

The physical principles of operation and principles of construction of measuring transducers of various physical parameters are considered. The main attention is paid to semiconductor sensors of temperature, mechanical deformation, and magnetic fields. Certain issues of the operation of humidity sensors, ionization devices, various phototransducers, flow rate meters, fill levels, pressure, etc. are considered. The results of a study of the characteristics of the considered sensors and the influence of various external influences on them are presented. The monograph is dedicated to engineering and technical workers involved in the development and use of measuring transducers and sensors, researchers, graduate and university students.

Sensors, Transducers, Measurements



Nikolay Gorbachuk is Associate Professor of the Department of Applied Physics and Higher Mathematics at the Kyiv National University of Technology and Design, Ukraine.

FOR AUTHOR USE

Nikolay Gorbachuk

# Measuring Transducers and Sensors

Monograph



Nikolay Gorbachuk



**Nikolay Gorbachuk**

**Measuring Transducers and Sensors**

FOR AUTHOR USE ONLY

**Nikolay Gorbachuk**

# **Measuring Transducers and Sensors**

**Monograph**

FOR AUTHOR USE ONLY

**LAP LAMBERT Academic Publishing**

## **Imprint**

Any brand names and product names mentioned in this book are subject to trademark, brand or patent protection and are trademarks or registered trademarks of their respective holders. The use of brand names, product names, common names, trade names, product descriptions etc. even without a particular marking in this work is in no way to be construed to mean that such names may be regarded as unrestricted in respect of trademark and brand protection legislation and could thus be used by anyone.

Cover image: [www.ingimage.com](http://www.ingimage.com)

Publisher:

LAP LAMBERT Academic Publishing

is a trademark of

Dodo Books Indian Ocean Ltd. and OmniScriptum S.R.L publishing group

120 High Road, East Finchley, London, N2 9ED, United Kingdom

Str. Armeneasca 28/1, office 1, Chisinau MD-2012, Republic of Moldova,  
Europe

Printed at: see last page

**ISBN: 978-620-7-47057-0**

Copyright © Nikolay Gorbachuk

Copyright © 2024 Dodo Books Indian Ocean Ltd. and OmniScriptum S.R.L  
publishing group

FOR AUTHOR USE ONLY

## Table of Contents

Introduction.....	5
Chapter 1. Temperature. Transducers, measurement .....	7
1.1. Mechanical contact thermometers .....	7
1.2. Thermometers based on the thermoresistive effect.....	7
1.3. Semiconductor resistance thermometers .....	8
1.4. Examples of some industrial thermistors .....	12
1.5. Platinum resistance thermometers .....	12
1.6. Own heating of resistance thermometers.....	13
1.7. Low-temperature (cryogenic) resistance thermometers - thermistors. Temperature measurement in the cryogenic region.....	14
1.8. Cryogenic thermistors based on dispersed germanium.....	15
1.9. Thermodiodes and thermotransistors.....	19
1.10. Thermoelectric transducers (thermocouples). Principle of operation, schemes of switching on and use of thermocouple.....	20
1.11. Thermocouple manufacturing .....	23
1.12. Graduation of the thermocouple .....	25
1.13. Alloys for thermocouples .....	26
1.14. Examples of temperature measurement and calculation using thermocouples.....	27
1.15. Pyrometers .....	31
Bibliography .....	34
Chapter 2. Mechanical quantities. Transducers, sensors, measurement .....	36
2.1. Load cells.....	36
2.2. Foil strain gauges .....	38
2.3. Measurement of mechanical stresses by vibrating string. Tenzometer.....	39
2.4. Adhesives, binders for mounting of strain gauges .....	40
2.5. Attestation, calibration, verification of strain gauges.....	41
2.6. Measurement of mechanical deformations (stresses) with the help of strain gauge .....	42

2.7. Hydroprotective strain gauge materials .....	44
2.8. Mounting of general purpose strain gauges .....	45
2.9. Semiconductor strain gauges.....	47
2.10. Piezoresistive effect in semiconductors and strain gauge based on it.....	49
2.11. Strain and pressure transducers for measuring force and pressure .....	58
2.12. Electromechanical transducers .....	59
2.13. Acceleration transducers. Accelerometers.....	59
2.14. Integral semiconductor beam accelerometer.....	60
2.15. Measuring transducers of vibrations. Vibrometers .....	61
2.16. Silicon strain gauge pressure transducer.....	62
2.17. Some commercially available pressure sensors. Sapphire, Motorola.....	63
2.18. Displacement transducers.....	65
2.19. Flow measurement instruments. Flow meters.....	67
2.20. Switches and sensors for proximity detection (motion sensors).....	70
2.21. Weight sensors. Methods and means of conversion.....	72
2.22. Fill level sensors. Fill level measurement.....	73
2.23. Speed measurement. Tachometers .....	78
Bibliography .....	80
Chapter 3. Magnetic Fields. Transducers, sensors, measurement .....	83
3.1. Hall sensors. Principle of operation, description, device .....	83
3.2. Principle of operation of a Hall sensor .....	84
3.3. Modern Hall Effect Sensors .....	86
3.4. A series of precision Hall EMF generators (Hall sensors).....	89
3.5. Estimated measurements of alternating magnetic fields in the environment... 91	
3.6. Automotive Hall Sensor. Hall sensor in the ignition system.....	94
3.7. Magnetoresistive transducers. Magnetoresistive effect.....	96
3.8. Magnetoresistor designs.....	97
Bibliography .....	99
Chapter 4. Humidity, gases. Methods of measuring humidity. Hygrometer.....	102
4.1. Hygrometers .....	102
4.2. Resistive gas analysis. Gas concentration transducer .....	104

Bibliography .....	105
Chapter 5. Light. Transducers, photocells .....	106
5.1. Photoconductivity .....	106
5.2. The photoeffect of the confinement layer .....	108
5.3. Solar battery .....	111
5.4. Bolometers .....	111
5.5. Selenium photocells .....	112
5.6. Selenium photoresistors .....	113
5.7. Photoelectric transducers. General principles of operation .....	114
5.8. Valve photocells. Designs .....	116
5.9. LEDs .....	118
5.10. Semiconductor lasers. <i>P-n</i> -junction laser .....	119
Bibliography .....	123
Chapter 6. Ionization transducers. Sensors .....	124
6.1. pH transducers .....	124
6.2. Ionization chambers. General principles of operation .....	124
6.3. Ionization measuring transducers .....	126
6.4. Ionization chamber. Radioactive radiation. Counters .....	127
Bibliography .....	132
Appendix .....	133

## **Introduction**

It is difficult to imagine modern techniques and technologies without various types of measuring transducers, sensors, transducers, sensing elements. Many works are devoted to the development of such devices, the principles and methods of measurement, the design of transducers and sensors are constantly being improved.

Measuring transducers include devices that convert a change in one quantity into a change in another quantity. As a rule, such a transducer converts a non-electrical physical quantity, called the measured physical quantity, into an electrical signal. Measuring transducers are used in electronic systems that display the result of measurements or observations. The primary generators of electrical signals about a non-electrical physical quantity are sensors (transducers, sensitive elements).

The monograph presents the results of development of various measuring transducers and sensors. Both author's and other methods and means of measurements known in the literature are described. Attention is paid to means of temperature measurement in a wide range of temperatures - from cryogenic to room temperature and melting temperatures of some solid materials. Methods of measuring mechanical parameters - deformations, pressures, displacements, flow velocities, etc., measuring magnetic fields by various means, gas parameters - humidity, etc., solar energy converters, ionization devices are considered.

## Chapter 1. Temperature. Transducers, measurement

There is a wide variety of methods and means for measuring temperature. To create a temperature sensor (thermometer), any properties of solid, liquid, gaseous substances that depend on temperature can be used. For example, physical and chemical states, dimensions, electrical characteristics, etc. At the same time, thermometers (sensors) that use a fairly limited number of electrophysical properties of materials and measurement methods have found wide practical application.

### 1.1. Mechanical contact thermometers

Such thermometers are based on the thermal expansion of substances. They are characterized by low cost and satisfactory accuracy. They are intended mainly for everyday practical use and for laboratory work.

In a contact thermometer, the sensing element can be a metal rod whose elongation depends on the temperature (dilatometric thermometers):

$$l = l_0(1 + \alpha t), \quad (1.1)$$

where  $l_0$  - length at 0 °C,  $\alpha$  - coefficient of thermal expansion,  $t$  - temperature °C.

Even more often the difference in thermal expansion of two dissimilar metals is used - bimetallic thermometers. Such thermometers can be made in small sizes, easy to manufacture, low cost.

Glass liquid thermometers are widely used. The main part of the liquid is concentrated in a volumetric reservoir, which is practically a sensor (sensing element). Any liquid can be used for filling, depending on the operating conditions. Most often mercury, alcohol are used. Such thermometers are not highly accurate, but they are the most common in households, laboratories. In industry, they are gradually being replaced by thermometers that allow you to automate production.

Mechanical contact thermometers have a major disadvantage: their information (signal) cannot be transmitted over a distance for processing. Therefore, thermometers that utilize electrical changes in the properties of a substance with a change in temperature are used in industry.

### 1.2. Thermometers based on the thermoresistive effect

The electrical resistance of most substances changes significantly with temperature. This dependence is used to create thermometers - thermoresistors. A thermistor is a device consisting of a current conductor whose electrical resistance depends on temperature and to which electrical leads are connected.

The temperature dependence of the electrical resistance of metals is caused by the dependence of the mobility of current carriers (electrons), in semiconductors the main role is played by the temperature dependence of the concentration of current carriers.

The measuring range of thermometers is limited mainly by high temperatures, which affect the linearity of the sensor characteristic, as well as the mechanical properties of the material of the sensor sensing element and housing.

The temperature dependence of the resistance of metals can be expressed as:

$$R = R_0(1 + \gamma t) \quad (1.2),$$

where  $R_0$  - resistance at 0 °C,  $\gamma$  - temperature coefficient of resistance,  $t$  - temperature in °C.

As materials for the sensitive element of the thermistor thermometer are used: platinum, nickel, copper and others. Metal-based thermometer sensing elements are very thin wires wound on a frame or a film deposited on an insulating substrate.

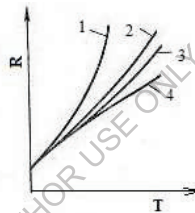


Fig. 1.1. Characteristic dependences of resistance  $R$  of some metals on temperature  $T$ :  
1 - nickel, 2 - tungsten, 3 - copper, 4 - platinum.

*Source: built by the author based on [2].*

Typical dependences of resistance of some metals on temperature are shown in Fig. 1.1. They indicate the possibility of obtaining a high degree of linearity of the relationship between resistance and temperature.

### 1.3. Semiconductor resistance thermometers

They are temperature sensors (thermistors) that use the dependence of the electrical resistance of a semiconductor on temperature. This dependence can be expressed as:

$$R = R_0 \cdot e^{B/T} \quad (1.3),$$

where  $R_0$  is the resistance at temperature  $T$  tending to infinity,  $B$  is the coefficient determining the sensitivity  $t_0$  temperature.

Exponential dependence shows a strong nonlinearity of the characteristic of such a thermometer and this is one of the main disadvantages of such a sensor. On the

other hand such thermometers are the most sensitive to temperature change. At liquid helium temperatures their sensitivity can reach 100-200 %/K. In addition, the high resistance (up to 1 megohm) allows neglecting interference at the connection points of the wires of the electrical circuit. Semiconductors such as silicon, germanium, gallium arsenide, etc., as well as metal oxides are used for manufacturing such thermometers.

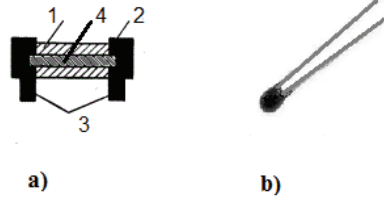


Fig. 1.2. a) - one of typical designs of semiconductor thermometer - thermistor. 1 - glass, 2 - steel, 3 - silver, 4 - sensing element, b) - sample of semiconductor miniature thermistor.

*Source: built by the author.*

Semiconductor thermometers can be of various kinds. With the help of microelectronics technology, the sensing element of thermistor can be made micro-miniature. Figure 1.2 shows some designs of semiconductor thermometers.

Semiconductor thermistors are widely used. A semiconductor in the form of a film on an insulating substrate or in a bulk design serves as a conductor of electric current. The total size of thermistors can be less than 1 mm<sup>3</sup>, electrical resistance from several Ohm to 100 kOhm, supply currents, as a rule, 10 - 100 μA, sensitivity from 3 %/K in the area of room temperature to 100 %/K in the area of cryogenic temperatures, inertia can reach several tens of milliseconds and less.

Semiconductor thermistors are widely used to measure and control temperature in a wide range, but, as a rule, not above 200 °C, as at high temperature comes intrinsic conductivity and temperature dependence of resistance falls sharply, becomes non-monotonic, not stable. In a wide temperature range, the temperature dependence of semiconductor resistance  $R(T)$  has a complex character and depends on the type of doping impurity and doping level. Therefore, it is impossible to express the dependence of  $R(T)$  by a simple formula that would allow to perform calibration with high accuracy. As a rule, the whole temperature interval is divided into separate sections, in which the dependence  $R(T)$  is described by its interpolation formula.

The group of semiconductor temperature-sensitive transducers used in thermometers is often referred to as thermistors. They have a highly nonlinear characteristic, but can be effectively used in systems for temperature measurement.

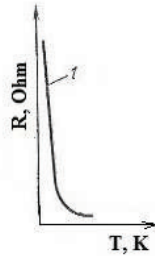


Fig. 1.3. Temperature dependence of resistance of a typical thermistor.

*Source: built by the author.*

A typical characteristic of a thermistor is shown in fig. 1.3. Comparing the characteristics of metallic resistive transducers with those of a thermistor allows us to conclude that the latter:

- 1) are steeper, i.e., their temperature coefficient of resistance is significantly larger than that of metals, at least in the main part of the curve;
- 2) fall with increasing temperature, i.e. their temperature coefficient of resistance is negative.

Thermistors with a negative temperature coefficient of resistance are better known as NTC thermistors. It should be noted that there are also thermistors with a positive resistance coefficient, which are referred to as PTC thermistors. The latter are more often used not for temperature measurement but, for example, to prevent overheating.

Thermistors are significantly smaller in size than metal resistive transducers and therefore react faster to temperature changes. On the other hand, the small size of thermistors means that a small current is required for self-heating. Consequently, it can be assumed that the current affects the accuracy of the measurement.

The methodology for calibrating a semiconductor thermistor can be examined using the following example. For example, in the room temperature region, the dependence of  $R(T)$  for semiconductor thermistors can be expressed by formula (1.3).

For thermistor calibration (obtaining tables of electrical resistance dependence on temperature), we transform formula (1.3):

$$\ln R = \ln R_0 + B(1/T) \quad (1.4),$$

The obtained expression (1.4) is the equation of a straight line in coordinates  $1/T$  and  $\ln R$ .  $\ln R_0$  is the value of the logarithm of resistance when  $T$  tends to infinity.

The coefficient  $B$  is equal to the tangent of the angle  $\alpha$  of the slope of the straight line to the  $1/T$  axis. If at two fixed temperatures  $T_1$  and  $T_2$  we measure the resistances of the thermistor  $R_1$  and  $R_2$  respectively, we can plot the dependence of  $\ln R(1/T)$  on the two points:

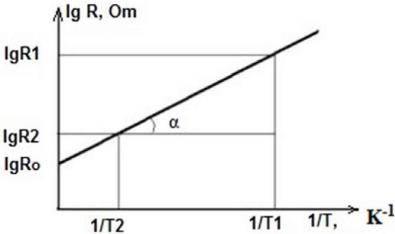


Fig. 1.4 Temperature dependence of resistance  $R$  of semiconductor thermistor.  
 Source: built by the author.

Using the formula (1.4) and the obtained graph it is possible to find for any value of  $R$  from the interval from  $R_1$  to  $R_2$  the corresponding temperature value - to make calibration tables.

For accurate temperature measurements thermistor calibration is carried out in specialized laboratories with the use of appropriate high-precision measurements and approximating formulas for the required temperature range, computer data processing, etc. In a wide temperature range, the temperature dependence of the resistance of semiconductor thermistors has a rather complex character.

Resistance thermometers are used in devices for temperature measurement, control and automatic regulation. In them, in addition to the sensing element, there is a current source and a measuring circuit. The measuring circuit, for example, of a balanced dc bridge is shown in fig. 1.5.

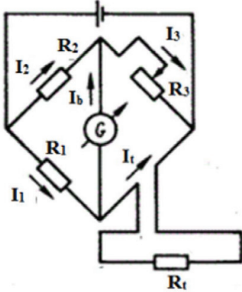


Fig. 1.5. Schematic diagram of the balanced DC bridge.  
 Source: built by the author based on [2].

By moving the slider of the rheostat  $R_3$ , bring the bridge to the balanced state, at which the galvanometer  $G$  fixes the absence of current in the diagonal of the bridge ( $I_d=0$ ). Thus, the value of  $R_3$  is proportional to the measured resistance  $R_x$ , which depends on the temperature. The equilibration of the bridge can be realized automatically. For this purpose, for example, the resistance of the resistor changes under the influence of the zero arrow of the galvanometer  $G$ .

In addition to balanced measuring bridges, unbalanced bridges are also used, which are characterized by higher reliability but lower accuracy due to the influence of source voltage fluctuations.

#### 1.4. Examples of some industrial thermistors

For example, we can consider well-known industrial thermistors of MMT and KMT series. The MMT-1 and KMT-1 types of thermistors represent a semiconductor rod covered with enamel paint, with contact caps and leads. These thermistor leads can be used only in dry rooms. Thermistors of MMT-4 and KMT-4 types are mounted in a metal case and sealed. They can be used in any humidity and any environment that is not aggressive to the housing. Sealing is carried out by glass and tin. The core of MMT-4 type thermistor is wrapped with metal foil. The current sink is made of nickel wire. These thermistors are produced for nominal resistance values from 1 to 200 kOhm (at 20°C) and can be used for operation in the temperature range from -100 to 129°C.

Pure metals are also used as materials for resistance thermometers: for example, platinum in the form of thin wire with a diameter of 0.05-0.07 mm for measuring temperatures up to 630°C. Copper, nickel or iron for measuring temperatures of 100-150°C. They are used in the form of wire with a diameter of 0.1 mm or in the form of films of the respective materials.

There are the following ways of winding the material of resistance thermometers:

- on a glass plate
- on a glass tube
- on a mica or porcelain cross.

The most widely used in the manufacture of metal sensitive elements of thermistors are platinum, nickel, copper.

#### 1.5. Platinum resistance thermometers

These transducers use the change in resistance of a platinum wire or film to determine temperature. They are also called resistive temperature detectors. It does

not follow that other metals cannot be used to measure temperature, but platinum sensing elements are most commonly used in such transducers.

The sensitivity of such resistive temperature detectors is quite low and the dynamic response is quite slow (due to the design of the device). They are also quite susceptible to destruction by vibration and shock.

There are two basic types of platinum wire resistive transducers: the immersed probe and the surface-mounted sensing element. The wire elements are usually mounted on a ceramic base with minimal tension and are usually coated with a protective material to prevent them from being exposed to the environment.

The design of a typical platinum wire probe is shown in fig. 1.6(a), and the surface-mounted temperature sensing element in fig. 1.6(b). Transducers with film sensing elements (fig. 1.6,c), which utilize a metal foil on an insulating substrate, are not as common as wire probes, although their use is constantly expanding because of their small size, improved dynamic response, higher sensitivity, and relatively low cost.

Platinum resistive transducers are usually included in one of the arms of a Wheatstone bridge, by means of which high accuracy of measurement is assured. Of course, the low resistance of the device (about 100 ohms) creates problems when switching it with measuring equipment, since the resistance of the wires connecting the transducer to the measuring circuit may be commensurate with the resistance of the transducer.

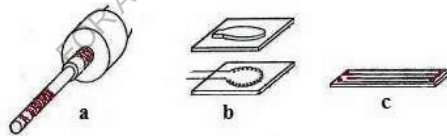


Fig. 1.6. Designs of platinum wire resistive transducers: a - wire probe, b - wire transducer mounted on the surface of the sensing element, c - thin-film transducer mounted on the surface of the sensing element.

*Source: built by the author based on [1].*

## 1.6. Own heating of resistance thermometers

The intrinsic heating of resistance sensing elements is understood as an increase in temperature  $\Delta T$  over the measured ambient temperature due to the release of joule heat in them during the passage of the measuring current. This temperature excess is an additional measurement error, depending not only on the current, but primarily on the amount of heat that can be dissipated into the environment.

The heat transfer is determined by the material and dimensions of the sensing element as well as by the condition and thermodynamic properties of the environment. Thermometer sensing element manufacturers usually indicate for each type of element the maximum permissible current and voltage drop across it in the form of a diagram, e.g. (fig. 1.7). The sensing element may be used only in the left ascending branch of the characteristic so that under certain boundary conditions no interference from its heating by the measuring current will occur. For example, a platinum sensing element (Pt 100) on a ceramic frame in a metal tube heats up by about 0.01-0.02 K in still water and by 0.1 K in still air when a current of 3 mA passes through it. The maximum current should not exceed 10 mA. With small NTC thermistors, the maximum allowable current may be only a few microamperes.

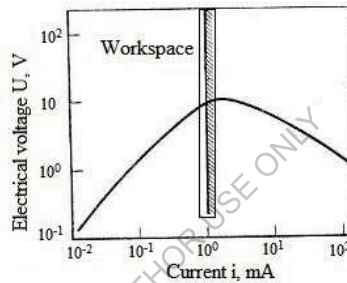


Fig. 1.7. Example diagram of permissible values of current flowing through the thermistor and voltage drop on it.

*Source: built by the author based on [2].*

### 1.7. Low-temperature (cryogenic) resistance thermometers - thermistors. Temperature measurement in the cryogenic region

Semiconductor and metal sensors - resistance thermometers (thermistors) and thermocouples with suitable characteristics are used for temperature measurement in the cryogenic region.

Very often measurements at low temperatures have to be carried out in the presence of rather strong magnetic fields. Therefore, low-temperature thermometers (sensors), in addition to good sensitivity to temperature and stability of characteristics, should have weak sensitivity to the influence of magnetic fields. Such well-known organizations as VNIIFTRI (Russia), LakeShore (USA), Institute of Semiconductor Physics (Ukraine), etc. are engaged in development, research, manufacturing of cryogenic thermistors (as well as other sensors for cryogenic range).

Among the known metallic resistance thermometers we can mention platinum thermistors, which are characterized by high metrological characteristics. However, for example, the magnetic field  $B=2$  Tesla at a temperature of 12 K causes the resistance growth equivalent to 5 K. It is considered possible to take into account the influence of magnetic field only at temperatures higher than liquid nitrogen temperatures (77 K).

Rhodium-iron thermistors are less sensitive to magnetic fields. At a temperature of 4.2 K, a field of 3 Tesla leads to an increase in resistance by 3% (equivalent to about 0.5 K). Of semiconductor thermistors, germanium thermistors are the most widely used. They have good long-term stability, high sensitivity ( $\cong 100$  %/K at 4.2 K) can provide accuracy of about 0.01 K. Germanium resistance thermometers are made of bulk germanium, dispersed germanium, germanium films on insulating substrates. There are known germanium thermistors, which due to low magnetoresistance value and in magnetic fields up to 6 Tesla provide accuracy at the level of 0,01 K. In addition to germanium, other semiconductor materials, such as gallium arsenide, are also used for cryogenic thermistors. However, it is considered that metrological characteristics of such thermometers, as a rule, are worse than those of germanium thermometers.

There are also carbon sensors - resistance thermometers, which are often used in measuring temperatures in the cryogenic region in the presence of magnetic fields. These are thermometers Allen-Bradley, Spear, Mitsushita, TSU (manufacturer VNIIFTRI), as well as TVO. It is noted in the literature that, for example, TCU thermometers provide reproducibility of  $\Delta T/T$  with an error not exceeding 0.0002. In a 6 Tesla magnetic field at a temperature of 4.2 K, their error is 0.35 K. TBO thermometers in the 6 Tesla field provide accuracy not worse than 0.12 K.

### **1.8. Cryogenic thermistors based on dispersed germanium**

To improve the technical characteristics of semiconductor microelectronic devices and to create their varieties, both new design solutions using well-known materials and new technologies for obtaining materials with promising electrophysical properties are used. When creating thermometers, the operation of which is based on the thermoresistive effect, the stability of the temperature dependence of the electrical resistance of the material used and the design of the thermal converter, sufficient sensitivity, minimum error from the influence of extraneous external influences is of crucial importance. Instability of known semiconductor thermistors especially begins to appear at cryogenic temperatures.

At temperatures below 20 K, the lack of repeatability makes many resistance thermometers unsuitable for precision measurements. Practice shows that these

disadvantages are less inherent in germanium thermometers. However, pure germanium is not used in thermometry because at low temperatures it has a very high resistance and low sensitivity. Often measurements must be carried out under conditions of various external influences (presence of magnetic fields, etc.), which, affecting the resistance of pure germanium, can lead to significant errors. Currently, to obtain suitable electrophysical properties of bulk germanium, various rather expensive and labor-intensive doping methods are used. They also use germanium in film form. In some works cryogenic thermistors based on germanium films on semi-insulating gallium arsenide have been investigated. At 4.2 K they can have a sensitivity of about 20 %/K, some are resistant to neutron irradiation at 77 K to doses of the order of  $10^{15}$  cm<sup>-2</sup>.

Studies of experimental samples of thermistors based on bulk dispersed germanium obtained by mechanical pressing at different temperatures and pressures of finely dispersed powder of monocrystalline germanium are known. The aim of the study was to create thermistors for the temperature range of 4.2-300 K resistant to extraneous external influences. The temperature dependence of electrical resistance in the above temperature range, magnetoresistance at T=4.2 K and the effect of neutron irradiation on electrical resistance at room temperatures were studied.

Dispersed germanium was obtained from powder of monocrystalline germanium of p-type conductivity with a resistivity of 15 Ohm.cm. Samples were produced by exposure to high pressures and temperatures. It was found that the pressure and temperature at which the powder was pressed determine the electrophysical properties of the obtained dispersed germanium. For creation of thermoresistors for cryogenic temperatures the most suitable samples were used. The obtained dispersed germanium had p-type conductivity, specific resistance at room temperature  $\rho = (1-4)$  Ohm.cm. It can be assumed that the acceptor levels are due to the peculiarities of the crystal structure of the obtained material. It is known that the type of conductivity can be determined by various types of structural defects. The peculiarities of the structure of dispersed (powder) germanium can also explain the increased radiation resistance of such material. Experimental samples of thermistors had a sensitive element with dimensions of approximately 1 mm<sup>3</sup> (fig. 1.8).

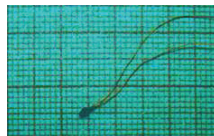


Fig. 1.8. Experimental sample of a thermistor based on dispersed germanium.

*Source: built by the author.*

The results of measurements of the temperature dependence of electrical resistance are presented in fig. 1.9. Here the temperature dependence of resistance of monocrystalline bulk germanium of p-type conductivity (curve 1) and experimental thermistors from dispersed germanium (curves 2,3) are shown.

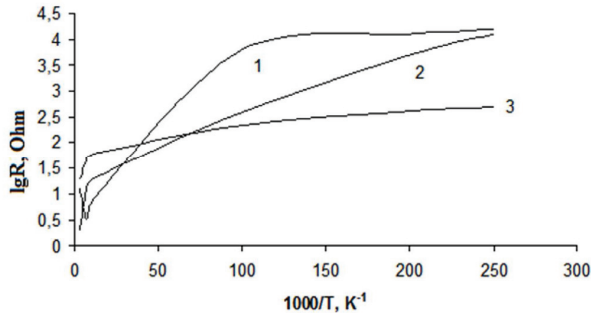


Fig. 1.9. Temperature dependence of electrical resistance: 1 - bulk initial monocrystalline germanium, 2- thermistor on the basis of dispersed germanium type A, 3- thermistor on the basis of dispersed germanium type B. Type A and B mainly differ in temperature and pressure value in obtaining dispersed germanium.

Source: built by the author based on [12,16,3].

Temperature dependence of electrical resistance of thermistors from dispersed (powder) germanium type A (curve 2) at low temperatures is steeper than the dependence of monocrystalline initial germanium and in the entire temperature range has a more monotonic character. The smooth character of the temperature dependence of the electrical resistance allows to approximate it with mathematical formulas quite simply and with good accuracy. For a sample of type A, for example, even for the temperature range 77-300 K using a polynomial of the form:

$$\ln R = \sum_{i=0}^n A_i (\ln T) \quad (1.5),$$

(where  $A_i$  - constant coefficients determined by the least squares method,  $n$  - determined from the condition of the smallest approximation error) already for  $n = 3$  we obtain the dependence:

$$\ln R = 15.1077031 + 1.6552736 * \ln T - 1.7901811 * (\ln T)^2 + 0.193233 * (\ln T)^3$$

with correlation coefficient  $r^2 = 0.9995$  and an error of about 0.1 K in the 77K region.

The sensitivity of type A thermistors in the temperature region of liquid helium (4.2 K) reaches values of more than 100 %/K. Sensitivity of thermistors made of type B material is about 20 %/K and at 4.2 K they have electrical resistance as a rule not exceeding 500 Ohm.

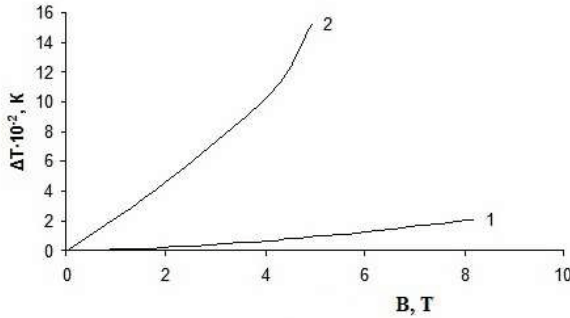


Fig. 1.10. Dependence of temperature measurement error  $\Delta T$  in the region of 4.2 K on the value of magnetic field  $B$  for thermistors of type A (curve 1) and type B (curve 2).

Source: built by the author based on [12].

Fig. 1.10 shows the dependence of the error  $\Delta T$  of temperature measurement in the region of liquid helium in the presence of magnetic fields on the magnitude of the magnetic field. The error of thermistors made of type A material (curve 1) in the field of 8 T is approximately 0.02 K, and that of type B thermistors in the field of 4 T reaches 0.15 K. It should be noted that the magnetoresistance  $\Delta R/R$  (where  $\Delta R$  is the change of resistance under the influence of the magnetic field,  $R$  is the initial resistance) in both types of thermistors is approximately the same. For example, in a 4 T field, the magnetoresistance of both is within (2.5 - 3.0) %. But the accuracy of measurement in magnetic fields of type A thermistors is higher due to higher temperature sensitivity.

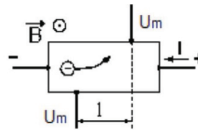


Fig. 1.11. Field-compensated temperature sensor:  $U_m$  - the measured voltage;  $l$  - distance between the contacts.

Source: built by the author based on [3].

In order to remove magnetic field-induced errors, a special configuration has been employed. The scheme is presented in fig. 1.11. The measuring wires are attached to the sensing head so as the electrical contacts are at the distance

$$l = aR_H/\rho M, \quad (1.6)$$

where  $a$  is the width of the plate;  $R_H$ , is the Hall constant;  $\rho$  is the resistivity;  $M = \Delta\rho/\rho B$  is magneto-resistance at field  $B$ .

As a result, the voltages generated on the contacts due to the Hall effect and magnetoresistance are mutually compensated so as to minimize the field effect on the measurement accuracy.

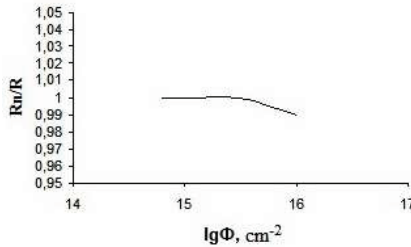


Fig. 1.12. Dependence of relative change of electrical resistance of a thermistor (type A) after neutron irradiation on the value of neutron fluxes  $\Phi$ .  $R$  - initial resistance,  $R_n$  - resistance after irradiation.

Source: built by the author based on [17].

The influence of radiation irradiation on the characteristics of thermistors based on dispersed germanium has been studied. Fig.1.12 shows the dependence of resistance of type A thermistors on radiation exposure. The effect of radiation on the resistance value has so far been investigated evaluatively and only at room temperatures. The characteristics were measured at a temperature of 300 K before irradiation and after irradiation with neutron fluxes  $\Phi$  from  $8 \cdot 10^{14} \text{ cm}^{-2}$  to  $1 \cdot 10^{16} \text{ cm}^{-2}$ . The temperature during the measurements was stabilized with an accuracy of 0.1 K. The neutron energy was 1 MeV and the flux intensity was  $(2-4) \cdot 10^8 \text{ fl/s}$ . The figure shows that the electrical resistance of the thermistors begins to change markedly when approaching neutron irradiation levels of  $10^{16} \text{ cm}^{-2}$ .

### 1.9. Thermodiodes and thermotransistors

Thermodiodes and thermotransistors are used in temperature sensors operating in the range from  $-80$  to  $+150$  °C. The upper limit of the temperature range is limited by thermal breakdown of the  $p-n$  junction and for some types of germanium sensors reaches 200 °C, and for silicon sensors up to 500 °C. The lower boundary of the temperature range of thermodiodes and thermotransistors is determined by the decrease in the concentration of the main carriers and can reach for germanium sensors  $-(240 - 260)$  °C, for silicon sensors  $-200$  °C.

The main advantages of thermodiodes and thermotransistors are small dimensions, interchangeability and, most importantly, cheapness, allowing their use in sensors of single use.

The relationship between the current  $I$  through a p-n junction (diode or transistor) and the voltage drop  $U$  across it is defined by a certain equation. This equation defines the current through the junction, both at forward and reverse bias of the junction. From the known equations and formulas we can see that both forward and reverse currents of a p-n junction are functions of temperature. Open p-n junctions are mostly used for temperature measurement. Theory shows that the voltage drop across an open p-n junction at current  $I$  through the junction is determined by an approximate formula, from which it can be seen that the voltage drop depends linearly on temperature and decreases with increasing temperature. The temperature sensitivity of the p-n junction in terms of voltage is  $\approx 1.5$  mV/K. Comparing the temperature sensitivity coefficients for the voltage drop across the p-n junction and the thermo-EMF of thermocouples operating in the same temperature range (e.g., chromel - copel), we can say that the sensitivity of the p-n junction is about 100 times higher than the sensitivity of thermocouples.

**1.10. Thermoelectric transducers (thermocouples). Principle of operation, schemes of switching on and use of thermocouple**

The principle of operation of a thermocouple is based on the thermoelectric effect, which consists in the fact that in a closed loop consisting of two dissimilar conductors, a thermo-EMF (voltage) occurs if the junction points of the conductors have different temperatures. If we take a closed circuit (see fig. 1.13) consisting of dissimilar conductors (thermoelectrodes), then on their junctions there will appear thermal EMF  $E(t)$  and  $E(t_0)$ , which depend on the temperatures of these junctions  $t$  and  $t_0$ . Since the considered thermoelectrodes are included in a countermeasure, the resulting thermoelectric EMF acting in the circuit will be defined as  $E(t) - E(t_0)$ .

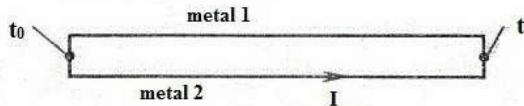


Fig. 1.13. Schematic of a closed circuit of two conductors.

Source: built by the author.

In the case of equal temperature of both junction, the resulting thermal EMF will be equal to zero. In practice, one of the junction of the thermocouple is immersed in a thermostat (as a rule, melting ice) and the temperature difference and temperature

of the other junction are determined relative to it. The junction that is immersed in the controlled (investigated) medium is called the working end of the thermocouple, and the second junction (in the thermostat) is called the free end.

In any pair of homogeneous conductors, the magnitude of the resulting thermoelectric EMF does not depend on the temperature distribution along the conductors, but depends only on the nature of the conductors and the temperature of the junction. If a thermoelectric circuit is disconnected in any place and included in it dissimilar conductors, then, provided that all the resulting junction points are at the same temperature, the resulting thermal EMF in the circuit will not change. This phenomenon is used to measure the thermal EMF of a thermocouple. The resulting EMF in thermocouples is small: it is less than 8 mV for every 100 °C and, as a rule, does not exceed 70 mV in absolute value.

Thermocouples can be used to measure temperatures in the range from -270 to 2200 °C. To measure temperatures up to 1100 °C, thermocouples made of base metals are used; to measure temperatures between 1100 and 1600 °C, thermocouples made of noble metals and platinum group alloys are used. To measure even higher temperatures, thermocouples made of heat-resistant tungsten-based alloys are used.

Currently, platinum, platinum-rhodium, chromel, alumel are most often used for thermocouples.

When measuring temperature in a wide range, it is necessary to take into account the nonlinearity of the thermocouple conversion function. For example, the conversion function of copper-constantane thermocouples for the temperature range from -200 to 300 °C with an error of approximately  $\pm 2 \mu\text{V}$  is described by the formula

$$E = At^2 + Bt + C \quad (1.7),$$

where  $A$ ,  $B$  and  $C$  are constants that are determined by measuring the thermal EMF at three temperatures,  $t$  is the working junction temperature at °C.

The time constant (inertia) of thermoelectric converters depends on the thermocouple design, the quality of thermal contact between the working junction of the thermocouple and the object under study. For industrial thermocouples the time constant is at the level of several minutes. However, there are also low-inertia thermocouples, whose time constant is within 5 - 20 seconds and even lower.

The measuring instrument is connected to the thermocouple circuit at the free end of the thermocouple and one of the thermoelectrodes.

As noted above, the free end of the thermocouple must be at a constant temperature when measuring temperature. If the length of the thermocouple itself is insufficient, in order to take this end to a zone of constant temperature, wires are used, which consist of two cores made of materials (metals) having the same thermoelectric properties as the electrodes of the thermometer.

For thermocouples made of base metals, extension wires are most often made of the same materials as the main thermoelectrodes. For thermocouples made of noble metals, extension wires are made of other (not expensive) materials that develop the same thermal EMF as the thermocouple electrodes in the temperature range 0 - 150 °C. For example, for platinum - platinum-rhodium thermocouple, extension thermoelectrodes are made of copper and a special alloy. These metals form a thermocouple identical to platinum-platinum-rhodium thermocouple in the range of 0 - 150 °C. For chromel-alumel thermocouple extension thermoelectrodes are made of copper and constantan, and for chromel-copel thermocouple extension thermoelectrodes can be the main thermoelectrodes made in the form of flexible wires. If the extension thermoelectrodes are connected incorrectly, a significant error may occur.

In laboratory conditions, the temperature of the free end of the thermocouple is maintained at 0°C by placing it in a Dewar vessel filled with crushed ice and water. Under industrial conditions, the temperature of the free end of the thermocouple is usually different from 0 °C and is usually equal to room temperature (room temperature). Since thermocouples are calibrated at a free end temperature of 0 °C and calibration tables are given relative to 0 °C, this difference can be a source of significant error. To reduce this error, as a rule, introduce a correction in the readings of the thermometer (thermocouple). When selecting the correction, both the temperature of the free ends of the thermocouple and the value of the measured temperature are taken into account (this is due to the fact that the thermocouple conversion function is nonlinear); this makes it difficult to accurately correct the error.

To eliminate the error, automatic correction for the temperature of the free ends of the thermocouple is widely used. For this purpose, a bridge is included in the circuit of the thermocouple and millivoltmeter, one arm of which is a copper thermistor, and the other arms are formed by manganin thermistors. At the temperature of the free ends of the thermocouple, equal to 0 °C, the bridge is in equilibrium; when the temperature of the free ends of the thermocouple deviates from 0 °C, the voltage at the output of the bridge is not equal to zero and is added to the thermal EMF of the thermocouple, thus making a correction in the readings of the device (the value of the correction can be adjusted by a special resistor). Due to the non-linearity of the thermocouple conversion function, full compensation of the error cannot be achieved, but the error is significantly reduced.

Depending on the required accuracy in practice when using a thermocouple, the following connection schemes are most often used (see fig. 1.14). For example, the thermocouple copper (M) - constantan (K) is taken:

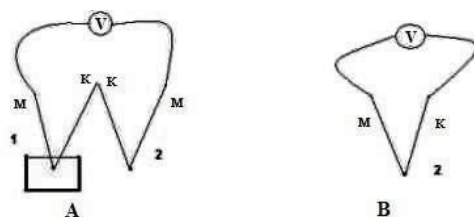


Fig. 1.14. Thermocouple connection schemes.

A) differential circuit. B) in this scheme, the temperature of the free end can be considered equal to the room temperature (temperature at the points of connection of the measuring device to the thermocouple).

*Source: built by the author.*

In the differential connection scheme (fig. 1.14.A), the free end 1 is at a constant temperature (melting ice,  $0^{\circ}\text{C}$ ). Thermo EMF is formed due to the temperature difference between the working 2 and free 1 junction. In the connection scheme shown in fig. 1.14.B, the temperature of the free end can be considered equal to the room temperature (temperature at the points of connection of the measuring device to the thermocouple) and the temperature in the area of the working junction 2 is calculated (corrected) relative to it. In this case, the thermal EMF in the thermocouple is formed due to the temperature difference between the working junction and the room temperature.

To measure the thermal EMF, voltmeters with a high impedance input or other type of galvanometers are used. To determine the temperature use calibration tables (see APPENDIX), which are built for the condition that the free end of the thermocouple is at zero degrees Celsius. Some calibration tables, e.g., for chromel-alumel thermocouples, etc., are presented in the tables at the end of the monograph.

### 1.11. Thermocouple manufacturing

For measurements and researches in laboratory (home) conditions thermocouples can be made independently. For this purpose, industrially produced wires from materials suitable for thermocouple manufacturing are used. The diameter of the wire is important when measuring thermal processes in small volumes (investigation of small objects). The smaller the diameter of the thermocouple wire, the smaller the error in determining the temperature and determining the parameters of thermal processes, as the influence of the thermocouple itself on the heat exchange is reduced. The material of the thermocouple is selected depending on the expected range of operating temperatures, the required sensitivity, the presence of secondary

equipment, etc. The most widely used thermocouples are chromel-alumel, copper-constantane, etc.

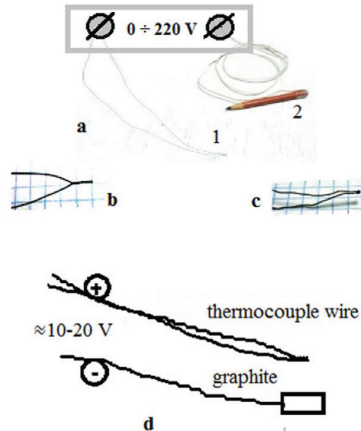


Fig. 1.15. Thermocouple welding: a - use of laboratory transformer, 1 - connected thermocouple wires, 2 - graphite (pencil), b - pre-connected wires, c - welded connection, d - general connection scheme during welding.

Source: built by the author.

Making a thermocouple consists in creating a strong connection (welding, fig. 1.15) of two materials (wires). For this purpose, you can use a voltage source of sufficient power (for example, LATR - laboratory autotransformer (a), automobile battery). A thermocouple (both free ends) is connected to one pole of the voltage source - fig. 1.15.a (1), d with pre-mechanically connected wires - fig. 1.15.b, and a lead connected to a piece of graphite (e.g. a pencil fig. 1.15.a (2)) is connected to the other pole.

When the connected ends of the thermocouple touch the graphite, an electric arc of sufficient power is generated and the thermocouple wires are welded. The voltage required for welding is selected experimentally, starting with small voltages of 3-5 V.

The optimum voltage for welding depends on the thermocouple material, diameter, length and, as a rule, does not exceed 30-40V. When working, it is necessary to ensure compliance with safety precautions: do not use too high voltages, do not touch bare parts of the electrical circuit. For convenience, a small section of thermocouple wires can be covered (insulated) with insulated tape, ceramic tubing, etc.

A sufficiently good connection can also be obtained by heating thermocouple wires by means of an arc discharge ignited between them and a strong aqueous solution of table salt.

### 1.12. Graduation of the thermocouple

Graduation of a thermocouple consists in establishing the dependence of the thermoelectromotive force on the temperature difference between the junction wires of the thermocouple. This is done, as a rule, in order not to use standard calibration tables, etc. in the future. Graduation can be done, for example, as follows.

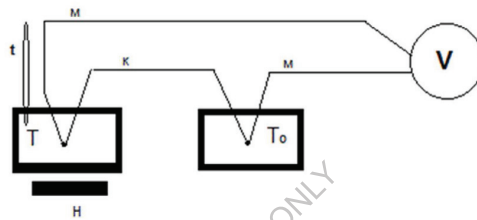


Fig. 1.16. Scheme of connections at thermocouple calibration.

*Source: built by the author.*

A simple experimental setup, from which the essence of the graduation technique is clear, is shown in fig. 1.16. One junction (working) of the thermocouple (for example, copper (m) - constantan (k)) is immersed in a vessel with oil (with temperature  $T$ ), the other free - in a vessel with ice  $T_0 = 0$  °C. Since the calibration tables in the literature are given relative to 0 °C, it is best to adhere to this condition, because in the future it will be easy to compare the obtained experimental results with the tabular ones. In addition, melting ice makes it possible to simply and accurately fix one of the temperatures relative to which the calibration is performed, and subsequently measurements with this thermocouple. A vessel with oil is heated by an electric heater  $H$ , and the temperature  $T$  is measured with a thermometer  $t$  of the required accuracy. The thermal EMF resulting from the heating of the junction of the thermocouple is measured with a dc potentiometer  $V$ . Make a table or plot the dependence of EMF on temperature  $T$ .

If high accuracy of graduation and measurement is not required, it is possible to graduate relative to room temperature. In this case, the free junction can be placed in room temperature oil ( $T_0$  about 20 °C).

### 1.13. Alloys for thermocouples

For the manufacture of thermocouples are used mainly alloys based on metals, although there are materials with values of thermal emf much higher than the thermal emf of metals. Semiconductors can be referred to such materials. However, it is very difficult to manufacture thermocouples from semiconductors and due to their technical and design features such thermocouples are not widely used.

The alloys most commonly used for thermocouples are:

- 1) copel (56% Cu and 44% Ni);
- 2) alumel (95% Ni, the rest - Al, Si and Mn);
- 3) chromel (90% Ni and 10% Cu);
- 4) platinum-rhodium (90% Pt and 10% Rh).

Fig. 1.17 shows the dependences of the thermal EMF on the temperature difference between the hot and cold junction for different thermocouples.

Inconsistency of alloy compositions can lead to significant changes in the values of thermoelectric emf. In such cases, preliminary calibration is necessary to achieve high accuracy instead of using standard tables.

Depending on the composition, thermocouples are used to measure temperatures in the following ranges: platinum-rhodium - platinum up to 1600°C; copper - constantan and copper - copel up to 350°C; iron - constantan, iron - copel and chromel - copel up to 600°C; chromel - alumel up to 900-1000°C.

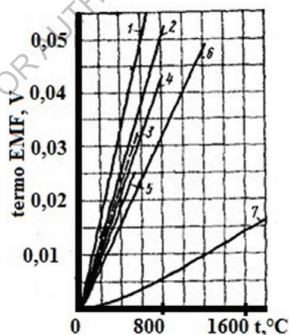


Fig. 1.17. Dependence of thermal EMF on temperature difference between hot and cold junction for thermocouples: 1 - chromel - copel, 2 - iron - copel, 3 - copper - copel, 4 - iron - constantan, 5 - copper - constantan, 6 - chromel - alumel, 7 - platinum-rhodium - platinum.

Source: built by the author based on [13].

Of the metallic thermocouples the greatest thermal EMF at the same temperature difference has a thermocouple chromel - copel. The sign of the thermal EMF of the thermocouples shown in fig. 1.17 is as follows: in the cold junction the

current is directed from the first material named in the pair to the second (from chromel to copel, from copper to constantan, etc.), and in the hot junction - vice versa.

Most thermocouples operate steadily in an oxidizing environment. In the process of long-term operation, a gradual change in the thermocouple's thermal emf can be observed. The reasons for such instability are contamination by impurities from the surrounding atmosphere, oxidation of wires, volatility of components, sharp bends and mechanical deformations, which introduce internal stresses and create inhomogeneity of the structure. The platinum-rhodium thermocouples have the highest stability, accuracy, reproducibility, despite the low value of thermal EMF. This is due to the chemical inertness of the material and a high degree of purity of the obtained material.

#### **1.14. Examples of temperature measurement and calculation using thermocouples**

##### **a) Calculation from the thermoelectric emf value of a copper-constantan thermocouple.**

Depending on the accuracy required, the temperature can be calculated differently from the thermocouple thermoelectric emf value.

In measurements, when it is enough accuracy in a few fractions of degrees, you can use the calibration tables and according to their data and readings of the voltmeter (galvanometer), measuring the value of the thermal EMF, to determine the temperature. In this case, if the thermocouple is included in the scheme of fig. 1.14.A and the free end is at 0 °C, the temperature determined by the above method by the value of the thermoEMF between the working and free junction should coincide with the true temperature (within the error determined by the quality of the thermocouple, the method of using the tables) in the area of the working junction of the thermocouple.

If a simpler scheme of thermocouple inclusion fig.1.14.B is used (conditionally speaking, the free end of the thermocouple is at room temperature and EMF in the thermocouple is generated due to the temperature difference between the working junction and the room temperature), it is necessary to make a correction when using the tables.

For example, the temperature in the region of the working junction can be determined by the value of the measured thermal EMF ( $E_i$ ) summed with the tabulated thermal EMF ( $E_{t_0}$ ) for a given room temperature (the temperature at which the measuring device is located):  $E = E_i + E_{t_0}$ . If, for example, the room temperature is 20 °C, the value of  $E_{t_0} = 0.790$  mV for the copper-constantan thermocouple for this

temperature - see the calibration table. Suppose the reading (measured EMF) of the copper-constantan thermocouple  $E_i = 2.119$  mV. In this case, the EMF to be used to determine the working junction temperature from the tables is:  $E = 0.790 + 2.119 = 2.909$  (mV). Using the tables we obtain the temperature value in the working junction area  $t = 70$  °C. Figure 1.18 shows the dependence of the measured EMF value ( $E_i$ ) and the table value ( $E_t$ ) on temperature for this case.

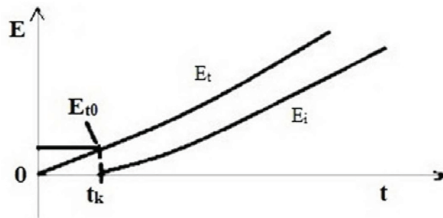


Fig. 1.18. Graph-scheme of the temperature dependence of the thermal EMF  $E$  of a differential thermocouple  $E_t$  and a single-junction thermocouple  $E_i$ .

Source: built by the author.

At the same time, sometimes the thermal EMF of thermocouples can significantly differ from the tabulated values, even when using a differential thermocouple and switching it on according to the scheme in which one junction is at 0 °C. This may be due to the presence of impurities, inhomogeneities, mechanical deformations, deviation from the ratio of materials in the alloy in the thermocouple wire. Therefore, if more accurate measurements are needed, a special thermocouple graduation is carried out (see graduation). It is also possible, for example, to select several points from the working temperature range, where the temperature can be stabilized and determined in a sufficiently accurate and independent way. Then, having plotted the dependence of the difference  $\Delta E$  of the thermal EMF values (according to the table data and measured ones) on the temperature, it is possible to make corrections - to add or subtract the value of  $\Delta E$  from the measured thermal EMF. In this way it is possible to achieve the accuracy of temperature measurement at the level of 0.05 °C. If even higher accuracy is required, calibration is carried out in specialized metrology laboratories.

### **b) Measuring and calculating temperature with a thermocouple made of chromel-copel alloys.**

Here we describe temperature measurement with a thermocouple made by our own hands, but the information given is also useful for understanding the operation of thermocouples manufactured commercially.

If you need the accuracy of temperature measurement at the level of 0,5 K (may be higher; the error depends on the capabilities of the measuring device V), it is necessary to make and use a differential thermocouple (see fig. 1.19.a). m1, m2 - metal 1 and 2 of the thermocouple wire, respectively.

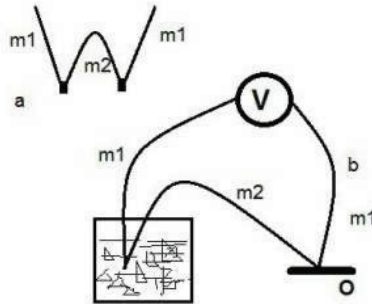


Fig. 1.19. Differential thermocouple - a, and the scheme of measuring the temperature of the object **O** - b.

*Source: built by the author.*

Here we note that for temperature measurement in the climatic range (room temperatures) the chromel-copper thermocouple is best suited, the main advantage of which is high sensitivity in the area of room temperatures. For measurements in the area of low temperatures it is possible to use thermocouples chromel-alumel, copper-constantan etc. (see calibration tables). For high temperatures, platinum-based thermocouples, chromel-alumel thermocouples, etc. are used.

Recall that the thermocouple calibration tables are made for the condition when one of the junction of the differential thermocouple is at 0 °C. In order to use this condition in practice, one of the junction of the thermocouple is immersed in a vessel (thermos) with melting ice, the temperature of which is known to be 0 °C.

The scheme of such a measurement of the temperature of the object **O** by a differential thermocouple is shown in fig. 1.19.b.

For the example, we consider that the measurements are carried out using a chromel-copper thermocouple. The temperature of the object **O** is determined by the readings of the voltmeter (galvanometer) V. For example, we know that the object is at a temperature above 0 °C, the voltmeter reading  $U = 6.43$  mV. We look at the table and determine that such a value of the thermal EMF corresponds to a temperature of +93 °C. It should be borne in mind that the sign of the thermal EMF

depends on the polarity of the thermocouple connection to the measuring device V and at the transition of the object temperature through  $0^{\circ}\text{C}$  will be reversed.

If the technical conditions suit the accuracy of measurement at the level of units of degrees, it is possible to use a thermocouple with one junction (see fig. 1.20).

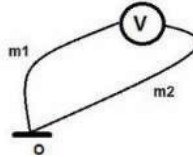


Fig. 1.20. Scheme of measuring the temperature of object **O** with a single junction thermocouple.

*Source: built by the author.*

If we analyze the physical processes in such a measuring circuit, we can see that in this case (as noted above) the role of temperature, relative to which the thermo-EMF is formed, plays the room temperature (the temperature at which the terminals of the measuring device - voltmeter). Accordingly, this is taken into account when using calibration tables and determining the temperature of the object. The value of thermal EMF  $U$ , by which, using the tables, the temperature of the object is determined, will be equal to:

$$U = U_k + U_v \quad (1.8),$$

where  $U_k$  - table value of EMF of differential (with two junction) thermocouple at room temperature  $t_k$  (device temperature - for example,  $t_k = 24^{\circ}\text{C}$ , in this case  $U_k = 1.57\text{ mV}$ ),  $U_v$  - measured thermal EMF (voltmeter reading V).

We took for example the temperature in the room  $24^{\circ}\text{C}$  ( $U_k = 1.57\text{ mV}$ ), if the voltmeter readings, for example,  $3.05\text{ mV}$ , then, respectively,  $U = 4.62\text{ mV}$  and using the tables determine that the temperature of the object **O** -  $68^{\circ}\text{C}$ .

To simplify the calculation (if a small decrease in accuracy is acceptable) when determining the temperature using a thermocouple with a single junction can approximate the dependence of the EMF of the thermocouple on temperature by a linear dependence. In this case, the temperature of the object to is determined:

$$t_o = t_k + U_v / j \quad (1.9),$$

where  $j = \Delta U / \Delta t$  is the average temperature sensitivity of the thermocouple in a certain temperature range.

For example, for a chromel-pin thermocouple in the temperature range (0 - 200)  $^{\circ}\text{C}$ , the average sensitivity  $j$  is approximately  $0.074\text{ mV}/^{\circ}\text{C}$ .

### 1.15. Pyrometers

Pyrometers are instruments that use the electromagnetic radiation of bodies to determine their temperature.

The surfaces of all bodies of substances whose temperature is above absolute zero emit electromagnetic waves. The nature of this radiation and its characteristics depend on the temperature.

The wavelength range of thermal radiation is between 0.1 and 1000  $\mu\text{m}$ . In addition to radiation, bodies also absorb radiation from other bodies. In general, a body absorbs part of the energy, part reflects it, and part transmits it further. All this is characterized by appropriate coefficients. In the physics of thermal radiation there is the concept of an absolutely black body. Absolutely black body is a body that absorbs all the radiation falling on it. Absorption and radiation of bodies are considered in relation to such a body.

In practice, no body absorbs and radiates as an absolutely black body. A model of an absolutely black body can be the opening of a chamber, the inner surface of which has a good absorption capacity and the same temperature.

The emissivity of an absolutely black body and its dependence on temperature is shown in fig. 1.21:

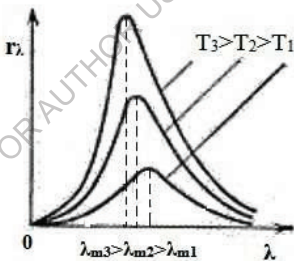


Fig.1. 21. Dependence of emissivity  $r_\lambda$  of a completely black body on temperature  $T$  and wavelength  $\lambda$ .

Source: built by the author based on [2].

The wavelength of the maximum intensity of radiation is determined by Wien's law:

$$\lambda_m = b/T \quad (10),$$

$b$  is Wien's constant,  $T$  is absolute temperature.

Knowing the laws of radiation it is possible to determine the temperature of the radiated surface by the measured radiation flux falling on a certain surface.

There are the following radiation receivers:

A) Black and gray receivers (thermal). These receivers include temperature sensors (thermistors, thermocouples) fixed on blackened plates receiving radiation. Their sensitivity is independent of wavelength.

B) Selective sensing elements. These are photocells, photoresistors, photodiodes, phototransistors. Absolute sensitivity of selective sensitive elements is much higher.

Radiation receivers cause a change in current, resistance, and voltage in the corresponding electrical signal processing circuitry.

At high temperatures of the radiating surface (above 650 °C), when the color begins to change, the eye of the observer can also serve as a radiation receiver.

*A distinction is made between pyrometers:*

**Optical pyrometers.** Optical pyrometers are sensitive only in a narrow wavelength range. This is achieved by using a special filter.

The radiation of the object under study is analyzed either by a radiation receiver or by comparison with a reference radiation source. The most widely used pyrometers are those with a disappearing filament. When working with such pyrometers, the researcher compares in a narrow wavelength range of the visible spectrum the brightness of the measured radiation and the control radiation (glowing tungsten filament). When both brightnesses are equal, the filament disappears.

The heating power (current) of the filament is an indication of the optical temperature of the monitored object. The temperature is determined by a graduation curve or the pyrometer may already have a scale. The brightness (spectral, optical) temperature measured by a pyrometer is equal to the true temperature if the spectral emission coefficient of the surface of the controlled object is equal to one (absolutely black body). In practice, the measured temperature is always less than the true temperature and it is necessary to introduce a correction in the measured value, which is determined depending on the measured temperature and spectral emission coefficient  $k_r$  (determined by tables) (for example, for a wavelength  $\lambda = 0.65 \text{ nm}$  - porcelain  $k_r = 0.78$  at 1200 °C, iron  $k_r = 0.35$  at 800 °C).

Disappearing filament pyrometers are very convenient and simple pyrometers. The disadvantage is the limitation of the lower temperature limit, as well as some subjectivity of the measurement results. At the same time, the correction made in the measurement result for non-black radiating objects is more accurate than for radiation pyrometers. Optical pyrometers with an objective radiation receiver - photoelectric element, etc. have also been developed.

Measurements with a disappearing filament pyrometer are carried out from a distance of 2 m to infinity. The distance can be corrected with the help of special optics. The lower temperature limit is 650 °C or 200 °C for the objective receiver.

The upper limit usually does not exceed 2500 °C. Pyrometers are graduated on a black emitter or a tungsten filament lamp.

**Radiation (full radiation) pyrometers.** These are pyrometers that sense radiation over the entire spectral range. They are considered as such if at least 90% of the radiation of the object is used in the pyrometer. For such pyrometers, only thermal receivers - thermocouples, thermistors - can be used as a receiver. Such pyrometers can measure temperature in the range of -50 °C - 2000 °C and higher. Correction of readings to the radiation coefficient in many pyrometers is carried out automatically and the pyrometer immediately shows the true temperature, if you set a known value of the radiation coefficient in advance.

FOR AUTHOR USE ONLY

## Bibliography

1. Orlova M.P., Pogorelova O.F., Ulybin S.A. *Nizkotemperaturnaya termometriya* [Low temperature thermometry]. M.: *Energoatomizdat*, 1987.-280 p.
2. P. Profos. *Spravochnik «Izmereniya v promyshlennosti»* [Directory "Measurements in Industry"] 1-3 volumes. M.: *Metallurgiya*, 1990.
3. N.Gorbachuk, M.Larionov, A.Firsov, N.Shatil Semiconductor Sensors for a Wide Temperature Range. *Sensors & Transducers Journal and Magazine*, Vol. 162, Issue 1, January 2014, pp.1-4.
4. N.S. Boltovets, V.K. Dugaev, V.V. Kholechuk et al., New Generation of Resistance Thermometers Based on Ge Films on GaAs Substrates, *Temperature: Its Measurement and Control in Science and Industry 7*, 399-404 (2003).
5. Zarubin L.I., Nemish I.Yu. *Miniatyurnyy termometr soprotivleniya na 1,3-200K*. [Miniature resistance thermometer for 1.3-200K]. *Pribory i tekhnika eksperimenta*, 1971, No. 4, p. 260.
6. Astrov D.I., Abilov G.S., Alshin B.I. *Izmerenie nizkikh temperatur v prisutstvii sil'nykh magnitnykh poley*. [Measuring low temperatures in the presence of strong magnetic fields]. *Izmeritel'naya tekhnika*, 1977, No. 4, p. 39.
7. V. F. Mitin. *Termometry soprotivleniya na osnove plenok germaniya*. [Resistance thermometers based on the germanium films]. *Fizika poluprovodnikov, kvantovaya elektronika i optoelektronika*. 1999. V. 2, N 1. P. 115-123.
8. Medvedeva L.A., Orlova M.P., Rabinkin A.G. *Termopara dlya izmereniya nizkikh temperature* [Thermocouple for measuring low temperatures]. *Pribory i tekhnika eksperimenta*, 1970, No. 5, p. 208.
9. Gorbachuk N.T., Shybyryn V. S. "SEMICONDUCTOR TEMPERATURE SENSORS - THERMORESISTORS", *Modern engineering and innovative technologies*, Germany, issue No16. April, 2021.
10. N. T. Gorbachuk, *Sposob izmereniya temperaturey*. [Method of measuring temperature], Patent of the Russian Federation. No. 2025736, No. 24, 1994.
11. Kiknadze G.I., Plesh A.G., Safronov A.N., Gorbachuk N.T. and others. *Rezultaty eksperimental'nogo issledovaniya protsessa okhlazhdeniya model'noy seksii i eksperimental'nogo bloka sverkhprovodyashchey obmotki toroidal'nogo polya ustanovki T-15 na komplekse SIMS* [Results of an experimental study of the cooling process of the model section and the experimental block of the superconducting winding of the toroidal field of the T-15 installation on the SIMS complex]. *Preprint IAE-4320/10*, M., 1986, 24 p.
12. Belyakov V.A., Gorbachuk N.T., Didenko P.I., Filatov O.G., Sychevskiy S.E., Firsov A.A. etc. *Poluprovodnikovye izmeritel'ne preobrazovateli deformatsii*,

*temperatury i magnitnogo polya dlya primeneniya v usloviyakh radiatsionnogo vozdeystviya, shirokom diapazone temperatur i magnitnykh poley* [Semiconductor measuring transducers of deformation, temperature and magnetic field for use in conditions of radiation exposure, a wide range of temperatures and magnetic fields]. *Voprosy atomnoy nauki i tekhniki*, Seriya: *Elektrofizicheskaya apparatura*, v.3(29), 2005, p.46-54.

13. Mykola Gorbachuk. ELECTROTECHNICAL MATERIALS. LAP LAMBERT Academic Publishing, 120 High Road, East Finchley, London, N2 9ED, United Kingdom, 2024, 112p. ISBN: 978-620-3-46212-8.

14. N. Stefan, S. A. Mulenko, N. T. Gorbachuk. "Laser Synthesis of Nanometric Chromium Oxide Films with High Seebeck Coefficient and High Thermoelectric Figure of Merit: An Experimental Study". Current Overview on Science and Technology Research Vol. 4, Chapter 1, p. 1-22. Print ISBN: 978-93-5547-861-0, eBook ISBN: 978-93-5547-862-7, DOI: 10.9734/bpi/costr/v4/6196F

15. S.A.Mulenko, N.T.Gorbachuk. Synthesis of nanometric iron oxide films by RPLD and LCVD for thermo-photo sensors. Applied Physics B: Lasers and Optics, v.105, #3, p.517-523, 2011.

16. Gorbachuk N.T., Didenko P.I. *Izmeritel'nye preobrazovateli na osnove GaAs, polikremniya i dispersnogo germaniya i perspektivy ikh ispol'zovaniya* [Measuring transducers based on GaAs, polysilicon and dispersed germanium and prospects for their use]. *Perspektivnye materialy*, 2004, N 5, p.93-97.

17. Gorbachuk N.T., Didenko P.I. *Vliyanie neytronnogo oblucheniya na kharakteristiki poluprovodnikovyykh izmeritel'nykh preobrazovateley temperatury, deformatsii, magnitnogo polya* [The influence of neutron irradiation on the characteristics of semiconductor measuring transducers of temperature, strain, and magnetic field]. *Poverkhnost'*, 2005, 4, pp.57-58.

18. N.T.Gorbachuk, S.A. Mulenko, Yu.N.Petrov. Photon synthesis of iron oxide thin films for thermo-photo-chemical sensors. Applied Surface Science. Volume 258, Issue 23, 15 September 2012, Pages 9186–9191.

19. Sergii Mulenko, Nicolaie Stefan, Floralice Miroiu, Nikolay Gorbachuk. Laser Synthesis of Transitional Metal Oxides in 2D Structure and Heterostructure for Thermo Sensors with High Seebeck Coefficient. *Frontiers in Sensors (FS) Volume 4*, 2016, p.16-26.

20. Sominskiy M.S. *Poluprovodniki* [Semiconductors].- L. Nauka 1967. 439p.

21. <https://sensorse.com>

22. Kucheruk I.M., Gorbachuk I.T., Lutsik P.P. *Zagal'niy kurs fiziki: Navchal'niy posibnik* [General course of physics: Study guide], T. 1-3. – K.: Tekhnika, 2001.

## Chapter 2. Mechanical quantities. Transducers, sensors, measurement

### 2.1. Load cells

Since the resistance of a conductor is defined by the relationship

$$R = \rho l/S \quad (2.1),$$

where  $\rho$  is the resistivity of the material;  $l$  is the length  $S$  is the cross-sectional area, then the resistance can change at any fluctuation of the measured value, which affects one or more of the arguments included in this expression.

This relationship is used in strain gauges, which are transducers that convert a change in applied force into a change in resistance. Typically, such a transducer is used in conjunction with a Wheatstone bridge, where one, two, or even all four arms are load cells and the output voltage changes in response to variations in the force being measured.

Strain gauges use, for example, metal transducer elements, which, when a mechanical load is applied to them, change their length and cross-sectional area. This in turn leads to a change in resistance. Some strain gauge materials, such as semiconductor materials, exhibit a piezoelectric effect in which a load applied to the material causes a large change in its resistivity. Strain gauges of this type have two orders of magnitude greater sensitivity than the previously discussed metallic ones.

In general, any parameter that tracks motion or force can be used to create strain gauge transducers.

**Wire strain gauges** (fig. 2.1) are produced in the form of conductors rigidly connected with paper or film base 2. Conductor 3 is a zigzag thin wire of 0.02-0.05 mm diameter, to the ends of which leads (copper conductors 4) are connected by soldering or welding. Conductors are covered with paper, film or varnish 1. After gluing the strain gauge substrate to the deformable surface under study, the deformation of this surface is transmitted to the conductors and leads to a change in their resistance.

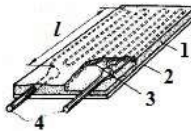


Fig. 2.1. Design of a wire strain gauge resistor.

*Source: built by the author based on [15].*

The resistance  $R$  of the resistor made in the form of a wire of length  $l$  is determined by the above expression (2.1).

The strain effect is characterized by the output signal associated with the relative change in the resistance of the resistor  $\Delta R/R$ . The ratio of the relative change of the output signal to the relative deformation  $\varepsilon$  that caused it at fixed values of current, temperature, etc., is called the strain-sensitivity coefficient of the strain gauge.

$$k = \Delta R/R\varepsilon \quad (2.2).$$

The ratio  $\Delta R/R$  is determined (mathematically it can be obtained by differentiating (2.1)) by  $\Delta R/R = \Delta\rho/\rho + \Delta l/l - \Delta S/S$ , where  $\Delta R$ ,  $\Delta\rho$ ,  $\Delta l$ ,  $\Delta S$  - changes in resistance, resistivity, length and cross resistance area of the conductor, respectively.

In the field of elastic deformations, using the theory for solid bodies, we can obtain an expression for the strain sensitivity coefficient in the form of:

$$k = 1 + 2\mu + \nu \quad (2.3).$$

For conductors, the components  $\mu$  (Poisson's ratio) and  $\nu$  (elastoresistance coefficient) do not differ much in magnitude. For semiconductors, the value of  $\nu$  can be two orders of magnitude larger than  $\mu$  and depends on temperature, strain, and crystallographic direction. Therefore, semiconductor strain gauges have much higher strain sensitivity, but are also more susceptible to external influences.

The quality of strain gauges is determined by their strain sensitivity coefficients  $k$  and the value of the temperature coefficient of resistance (TCR) -  $\Delta R/RA\Delta T$ . The higher the strain sensitivity coefficient  $k$  and the lower the temperature coefficient of resistance (TCR) of the material from which the strain gauge is made, the higher its quality.

For example, for wire strain gauges made of constantan and manganin alloys  $k \approx 2$ , TCR =  $30 \cdot 10^{-6} \text{ K}^{-1}$  and  $10 \cdot 10^{-6} \text{ K}^{-1}$ , respectively. For semiconductor strain gauges  $k$  reaches the value of 100 and more (e.g., silicon).

In foil strain gauges, the sensitive element is made of foil with a thickness of 3-6 microns. The main advantages of foil strain gauges are the possibility of forming strain gauges of any shape and effective heat dissipation during measurements, which allows to obtain a higher output signal. Foil strain gauges are insensitive to transverse deformations and can be produced in sizes from 0.3 mm.

One of the main metrological characteristics of strain gauges include strain sensitivity, creep, mechanical hysteresis, temperature instability.

Strain sensitivity is determined mainly by the strain-resistive properties of the material of the sensing element. Strain sensitivity is the main parameter by which the value of the measured strain is determined:

$$\varepsilon = \Delta R/Rk \quad (2.4).$$

Creep manifests itself as a change in the output signal at a given and unchanged value of  $\varepsilon$ . Creep is mainly caused by elastic imperfections in the substrate and adhesive.

Mechanical hysteresis, like creep, is caused by the elastic imperfection of the substrate and adhesive and is numerically determined through the difference in output resistance values for the same strain value, provided that the given strain value is achieved with its smooth increase and smooth decrease.

Temperature instability, consists in the change of resistance of the strain gauge due to its TCR, and also due to the appearance of additional mechanical stresses due to the difference in the temperature coefficients of linear expansion of the material of the strain gauge and the part under study.

An important parameter of strain gauges is the permissible power that can be dissipated in the strain gauge, provided that its overheating does not exceed the permissible value. The allowable power of a strain gauge is dependent on its geometric dimensions.

## 2.2. Foil strain gauges

In foil strain gauges the sensitive element is made of foil with thickness of 3...6 microns.

The thickness of foil strain gauges is less than wire strain gauges and is 30...50 microns. The main advantages of foil strain gauges are the possibility of forming strain gauges of any shape and effective heat dissipation during measurements, which allows to obtain a higher output signal at the same deformations. Foil strain gauges are insensitive to transverse deformations and allow for small-base designs starting from 0.3 mm and up.

Foil strain gauges are usually made of constantan foil. Electromechanical properties of foil are less constant within one batch compared to constantanum strain gauge wire. Its heat treatment is less effective, so the operating range of foil strain gauges does not exceed  $\pm(3-5)10^{-3}$  relative strains ( $\pm 3000...5000$  URD, where  $1\text{URD} = 1\text{m}\ln^{-1} = 10^{-6}$  - a unit of relative deformation)), and the temperature range is 75...575 K. The technology of fabrication of foil strain gauges, as a rule, is based on the use of photochemical processes. The technology is most adapted for mass production. Depending on the shape of tensor gratings, foil strain gauges are divided into the following typical modifications (fig. 2.2):

- single-element rectangular for linear measurements;
- two- or three-element rectangular or rosette strain gauges for measurements in areas with flat stress state;
- special ones used as strain gauges in membrane sensing elements;

- etc.

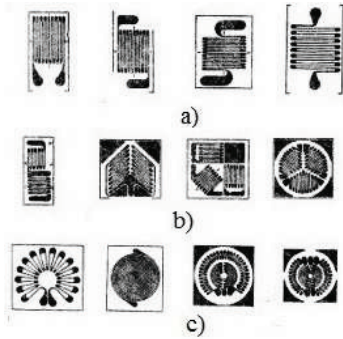


Figure 2.2. Shapes of some tensor lattices of foil strain gauges.

a - single-element rectangular; b - multi-element rectangular and rosette; c - membrane.

Source: built by the author based on [15].

### 2.3. Measurement of mechanical stresses by vibrating string. Tenzometer

This method of measuring mechanical stresses (strains, elongations) uses as a sensing element a steel string stretched between two clamps fixed in the structure whose deformations are being studied. A change in the mechanical tension of the string leads to a change  $v$  in the frequency of its oscillation, and the measurement of  $\Delta v$  makes it possible to determine the deformations. One of the advantages of the method under consideration is a long service life of the sensor (transducer, strain gauge), reliability, weak susceptibility to external external influences (humidity, radiation, etc.). These advantages are provided by the strength of the string and the construction of the strain gauge. In this method, the carrier of information is the frequency of the output signal, which creates additional advantages in terms of resistance to interference in the form of noise, interference, influences of transmission lines. In addition, such a signal can be easily converted into digital form.

The fundamental frequency  $v$  of mechanical vibrations of a strain gauge string stretched between two points at a distance  $l$  and subjected to a force  $F$  is expressed by the formula

$$v = \frac{1}{2l} \sqrt{\frac{F}{S\rho}} \quad (2.5),$$

where  $S$  is the cross-sectional area of the string,  $\rho$  is its density.

Under the influence of mechanical stress  $F/S$ , the string of the tensometer experiences elongation  $\Delta l$ . Analyzing the stress-strain state of the string, we can

obtain an expression for the relative elongation (relative strain) through the change in frequency:

$$\Delta l/l = (4l^2\rho/E)(v_l^2 - v_0^2) \quad (2.6),$$

where  $E$  is the Young's modulus. Knowing  $v_0$  (initial frequency) and measuring  $v_l$  (frequency after deformation of the structure), it is thus possible to determine the deformation of the structure.

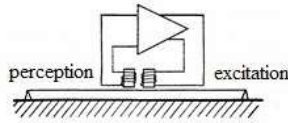


Fig. 2.3 Strain gauge with a vibrating string.  
*Source: built by the author based on [25].*

Fig. 2.3 shows a strain gauge (scheme) with a vibrating string. The steel string vibrates with frequency  $\nu$  in front of the signal coil, causing periodic oscillations of the magnetic resistance of its magnetic circuit, which generates an electrical signal of the same frequency  $\nu$ . This signal is amplified and transmitted to the excitation coil, which maintains the vibration. The frequency  $\nu$  can be measured using a frequency meter. The characteristics of this type of strain gauges can be found in the literature. For example, a strain gauge manufactured by “Telemac” has the following characteristics: maximum frequency  $\sim 1200$  Hz, minimum frequency  $\sim 400$  Hz, measurement range  $4000\mu\text{m/m}$ , resolution  $1\mu\text{m/m}$ , accuracy 1 to 2% of the measurement range.

The described type of elongation meter (strain gauge) is used for control of mechanical deformations and stresses in construction (dams, bridges, tunnels, etc.), in weight measurement, etc.

#### 2.4. Adhesives, binders for mounting of strain gauges

Adhesives, binders used for mounting of strain gauges on the surface under investigation should meet the following basic requirements:

A) Ensure the transfer of deformation of the surface under study to the strain gauge and the least possible creep of readings in the operating range of temperatures and strains. Creep is due to the plasticity of the adhesive.

B) Ensure electrical isolation of the strain gauge from the surface under test

As a rule, suppliers of strain gauges provide in their documentation a list of adhesives with optimal characteristics for this type of strain gauges and a description of the technology of their application.

The adhesives most often used in strain gauging are briefly described below.

For foil strain gauges:

Cyacrine EO adhesive. These are cold-setting, quick-setting adhesives. They are used for bonding non-porous materials and metals. They harden within 48 hours without compression forces. Operating temperature range  $-80 - +80$  °C.

Glue UVS-10T. Hot curing, one-component. Connects non-metallic non-porous materials and metals. Operating temperature range  $-70 - +200$  °C. Polymerization (curing) of the adhesive is carried out as follows: glued strain gauges should be kept for 0.5 hours under normal conditions. Then to keep 5 hours at temperature  $180$  °C with pressing pressure  $0,1 - 0,3$  MPa ( $1 - 3$  atm) in the conditions of the thermo-closet. Then cure for 5 hours at  $215$  °C under open curing conditions.

BFR-2K glue. Refers to one-component hot-set adhesives, phenol-formaldehyde. Polymerization conditions, technology of use are similar to UVS-10T glue.

## 2.5. Attestation, calibration, verification of strain gauges

For attestation, calibration (determination of calibration characteristics) of strain gauges, reference elastic elements (beams) are used. The beam, as a rule, has dimensions (shape) that provide equal resistance to bending (fig. 2.4.a) or has a constant cross-section (fig. 2.4.b). The beam has a section (working area, shaded in the figure) within which the deformation is practically constant.

The value of deformation of the beam surface of equal resistance is determined by the formula:

$$\varepsilon = \frac{6PL}{EB(h+\Delta h)^2} \quad (2.7),$$

where:  $P$  is the value of loading force (load),  $H$ ,  $L$  is the distance from the beam attachment line to the point of force application,  $E$  is the modulus of elasticity of the beam material,  $B$  is the beam width at the attachment point,  $h$  is the beam thickness,  $\Delta h$  is the distance from the beam surface to the middle of the strain gauge thickness.

The magnitude of deformation of the beam surface of constant section is calculated through the deflection  $f$  by the formula:

$$\varepsilon = \frac{4(h+2\Delta h)f}{l^2+4f^2+4fh} \quad (2.8),$$

where:  $h$  - thickness of the beam,  $\Delta h$  - distance from the beam surface to the middle of the strain gauge thickness,  $l$  - base of the device with the help of which the deflection is determined,  $f$  - deflection boom at the base  $l$ .

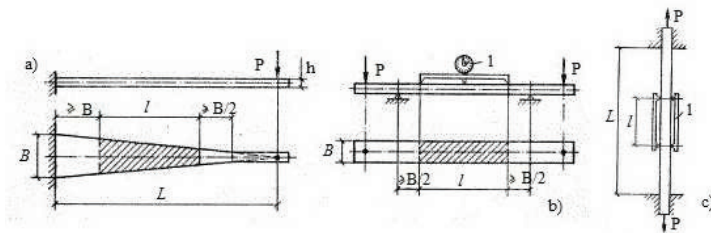


Fig. 2.4. Reference elastic elements: a - of equal resistance to bending, b - of constant cross-section, c - beam working in tension. 1- device for measuring the actual deformation.

Source: built by the author based on [15].

Beams working in tension (fig. 2.4.c) can also be used for calibration. In this case, direct measurement of the strain value in the working area is used. The disadvantage of this method is the difficulty of creating a stable axial loading.

## 2.6. Measurement of mechanical deformations (stresses) with the help of strain gauge

As noted above, a strain gauge is a device whose electrical resistance changes when it is deformed. This change in resistance is related to the magnitude of mechanical strain  $\epsilon$  through the strain sensitivity coefficient (see 2.2).

Currently, the most widely used for measuring mechanical deformations are foil (foil material is metal) strain gauges and for solving certain problems semiconductor strain gauges. Advantages and disadvantages of both types of strain gauges are well presented in the literature. The main advantage of semiconductor strain gauges is their higher (up to 100 times) strain sensitivity, but at the same time they are more fragile, rigid, higher temperature dependence of parameters. High strain sensitivity of semiconductor strain gauges is explained by changes in the zone structure of semiconductor material under the influence of mechanical stresses and, accordingly, a strong dependence of conductivity (resistance) on deformation. While in metallic strain gauges strain sensitivity is provided by changes in the size of the sensitive element (foil).

Foil strain gauges are differentiated by their purpose - for measuring uniaxial strains, distributed strains, for different temperature ranges, by the size and shape of the lattice (shape of electrically conductive foil), by the values of electrical resistance, as well as some other parameters.

One of the simplest foil strain gauge is shown in fig. 2.5. The design of the strain gauge is such that it reacts (changes its resistance) practically only when the

strain is directed (applied) along the axis of the strain gauge lattice or there is a component of complex-distributed strain in this direction (this is called "longitudinal strain sensitivity").

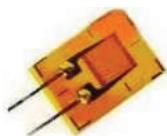


Fig. 2.5. Typical foil strain gauge.

*Source: built by the author.*

Moreover, the change in resistance is proportional to the magnitude of the longitudinal (or component of the complex) strain and is related to its magnitude through the coefficient  $k$ . It should be noted that there is also transverse strain sensitivity, i.e. sensitivity to strain directed perpendicular to the base (longitudinal axis) of the strain gauge, but it is insignificant, as a rule, for foil strain gauges is close to zero, and for wire strain gauges does not exceed 1% of the longitudinal.

The main reason for the change in the resistance of the foil strain gauge under the influence of deformation is the change in the size of the electrically conductive lattice. As it is known electrical resistance of materials is determined by the dependence (2.1). Under tensile strain the resistance will increase, under compression it will decrease. In the process of using strain gauges, this is taken into account to determine the sign of deformation of the object.

For foil strain gauges, the strain sensitivity coefficient depends on the foil material. Its value is in the range  $k = 2-4$  and is indicated in the passports and descriptions attached to the batch of strain gauges. The value of electrical resistance, as a rule, is from 50 Ohm.

To measure the magnitude of deformation of the object under study, the strain gauge is mounted (glued) at the point of the object in which it is necessary to measure the deformation. In order to measure the deformation of the object as accurately as possible, it is necessary to ensure that the deformation is transferred from the object to the strain gauge array almost without losses. This is achieved by selecting the appropriate binder (adhesive) and mounting technology. The main requirement for the binder is the absence of plastic deformation in the operating range of the strain gauge. Optimal binder and technology of work with it are specified in the technical descriptions to the batches of strain gauges. Very often glues of BF-2 type are used as a binder.

The resistance indicated in the data sheet and measured after mounting the strain gauge on the object may slightly differ - in the process of polymerization of the

binder, deformations of the strain gauge lattice may occur. It is necessary to take this into account during precise measurements.

Further, after mounting the strain gauge on the object during mechanical testing of the object, the electrical resistance of the strain gauge is measured. If, for example, the strain gauge sensitivity coefficient  $k = 2$ , the initial resistance (specified in the passport or measured after mounting the strain gauge on the object)  $R_o = 200.1$  Ohm, and during mechanical loading of the object  $R_e = 200.9$  Ohm, then the amount of mechanical deformation (in this case, stretching) at the mounting point of the strain gauge and in the direction of its base is equal:

$$\varepsilon = \Delta R/kR_o = (R_e - R_o)/kR_o = 0,002 = 2 \cdot 10^3 \text{ mln}^{-1} = 2 \cdot 10^3 \text{ URD.}$$

I.e. the value of relative strain is equal to 0.002. Relative strain values are sometimes expressed in URD - unit of relative strain, which is equal to  $1/1000000$  (one millionth part -  $\text{mln}^{-1}$ ) of the strain unit.

In practice, special equipment is used to measure deformations in order to automate measurements, measurement technologies are more complex to achieve maximum accuracy, calculation of errors according to certain methods, etc.

If it is necessary to determine the mechanical stresses of the object at the point of strain measurement, the known relationship between mechanical strain  $\varepsilon$  and mechanical stresses  $\sigma$  is used:

$$\sigma = \varepsilon E \quad (2.9),$$

where  $E$  is Young's modulus (elasticity) of the object material.

The technique and sequence of measuring mechanical strains with a semiconductor strain gauge is basically the same as described above for a foil strain gauge.

## 2.7. Hydroprotective strain gauge materials

Waterproofing of strain gauges after their installation at the measuring object is carried out, as a rule, in all cases when the humidity of the environment can increase above 50%.

The most widespread is the method of relative waterproofing, which consists in applying hydrophobic compositions and sealants to the places of installation of strain gauges. Usually such compositions have a good adhesion to the base of strain gauges and the surface under study, so that, as well as adhesives, after curing make one whole with the strain gauge.

Hydrophobic compositions and sealants must not deform as a result of shrinkage or changes in the environmental conditions and must not visibly reinforce the measurement sites and must retain the ability to elastoplastic deformation. They shall also not chemically attack the materials of strain gauges and patch wires.

The waterproof coatings used for strain measurement purposes are subdivided into:

- film coatings applied in several layers with a total thickness of 50... 100 microns;
- soft sealants with modulus of elasticity up to 100 MPa, usually applied in one layer with thickness of 2...3 mm.
- hard with modulus of elasticity more than 100 MPa, applied in one or several layers with total thickness from 0.5 to 2...3 mm.

Thin film coatings are made of adhesive solutions such as BF-2 and others. Soft waterproof coatings are made of technical vaseline, paraffin-vaseline mixtures, wax greases and lubricants, as well as sculptural plasticine.

Wax grease mixtures and greases or compounds include, in addition to beeswax, a number of plasticizing and sealing components, since wax has insufficient adhesion and is prone to cracking at subzero temperatures.

Solid waterproof coatings are made of polymer and bituminous compounds. For example, carbinol-cement and epoxy, epoxy putties and others.

Epoxy compounds and putties are prepared on epoxy resins ED-5 and ED-6 with the addition of hardeners. Plasticizers are added to the compound to reduce stiffness. Epoxy compounds are characterized by low coefficient of moisture absorption (less than 0,05% in 24 hours); good adhesion to most materials and sufficient resistance to aggressive media. Their disadvantages include brittleness, tendency to cracking and disruption of adhesive bonds on the contact surface during deformation, as well as toxicity.

## **2.8. Mounting of general purpose strain gauges**

Mounting of strain gauges, depending on their type and test conditions, is performed by sticking or welding to the surface under test, as well as by embedding inside the elements under test made of adhesive materials, e.g. fiberglass plastics.

Gluing of general-purpose strain gauges intended for strain measurements up to  $\pm 1$  % in the climatic temperature range is done in most cases with cold-curing adhesives of nitrocellulose and cyanoacrylate groups. Gluing of thermocompensated strain gauges used in the range of 175...475 K is carried out with thermosetting adhesives of phenolic, viniflex and furan groups depending on the material of the measuring object and the operating temperature range. When mounting high-temperature strain gauges operating at temperatures 525...575 K, organosilicon binders are used.

The technology of gluing with adhesives of all listed groups, except for express adhesives of cyanoacrylate group, is reduced to the following operations:

- immediately before gluing the strain gauge mounting locations are cleaned from dust and wiped with a swab moistened with ethyl alcohol or ether to remove water condensation;

- a thin layer of glue is applied to the prepared areas of the measurement object by brush; at the same time the same layer is applied to the contact surface of the strain gauge base and dried for 10-15 min;

- the second, thicker layer of glue is applied to the strain gauge and kept for 2-3 minutes until it thickens;

- the strain gauge is oriented according to the marking marks in the place of installation and pressed firmly to the surface;

- fluoroplastic or triacetate film is placed over the strain gauge, after which excess glue is removed with a finger or rubber roller;

- the glued strain gauge is kept for 1-2 hours under pressure (load) at the rate of about 0.2...0.3 MPa;

- after the pressure is removed, the strain gauge is freed from the film and dried until the excess solvent is completely removed, usually within 1-2 days. An objective sign of drying completion is stabilization of its insulation resistance relative to the surface under test (for conductive materials);

- in case if gluing of strain gauges is made with thermosetting adhesive, after drying normal heat treatment is performed according to the recommended mode for this adhesive; during the heat treatment period strain gauges should be under pressure up to 0,3...0,5 MPa;

- after drying or polymerization of glued strain gauges check the quality of gluing and the correct position of strain gauges relative to the marking marks; also check the straightness of the threads of the grid, the presence of an electrical circuit, resistance and insulation level of strain gauges relative to the surface under test.

Gluing of strain gauges with cyanoacrylate express adhesive cyacrin-30 can be performed after preliminary priming of the paper base with some strain gauge adhesive followed by drying or polymerization. Strain gauges with a film base do not require pre-priming. The polyethylene ampoule with glue is taken out of the refrigerator and kept at a temperature of  $295 \pm 10$  K for  $15 \pm 20$  min. Then a hole with a diameter of about 0,3 mm is pierced in the ampoule and a thin layer of glue is applied to the contact surface of the strain gauge base. Immediately after applying the glue the strain gauge is placed as accurately as possible on the marked place and kept under pressure for 1 min. Subsequent drying is carried out at normal temperature and humidity 50...80% for 6 hours.

In all cases it is necessary to use instructional materials with a detailed description of the technology of gluing with a particular mounting adhesive. General technological requirements for gluing of strain gauges are given in the descriptions.

At the same time with gluing of strain gauges install and glue mounting pads made of insulating material with terminated conductors for soldering of strain gauges and patch wires. The pads are glued close to the transverse edge of the strain gauge base from the side of the lead wires. Mounting pads protect strain gauges from breaks during mounting and eliminate the possibility of short circuits during measurements.

Insulation level of glued strain gauges should not be lower than 50...100 Mohm if measurements are performed under normal conditions and expected deformations do not exceed 1%.

## 2.9. Semiconductor strain gauges

The main materials for semiconductor strain gauges are currently silicon and germanium, with silicon being more widely used due to its lower sensitivity to temperature. Semiconductor compounds such as gallium arsenide GaAs and others are also used.

Depending on the materials used, semiconductor strain gauges can be divided into two groups: monocrystalline and polycrystalline. Monocrystalline strain gauges include strain gauges obtained by cutting from a single crystal; needle crystals obtained by growing from the gas phase; epitaxial films and dendrites. Polycrystalline ones include tensolites, which are artificial mixtures of, for example, carbon (or carbon black) and bakelite varnish.

Materials for semiconductor strain gauges should have the highest possible strain sensitivity coefficient (SSC) and the lowest temperature coefficient of resistance (TCR), as well as ensure the stability of strain gauge parameters.

A very important operation in the manufacture of semiconductor strain gauges is the creation of metal-semiconductor contact, which is obtained by various methods: soldering, fusion, welding, sputtering, electrochemical or chemical coating.

Of certain interest are semiconductor strain gauges made of dendritic ribbon of germanium, which have become widespread due to simple and affordable manufacturing technology. Dendrites are tree-shaped, needle-shaped or lamellar crystals of complex twin structure formed by crystallization in supercooled melt or from supersaturated gas phase.

Dendritic strain germanium strain gauges are characterized by reduced mechanical strength compared to strain gauges made of single-crystal ingot. The advantages of dendritic strain gauges include simplicity of manufacture and relative cheapness (compared to other semiconductor strain gauges, dendritic strain gauges are the cheapest). Manufacturing of germanium dendritic strain gauge does not require special equipment (for example, machines for grinding and cutting) and is reduced to cross-cutting dendritic ribbon corundum needle, breaking off the strain

gauge and soldering to it electrical leads with special solder. For manufacturing of strain gauges germanium dendritic ribbon is used mainly with specific resistance  $\rho=1\pm 0,2 \text{ ohm} \cdot \text{cm}$ . Parameters of such strain gauges strongly depend on temperature.

Semiconductor strain gauges can be divided into bonded and unbonded semiconductor strain gauges by design. Bonded semiconductor strain gauges can be used with or without a substrate.

Semiconductor strain gauges without a substrate differ in cross-sectional shape, material, and method of making ohmic contact. Their design is largely determined by the manufacturing technology. The most common type of strain gauge is a bar.

Strain gauges obtained by growing from the gas phase are monocrystalline needles with a diameter of 10 - 100 microns. The design of such a strain gauge with a substrate is shown in fig. 2.6.a. The construction of a film strain gauge is shown in fig. 2.6.b; the strain gauges are made in the form of a single conductive strip, which is covered with a layer of varnish. Parameters of some semiconductor strain gauges are given in table 2.1.

The main application of semiconductor strain gauges is in pressure, force and stress sensors. The application of semiconductor strain gauges in accelerometers is promising.

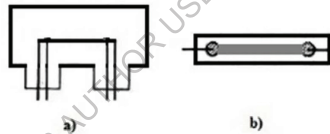


Fig. 2.6. Designs of some semiconductor strain gauges: a - needle crystal strain gauge with substrate, b - film strain gauge.

Source: built by the author.

Table 2.1. Specifications of some semiconductor strain gauges.

Source: built by the author based on [15,1,3].

Parameter	Strain gauge type				
	p-Si	p-Si	n-Si	n-Ge (dendrite)	n-Ge
$\rho, \text{ Ohm} \cdot \text{cm}$	0,017	0,02	0,35	0,25	0,8
Dimensions, mm					
length	12,7; 4,4	5	5	10	3,5
thickness	0,017	0,03-0,05	0,1	0,15-0,22	0,5
width	0,5	0,3	0,8	0,7-2,0	0,2
Nominal resistance at 20 °C	350;120	100-200	150-400	50-200	350
Strain sensitivity coefficient at 20 °C	130	135	-133	-100	-
Operating current, mA	20;35	20-40	10-20	20-35	5
Maximum operating temperature, °C	+300	+500	-	+150	-

## 2.10. Piezoresistive effect in semiconductors and strain gauge based on it

Using the methods of mathematical analysis, we will consider the physics of the piezoresistive effect in solid materials. We will focus on semiconductors such as Si in bulk and in the form of silicon films on insulating substrates. We will consider the practical use of the effect to create measuring transducers of mechanical deformations - strain gauges. Examples of sensor designs and their main characteristics and capabilities are given. We analyze the advantages and disadvantages of semiconductor strain gauges.

The results of experimental studies are presented here for ion-implanted silicon films on semi-insulating silicon substrates with a  $\text{SiO}_2$  layer on the surface. Most of the results obtained can be used in the development of strain gauges based on other semiconductors.

It is known that the electrophysical properties of semiconductors are 10-100 times more sensitive to mechanical stress than those of metals. At the same time, a number of reasons prevent the widespread practical use of semiconductor materials in strain measurement. The main ones are the temperature dependence of the electrophysical parameters of such strain gauges (measuring transducers), low mechanical strength and stiffness, which leads to creep in the readings, and significant transverse strain sensitivity.

The development of science and technology is impossible without improving the means of monitoring various physical parameters. This also applies to strain gauging, which is now required under such conditions as cryogenic temperatures, strong magnetic fields, radiation exposure, etc.

As you know, the piezoresistive effect is a change in the electrical resistance of a material under mechanical stress. It is known that the change in electrical resistance in this case occurs for two reasons - due to changes in geometric dimensions and due to changes in the mobility of charge carriers and, accordingly, the conductivity of the material. The first reason relates to metals, where the mobility of current carriers under mechanical impact practically does not change, and the resistance changes due to changes in size during deformation - fig. 2.7.

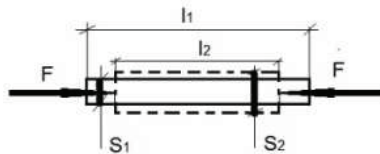


Fig. 2.7. Change in the dimensions  $l$  - length,  $S$  - cross-sectional area of the sample under mechanical action on it by a force  $F$ .

*Source: built by the author.*

The electrical resistance  $R$  of the material is determined by the above expression (2.1):

$$R = \rho l/S,$$

where  $\rho$  is the resistivity,  $l$  is the length of the sample, and  $S$  is the cross-sectional area.

As can be understood from fig. 2.7 and expression (2.1), the electrical resistance of the sample will decrease under compression due to a decrease in length  $\Delta l = l_1 - l_2$  and an increase in cross-sectional area  $\Delta S = S_2 - S_1$ , and increase under tension.

In semiconductors with a cubic lattice, for the general case when the direction of mechanical stress  $\sigma$  and current density  $j$  are arbitrary angles, the piezoresistive effect is theoretically described by piezoresistive  $\pi_{ij}$  ( $\pi = \Delta\rho/\rho_o X$ , where  $\Delta\rho$  is the change in resistivity,  $\rho_o$  is the initial resistivity,  $X$  is the mechanical stress) or elastoresistive  $m_{ij}$  coefficients, which are fourth-rank tensors. These coefficients are related to each other through the coefficients of malleability and elastic moduli. For crystals of the symmetry class to which silicon belongs, it is sufficient to know three coefficients in the crystallographic axis system to describe the piezoresistive effect:  $\pi_{11}$ ,  $\pi_{12}$ , and  $\pi_{44}$ , which are sometimes called the main piezoresistive coefficients. The principal piezoresistive coefficients depend on many factors: material, type of conductivity, resistivity, doping level, temperature, and the amount of mechanical deformation (stress).

For example, various combinations of piezoresistance coefficients are known in the literature for mechanical stress and current density directions that coincide with certain crystallographic axes. All three main piezoresistance coefficients can be determined by three measurements in different directions. The full piezoresistance tensor  $\pi_{ijkl}$  is defined as follows:

$$\frac{\Delta\rho_{ij}}{\rho_o} = \sum_{kl}^3 \pi_{ijkl} \sigma_{kl} \quad (2.10),$$

where  $\sigma_{kl}$  is the stress tensor,  $\Delta\rho_{ij}$  is the resistivity tensor. It is known that the stress tensor is a symmetric tensor and has six independent components. The same is true for the resistivity tensor.

With this in mind, in six-dimensional space, we can obtain:

$$\frac{\Delta\rho_{ij}}{\rho_o} = \sum_{j=1}^6 \pi_{ij} \sigma_{,i=1,2,\dots,6} \quad (2.11).$$

For bulk  $n$ -Si with uniform doping and  $\rho = 11.7$  Ohm-cm, the following values are given in scientific papers:  $\pi_{11} = -102.2 \cdot 10^{-11}$  m<sup>2</sup>/N,  $\pi_{12} = 53.7 \cdot 10^{-11}$  m<sup>2</sup>/N,  $\pi_{44} = -13.6 \cdot 10^{-11}$  m<sup>2</sup>/N, and for  $p$ -Si with  $\rho = 7.8$  Ohm-cm,  $\pi_{11} = 6.6 \cdot 10^{-11}$  m<sup>2</sup>/N,  $\pi_{12} = -1.1 \cdot 10^{-11}$  m<sup>2</sup>/N,  $\pi_{44} = 138.1 \cdot 10^{-11}$  m<sup>2</sup>/N.

In silicon layers with diffusion doping, the piezoresistive coefficients are determined by the concentration of the impurity on the surface of the layer  $N_n$  and almost do not depend on the law of impurity distribution. From the results obtained in various works, it is clear that for n-Si layers, the coefficient  $\pi_{11}$  at room temperature varies from  $17 \cdot 10^{-11} \text{ m}^2/\text{N}$  ( $N_n = 1 \cdot 10^{21} \text{ cm}^{-3}$ ) to  $88 \cdot 10^{-11} \text{ m}^2/\text{N}$  ( $N_n = 1.8 \cdot 10^{18} \text{ cm}^{-3}$ ). A noticeable temperature dependence of  $\pi_{11}$  begins with  $N_n = 9 \cdot 10^{19} \text{ cm}^{-3}$  (approximately 0.1 %/K).

Due to the peculiarities of the n-Si band structure, the assumptions for low-doped silicon are valid:

$$\pi_{44} \approx 0; \pi_{11} \approx -2 \pi_{12} .$$

As the impurity concentration increases, a violation of these assumptions occurs, which must be taken into account when analyzing the characteristics of the strain effects. For diffusion layers, violations occur at  $N_n \geq 5 \cdot 10^{19} \text{ cm}^{-3}$ .

Depending on the crystallographic orientation of the silicon sample, different combinations of longitudinal and transverse piezoresistance coefficients are obtained. This is important to take into account when designing strain gauges, especially those whose sensitive element will operate under uniaxial deformation and whose components of the sensitive element will be oriented in both the longitudinal and transverse directions. Using the literature data, it can be calculated that for low-alloyed p-Si, the optimal ratios of longitudinal and transverse orientations are  $110 \perp 110$ , and for n-Si  $100 \perp 010$ . For samples of weakly alloyed p-Si with a longitudinal orientation  $\langle 110 \rangle$ , for example, we can obtain  $\pi_{\parallel} \approx 72 \cdot 10^{-11} \text{ m}^2/\text{N}$ , and  $\pi_{\perp} \approx -65 \cdot 10^{-11} \text{ m}^2/\text{N}$  ( $\pi_{\parallel}$  is the longitudinal piezoresistance coefficient,  $\pi_{\perp}$  is the transverse piezoresistance coefficient).

Analyzing the data known in the literature, it can be observed that the relations valid for pure p-silicon are violated for p-Si in a heavily alloyed material. At the same time, the strain sensitivity for certain directions can increase compared to pure silicon, which can be explained by an increase in the contribution of heavy holes.

Other factors are known that significantly determine the characteristics of the strain gauge. For example, the influence of its geometric dimensions on the strain gauge parameters is significant. Some studies have shown that not all of the deformation is transmitted from the deformed object under study to the strain gauge sensing element, even with a rigid binder. The transmitted deformation depends on the size of the strain gauge, its elastic properties, and the properties of the binder with which the sensor is attached to the beam. This effect can be accounted for by the transmission coefficient, the value of which (for the case when the strain gauge is located in the center of the sample) can be determined by the formula:

$$k_{\text{trp}} = 1 - \frac{2}{bl} \left( 1 - e^{-bl/2} \right) \quad (2.12),$$

where ,  $b = \sqrt{GC/EQ}$  ,  $G$  is the shear modulus of the binder,  $E$  is the elastic modulus of the sensitive element (sample),  $Q$  is the cross-sectional area of the sample,  $C = \frac{2\pi}{\ln^4 h_c/h}$ ,  $h$  is the thickness of the sample,  $h_c$  is the thickness of the binder,  $l$  is the length of the sample.

For the study and development of measuring transducers, thin polycrystalline silicon films doped with phosphorus and boron by ion implantation were used on the plane (100) of single crystalline silicon with an insulating layer of SiO<sub>2</sub>. Such structures can be more technologically advanced when using planar technologies for manufacturing measuring transducers.

The resistivity  $\rho$ , the coefficients of longitudinal  $k_{||} = \Delta\rho_{||}/\rho_{||}\cdot\varepsilon_{||}$  (where  $\Delta\rho_{||}$  is the change in resistivity along the direction of deformation  $\varepsilon_{||}$ ), and transverse  $k_{\perp} = \Delta\rho_{\perp}/\rho_{\perp}\cdot\varepsilon_{||}$  (where  $\Delta\rho_{\perp}$  is the change in resistivity perpendicular to the direction of deformation  $\varepsilon_{||}$ ) strain sensitivity were experimentally measured, piezoresistance coefficients  $\pi_{||} = (\pi_{11} + \pi_{12} + \pi_{44})/2$  and  $\pi_{\perp} = (\pi_{11} + \pi_{12} - \pi_{44})/2$ , temperature and strain dependence of the parameters of the experimental transducers.

The piezoresistance coefficients were measured using a cantilevered steel beam of equal bending resistance, on which the sample was glued with BF-2 adhesive, and by directly loading the samples. By comparing the results obtained, it is possible to calculate the value of the strain transfer coefficient and assess how it coincides with the one calculated theoretically using formula (2.12). The films used are of the n-type on a (100) silicon plane. The thickness of the films is 0.6  $\mu\text{m}$ , the concentration of the alloying phosphorus impurity is  $5 \cdot 10^{18} \text{ cm}^{-3}$ . The resistivity is 0.013 ohm·cm. The measurements were performed on samples (strain gauges) with dimensions of  $8 \times 0.6 \times 0.4 \text{ mm}$  with a film on the surface.

When measuring with a beam and using the strain value calculated using the well-known formula  $\varepsilon_b = h\delta/l_b^2$  (where  $h$  is the thickness of the beam,  $l_b$  is the length of the beam,  $\delta$  is the displacement of the free end of the beam), the values of the strain sensitivity coefficients  ${}^b k_{||} (\varepsilon_{||} \langle 110 \rangle ; J_{||} \langle 110 \rangle)$   ${}^b k_{\perp} (\varepsilon_{||} \langle 110 \rangle ; J_{\perp} \langle 110 \rangle)$  -27,3 and -2.8, respectively.

When measuring the strain sensitivity by the direct loading method, the sample was cantilevered and a bending load was applied. The measurement error of the coefficients by this method did not exceed 4%. The following values were obtained at room temperature:  $\pi_{||} = -24.9$  and  $\pi_{\perp} = -2.4$ . If we use the known elasticity coefficients for silicon and calculate  $k$ , we obtain  $k_{||} = -39.1$ ,  $k_{\perp} = -3.8$ . Comparing, we obtain the experimental transmission coefficient  $k_{tr}^e = 0.71$

For comparison, measurements were made using the direct load method. Substituting the parameters of the measurement conditions into formula (2.12) (for  $h_c$

= 0.15 mm), we obtain the theoretical  $k_{tr} = 0.68$ . Thus, the experimentally and theoretically determined strain transfer parameters practically coincide.

It was also found that in ion-implanted  $p$ -Si films with an impurity concentration of  $N_p = (10^{18}-10^{19}) \text{ cm}^{-3}$ , for example, the longitudinal and transverse strain sensitivity coefficients  $k$  ( $k = \Delta\rho/\rho_0\varepsilon$ ,  $\varepsilon$  is the relative mechanical strain) for the longitudinal orientation  $\langle 100 \rangle$  were close in value and were at least  $k = 30$ . This can be explained by the polycrystallinity of the film and the peculiarities of the band structure of  $p$ -silicon, which can determine the strain effect by light holes in a weakly alloyed material, while their contribution decreases in a strongly alloyed material.

The mechanism of strain transmission leads to the fact that, as established by the ratio of the sensor width  $d$  to the height  $h$   $d/h < 2$ , the transverse deformation of the object is practically not transmitted to its surface. This property is used for the manufacture of experimental strain gauges (measuring transducers).

For the fabrication of mechanical strain transducers, polysilicon films of  $n$  and  $p$ -type conductivity,  $0.6 \mu\text{m}$  thick and with doping levels  $(1 \cdot 10^{17} - 5 \cdot 10^{19}) \text{ cm}^{-3}$  were used. Basically, samples with  $p$ -type films of longitudinal orientation  $\langle 100 \rangle$  and transverse orientation  $\langle 010 \rangle$  were used in the experiment, since for highly doped polycrystalline  $p$ -silicon the transverse and longitudinal coefficients for this orientation are shown to be close in value. The alloying impurity for  $p$ -silicon was boron.

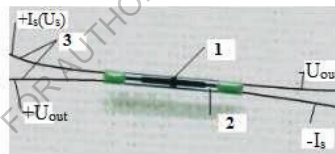


Fig. 2.8. Strain sensor. 1 - strain-sensitive microcircuit; 2 - substrate; 3 - electrical terminals;  $I_s(U_s)$  - supply current or voltage,  $U_{out}$  - output voltage.

*Source: built by the author based on [6].*

Fig. 2.8 shows an image of one type of strain (stress) transducer and the polarity of the power supply and measuring devices. It consists of an integral sensing element 1 made on the basis of a silicon film deposited on a single-crystal silicon substrate 2 with an oxide layer on the surface.

The electrical leads 3 are made of aluminum wire  $d=80 \mu\text{m}$ , the ends of which are equipped with strips of metal that can be soldered with conventional solder. The design and integral execution of the sensor sensing element provide thermal compensation of the main parameters, compensation for the influence of the magnetic field and the absence of transverse strain sensitivity. The size of the sensor base is 8 mm, the input  $R_{in}$  and output  $R_{out}$  electrical resistances depend on the level of doping

and film thickness and are in the range (200 - 3000) Ohm, the supply current depends on the resistance value and is usually in the range (1 - 10) mA. The difference in the electrical resistance of the sensors of one batch does not exceed 5%, and if necessary, a batch of sensors can be formed from almost identical technical characteristics.

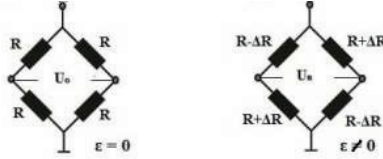


Fig. 2.9. Schematic diagram of the strain gauge sensing element.

Source: built by the author.

The principle of operation of the strain gauge is to change the electrical resistance of the resistive elements of the integrated circuit when a mechanical deformation is applied along the sensor axis (fig. 2.9), to compensate the circuit and, as a result, to generate an electrical voltage  $U_{out}$  on the measuring contacts when the sensor is powered by current or voltage (see fig. 2.9). After pre-programming the sensor, i.e., obtaining the dependence of the output voltage  $U_{out}$  on the value of mechanical deformation, the deformation of the object is determined by the value of the output voltage of the sensor rigidly fixed to the object:

$$\varepsilon = (U_{out} - U_o)/k \tag{2.13}$$

where  $U_{out}$  is the output signal of the sensor after the appearance of the deformation  $\varepsilon$  of the object under study,  $U_o$  is the initial output signal measured after mounting the sensor on the object,  $k = \Delta U_{out} / \Delta \varepsilon$  is the strain sensitivity of the sensor.

To mount the sensor on the test object, BF-2, BC-350 and other adhesives can be used, which are widely used in strain gauging and provide sufficient mounting rigidity. The permissibility of using this binder can be checked by the value of the sensor readings creep after loading the test beam, which should not exceed the permissible measurement error.

Below are the results of a more detailed study of the measuring transducers with  $R_{in} = 1.7 \text{ k}\Omega$  ( $N_p = 10^{18} \text{ cm}^{-3}$ ). The sensitivity at a supply current of 2 mA is approximately  $42 \text{ }\mu\text{V}/\text{mln}^{-1}$  ( $42 \text{ }\mu\text{V}/\text{URD}$ ). The value of the zero (initial) output signal of the sensor  $U_o$  is  $\sim 6.2 \text{ mV}$  and can be adjusted close to zero if necessary. The temperature dependence of the strain sensitivity is slightly more than  $0.02 \text{ \%}/\text{K}$ ,  $U_o \sim 8 \text{ }\mu\text{V}/\text{K}$ ,  $R \sim 0.03 \text{ \%}/\text{K}$ . The characteristics can be changed, for example, by increasing the supply current (without overheating and unacceptable noise), to increase the sensitivity.

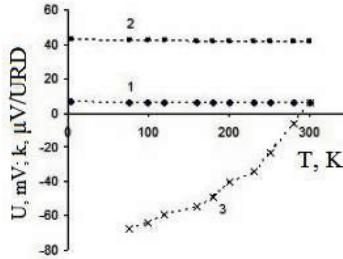


Fig. 2.10. Temperature dependences of the zero output signal (relative strain  $\varepsilon = 0$ ) (1), strain sensitivity  $k = \Delta U_{out} / \Delta \varepsilon$  (2) and the output signal of the sensor glued to a steel plate (3). Source: built by the author based on [6,27].

Fig. 2.10 shows the temperature dependence of the zero output signal (relative strain  $\varepsilon = 0$ ) (1), strain sensitivity  $k = \Delta U_v / \Delta \varepsilon$  (2), and the output signal of the sensor glued to the steel plate (3). The latter monitors thermal stresses.

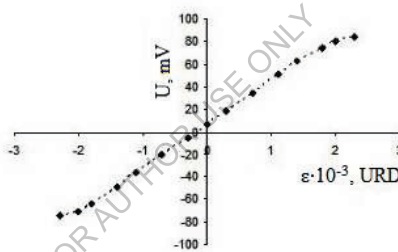


Fig. 2.11. Dependence of the output voltage  $U_{out}$  on the value of the applied strain. Source: built by the author based on [6,27].

Fig. 2.11 shows the dependence of the output voltage  $U_{out}$  on the value of the applied strain. The graph indicates good linearity of the characteristic up to deformations of approximately  $1 \cdot 10^3$  URD. The strain sensitivity of the investigated sensor, as can be seen from the graph, is equal to  $42 \mu\text{V}/\text{URD}$ .

If we consider the operation of a bridge-type strain gauge, in which one pair of resistors has one sign of the strain effect and the other has the opposite sign (provided that the resistances are equal), we can obtain the following expression for the voltage in the diagonal of the bridge:

$$U = I_o R_o [(k_{||} + k_{\perp}) / 2] \varepsilon \quad (2.14).$$

If  $|k_{||}| = |k_{\perp}| = k$ , then  $U = I_o R_o k \varepsilon$ ,

where  $k$  is the coefficient of the bridge arm (resistor) strain sensitivity,  $I_o$  is the supply current of the bridge circuit,  $R_o$  is the initial resistance of the circuit resistor.

That is, the output voltage at a constant supply current is linear in the region of linearity of the dependence of  $k(\varepsilon)$  of the strain gauge or the constancy of the value of  $k$ . The experimental nonlinearity observed after  $\varepsilon > 1 \cdot 10^3$  URD ( $\text{mln}^{-1}$ ) can be related to both the electrophysical properties of the sensitive silicon film and the properties of the binder.

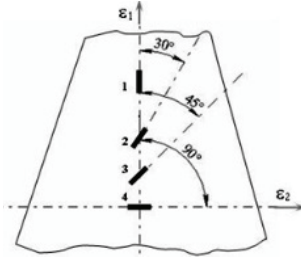


Fig. 2.12. Strain gauge arrangement in the study of the case of divergence of the sensor axis and the direction of the main deformation  $\varepsilon_1$ .

*Source: built by the author based on [6,27].*

We also studied the error of strain measurements using strain gauges under conditions when the axis of the sensor base does not coincide with the direction of the main deformation of the object. Fig. 2.12 shows the direction of the main deformation  $\varepsilon_1$  of the beam and the arrangement of the sensors on the beam. The sensors were attached using BF-2 glue. The base axis of sensor 1 coincides with the direction of the principal strain  $\varepsilon_1$ , sensor 2 is located at an angle of  $30^\circ$  to  $\varepsilon_1$ , sensor 3 at an angle of  $45^\circ$ , and sensor 4 at an angle of  $90^\circ$  (coinciding with the principal strain  $\varepsilon_2$ ). All the sensors were taken from the same batch produced in the same technological mode.

The value of the measured strain  $\varepsilon_\varphi$  was determined using formula (2.13). The calculated deformations used for comparison with those obtained experimentally were determined by the formula:

$$\varepsilon_\varphi = \frac{\varepsilon_1 + \varepsilon_2}{2} + \frac{\varepsilon_1 - \varepsilon_2}{2} \cos 2\varphi \quad (2.15),$$

where  $\varphi$  is the angle between the direction  $\varepsilon_1$  and the direction for which the strain is calculated.

The strain  $\varepsilon_2$  was calculated using the formula  $\varepsilon_2 = -\mu\varepsilon_1$  (where  $\mu$  is the Poisson's ratio). The results of the study are shown in table 2.2.

Table 2.2. Dependences of the calculated  $\varepsilon_\varphi$  and experimental  $\varepsilon_e$  deformations on the orientation of the sensor relative to the main axis.

Source: built by the author based on [27].

$\varphi$	$0^\circ$	$30^\circ$	$45^\circ$	$90^\circ$
$\varepsilon_\varphi$ , URD	$1 \cdot 10^3$	$0,68 \cdot 10^3$	$0,37 \cdot 10^3$	$-0,25 \cdot 10^3$
$\varepsilon_e$ , URD	$1 \cdot 10^3$	$0,64 \cdot 10^3$	$0,36 \cdot 10^3$	$-0,24 \cdot 10^3$

The largest difference between  $\varepsilon_\varphi$  and  $\varepsilon_e$  is observed for  $\varphi = 30^\circ$  and is 6%, which is at the level of the experimental error. The results indicate that the transverse strain sensitivity of the sensors is insignificant.

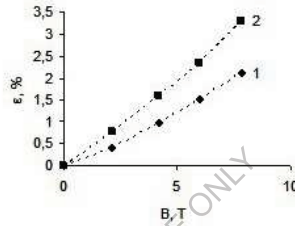


Fig. 2.13. Dependence of the measurement error arising in a magnetic field at 4.2 K: 1 - undeformed sensor, 2 - deformed to  $\varepsilon = 10^3$  URD.

Source: built by the author based on [27].

Fig. 2.13 shows the results of the study of one of the sensors in a magnetic field at  $T = 4.2$  K. Curve (1) corresponds to the strain value that seems to occur when a magnetic field acts on an undeformed sensor ( $\varepsilon = 0$ ), and curve (2) on a pre-deformed sensor to  $\varepsilon = 1 \cdot 10^3$  URD. A field of 7 T leads to an error of about 3%.

It is known that the accuracy of measurements largely depends on such a parameter as the creep of the readings. The creep is determined by the rigidity of the sensor and binder structure and is caused by the plastic deformation of the binder (glue) under mechanical deformation. As a rule, for semiconductor sensors, the creep is significantly higher than that of metal foil sensors.

For the sensors under consideration, creep is probably the main drawback and is due to the rather rigid design of the transducer. Ways to reduce the creep may include further miniaturization and optimization of the sensor shape, and selection of a binder.

### 2.11. Strain and pressure transducers for measuring force and pressure

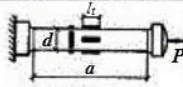
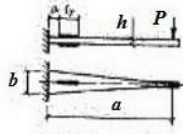
Strain-gage transducers of force and pressure are used in a wide variety of applications, as they can measure forces and pressures in the range from several milli- to several MN using elastic elements (beams) of various shapes and sizes. When designing strain gauges (pressure and force transducers), special attention is paid to ensuring the lowest possible deformation of the system that perceives the force and pressure, and to compensate for the influence of lateral force components that arise from eccentricities. To avoid eccentricities, intermediate ball and segment supports and elastic diaphragms flexible along and rigid across the force axis are commonly used. In order to reduce hysteresis at the mating points of elements in force and pressure transducers, it is recommended to use elastic joints.

When measuring large forces from 10 kN to 10 MN, various design forms of elastic elements (beams) are used in force and pressure transducers. The simplest is the bar elastic element used for measuring forces from 50 kN to 5 MN. In order to ensure uniform stress distribution across the cross-section of the elastic element in the strain gauge zone, the ratio of height to transverse dimension should be at least 3. Increasing this ratio above 5 may cause loss of stability. To increase stability, a centering elastic diaphragm or a system of elastic joints is used.

Force and pressure transducers for measuring small forces (up to 10 kN) have, as a rule, beam elastic elements. Strain-dynamometers in the form of bendable rings operating on two-digit deformation are also widespread. Ring-type elastic elements have relatively high sensitivity with sufficient stiffness from the plane of force action.

Table 2.3. Calculation schemes and formulas for characterization of some simple elastic elements of force and pressure transducers.

Source: built by the author based on [15].

Type of elastic element	Elastic element diagram	Calculation formula
Rods	 <p style="text-align: center;"><math>a &gt; 5d; l_g &lt; a/5</math></p>	$\frac{4P10^6}{\pi d^2 E}$
Beam	 <p style="text-align: center;"><math>a_t &gt; b; l_g &lt; a/2</math></p>	$\frac{6Pa10^6}{bh^2 E}$

## 2.12. Electromechanical transducers

Electromechanical transducers are made in the form of a mechanical contact device operating under the action of a changing physical quantity, which is measured. They can be manufactured in different designs. Usually contacts have a simple form and operate in a discrete mode, such as, for example, a bimetallic switch (fig. 2.13)

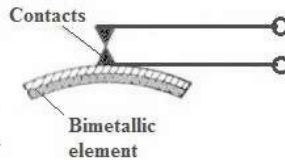


Fig. 2.13. Example of a bimetallic element working as an electromechanical transducer.

*Source: built by the author.*

When the value of the measured value exceeds the switching point, the contact opens or closes, resulting in a transducer output signal in the closed or open circuit.

Electromechanical transducers are usually digital (discrete) because their contacts can only be in two positions and represent an on-off element.

## 2.13. Acceleration transducers. Accelerometers

Accelerometers are transducers that measure the acceleration of an object, which it acquires when it is displaced relative to its initial position. Accelerometers are used to measure the acceleration of horizontal displacements, accelerations caused by the Earth's gravity and others. Nowadays accelerometers are mass produced on the basis of micro electromechanical systems (MEMS).

Let us consider the principles of operation of the main accelerometer circuits. Fig. 2.14 shows some designs of strain-gauge accelerometers. The simplest accelerometer (a) consists of a base, a cantilever sensing element with strain gauges and an inertial mass at the end. The calculation of such an accelerometer is reduced to determining the cross-section and span of the cantilever beam for the action of a force equal to the product of the mass by the measured acceleration. Accelerometers of this type are used to measure accelerations in the ranges from 0...20g to 0...20000g with a frequency range of 0...15 to 1500 Hz. 15 to 1500 Hz. The natural frequency of cantilever-type accelerometers is determined by the stiffness of the cantilever and inertial mass. The frequency range can be extended by using elastic elements without concentrated mass. The force acting on such an accelerometer is determined by the product of the measured acceleration by the cantilever mass.

The accelerometer shown in fig. 2.14.b) differs in that it has a frame sensing element with an inertial mass supported between two cantilever beams. Compared to the cantilever-type accelerometers, in this case a higher conversion factor can be achieved at the same natural frequencies. The frame element is designed to be rigidly fastened to the struts at both ends. Low-frequency accelerometers usually have liquid damping, for which the sensing element is located in a sealed housing filled, for example, with polyxyloxane liquid.

High-frequency accelerometers have an inertial mass, which is connected to the base through a force-meter of solid or tubular cross-section. The accelerometer is oriented so that the measured acceleration acts along the axis of the sensing element. The calculation of such an accelerometer is reduced to determining the dimensions of the force meter loaded with a force equal to the product of acceleration and mass.

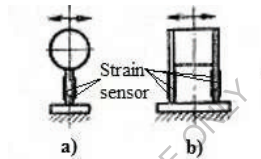


Fig. 2.14. Examples of some accelerometer designs.

*Source: built by the author based on [15].*

## 2.14. Integral semiconductor beam accelerometer

Technologies of modern microelectronics allow to create miniaturized accelerometers with stable metrological characteristics. This makes it possible to apply them in a wide variety of technical devices and solve various scientific, technical and production problems.

As an example, consider the well-known **integrated beam silicon accelerometer (MEMS transducer)**. It is a micro-miniature design shown in fig. 2.15. The accelerometer consists of a silicon crystal oriented in the optimal crystallographic plane in terms of tensometric properties. A beam with a mechanical stress concentrator and strain gauges on it and a massive part - inertial mass, which can be made either from the same silicon together with the beam or from another material, is fabricated in the crystal by means of anisotropic etching. The beam is separated from the base by a slotted hole. The silicon crystal is closed at the top and bottom by glass covers with etched cavities, which form a closed chamber protecting the beam and the strain cell from the external environment and limiting the free movement of the beam under overloads. The covers are connected to the silicon by means of an anodic fit. In addition, contact pads are fabricated on the top cover, to

which the external wire leads are connected. As the authors report, the dimensions of the considered example accelerometer are 2x3x0.6 mm, mass 0.02 g, range of measured accelerations from 0.1 to 500 m/s<sup>2</sup>, in the frequency range from 0 to 100 Hz.

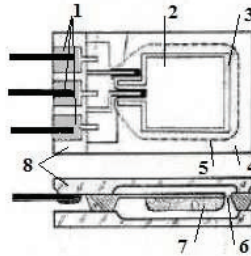


Fig. 2.15. Example of construction of the integral beam accelerometer. 1 - contact pads; 2 - beam; 3 - air gap; 4 - silicon; 5 - notch in the cover; 6 - air gap; 7 - inertial mass; 8 - glass cover.

*Source: built by the author based on [3].*

## 2.15. Measuring transducers of vibrations. Vibrometers

Inertial tensoresistor measuring transducers of vibrations (vibrometers) can be constructed according to the schemes of accelerometers and differ from the latter only by the ratio of natural frequencies and frequencies of the processes under study. Since the inertial masses of vibrometers are relatively larger, and the amplitude range should correspond to the amplitude of the measured vibrations, the design of low-frequency vibrometers and accelerometers is also somewhat different.

Figure 2.16 shows a schematic of an inertial vibrometer in which the inertial mass is supported on bearings. The mass is kept in a state of equilibrium by a spring of an elastic element (suspension) and its movements cause deflection of a beam with strain gauges of the displacement transducer 4. Vibrometers of this design can have a natural frequency of the order of several hertz. Low-frequency vibrometers are characterized by some instability of the zero reference due to the influence of friction forces in the bearings, which causes a limited measurement range.

There are also vibrometers with an inertial mass in the form of a pendulum. In it, the inertial mass on the lever is held in the equilibrium position by two springs or elastic sensing elements of displacement transducers.

In contact-type vibrometers, vibration is transmitted to the sensing element via a rod. During measurements, the body of the vibrometer is held in the hands or strengthened on a fixed support.

Vibrometers in the form of contact-type vibration probes are used in the study of structures, which connect the object of study and some fixed support. As vibration probes it is possible to use tensoresistor transducers of displacements of any type, the range of measurement of which corresponds to vibration displacements of the object of research. A variation of contact-type vibration probes are hand-held vibration probes. During measurement, the operator holds the stylus body in his hands, pressing the tip against the object so that the strain-gauge displacement transducer is in the middle of the measurement range.

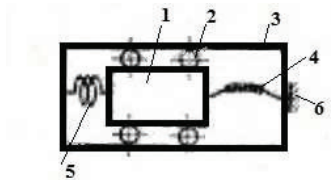


Fig. 2.16. Example of vibrometer design. 1- inertial mass, 2 - bearings, 3 - housing, 4 - beam with strain gauges, 5 - spring, 6 - beam mounting.

*Source: built by the author.*

## 2.16. Silicon strain gauge pressure transducer

Silicon membranes for creation of pressure transducers are used widely enough, tenso-effects in such membranes with different crystallographic orientations are well studied, technologies of work with them, creation of strain-resistive sensitive elements on them and their connection in integrated circuits are worked out. The use of silicon and modern microelectronics technologies make it possible to create miniature pressure sensors for medical applications and other special tasks in various fields of science and technology.

Let us consider one of the known integrated strain-gauge absolute pressure transducers described in the literature. It has the structure shown in fig. 2.17. The design consists of a glass flat cover, in which a recess is etched, and a silicon crystal with a thin membrane, in which four strain gauges are made, connected in a bridge circuit. The membrane is surrounded by a thick silicon ring base. A recess in the glass plate is located below the membrane, and the plate itself is bonded to the silicon crystal by means of an anode fit. Anode bonding is carried out by heating the glass and silicon plates up to 400 °C with subsequent application of 600 V voltage to the silicon relative to the grounded glass plate. The anode fit provides a completely hermetic connection, so that the recess in the glass plate together with the membrane form a closed hermetic chamber.

According to the authors the external dimensions of the transducer can be: 1.5x2.0x0.2 mm. The sensitivity is 0.2 mV/ (kPa·V). The temperature drift is equivalent to 250 Pa per 1 °C, and the output voltage varies linearly up to a pressure of 40 kPa.

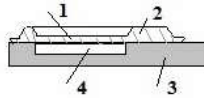


Fig. 2.17. Example of silicon integral absolute pressure transducer structure: 1 - silicon membrane; 2 - base; 3- glass plate; 4 - hermetic chamber.

*Source: built by the author.*

### 2.17. Some commercially available pressure sensors. Sapphire, Motorola

Pressure sensor (transducer) Sapphire. Pressure transducer of Sapphire 22 complex is designed for continuous conversion of the measured parameter value - absolute, gauge, vacuum, hydrostatic pressure and pressure difference of neutral and aggressive media, as well as level conversion into a unified current output signal. The pressure transmitter is designed for operation in systems of automatic control, regulation and management of technological processes in various industries, including application in explosive production of oil and gas industry, at nuclear power facilities (UAE) and for export.

The pressure transmitter consists of measuring and electronic units. All converters have a unified electronic unit and differ only in the design of the measuring unit.

The operating principle of Sapphire 22 pressure sensors is based on the effect of the measured pressure (pressure difference) on the membranes of the measuring unit, which causes deformation of the elastic sensing element and a change in the resistance of strain gauge strain gauge resistors. The change in resistance is converted into an electrical signal, which is transmitted from the strain gauge to the electronic converter. Further in the form of standard current unified signal.

The pressure transmitter has explosion protection version. Explosion-proof pressure transmitter is designed for installation in hazardous areas of premises and outdoor installations, according to documents regulating the use of electrical equipment in hazardous areas.

**Motorola pressure sensors.** Motorola is widely known for the creation and production of various types of sensors. The latest developments are semiconductor pressure sensors. Sensors are characterized by small size, ease of use. The design uses membranes developed a new patented sensing element. This sensing element works on the principle of a Hall sensor. In it, under the action of mechanical stress on

the output terminals of the sensor appears an electric voltage proportional to pressure. The voltage appears due to inhomogeneous deformation of resistive elements of the pressure sensor. As noted, the pressure sensor with the proposed design of the sensing element has such advantages as improved linearity, simplicity in thermal compensation, etc. According to the type of pressure to be measured, differential, relative and absolute pressure sensors are produced.

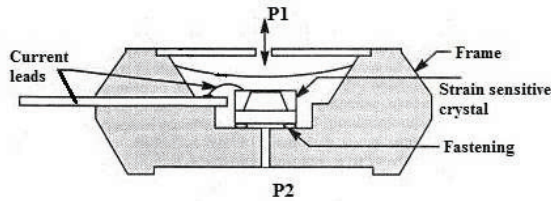


Fig. 2.18. General design of one of Motorola pressure transducers.  
*Source: built by the author based on Sensor instructions.*

**Piezoelectric pressure transducer. General scheme of the device.** Piezoelectric effect, which is used in transducers, is the appearance of electric charges on the surface of some crystalline dielectrics (quartz, barium titanate) under the action of mechanical stress or deformation.

Fig. 2.19 shows the scheme of a device for measuring gas pressure using a piezoelectric transducer. The measured pressure  $P$  acts on the diaphragm 1- bottom of the transducer body. Two quartz plates 2 are sandwiched between three metal spacers 3. A ball 4 is placed between the lid and the top to ensure a homogeneous distribution of the measured pressure. To the middle pad - the negative electrode - is attached a wire 5 passing through an insulating sleeve.

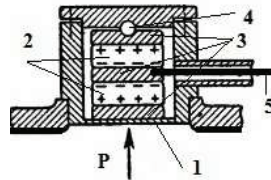


Fig. 2.19. Device of piezoelectric transducer for gas pressure measurement. General scheme of the device.  
*Source: built by the author based on [15].*

The potential difference between the negative electrode and the housing is proportional to the measured pressure. The pressure is determined by the measured potential difference.

Since the charges disappear when the pressure is removed, appropriate measuring circuits must be used so that the charge does not have time to change significantly.

## 2.18. Displacement transducers

One of the simple displacement transducers is a resistive potentiometric divider, in which the sliding contact or potentiometer slider moves along the resistive element (fig. 2.20). The slider is mechanically connected to a sensitive roller (pin), which follows the movements of the measuring object. When voltage is applied to the resistive element, the voltage removed from the potentiometer slider indicates the value of movement.

Linear and rotary angular displacement transducers based on the principle of voltage division are quite common. Angular transducers are used to measure angular displacements from a few degrees to a few turns of the disk, while linear transducers work in the range from a few millimeters to a few meters.

The shape of the resistive element determines the resolution of the transducer. When this element is made of wire, the resolution depends on the number of turns of wire per unit length of the element. Other types of voltage division based transducers use a film of metal, carbon, etc. to create the resistive element, allowing theoretically infinite resolution.

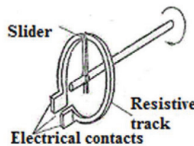


Fig. 2.20. The simplest potentiometric device for angular displacement detection.

*Source: built by the author.*

**Capacitive displacement transducers.** Capacitive displacement transducers work on the principle of a capacitor, which is formed by two plates separated by a dielectric. A change in the size of the plates, the distance between them or between them and the dielectric causes a change in capacitance.

Figure 2.21 shows one of the principles of operation of a capacitive displacement transducer. In it, the capacitance is changed by moving the dielectric

between the two plates of the capacitor. There are also other principles - moving one plate relative to the other, changing the area of overlapping of the plates. There is also known a design in which the dielectric, remaining stationary, changes its characteristics.

On this principle are based capacitive proximity sensors and capacitive proximity switch, capable of detecting the target at some distance from the device. The same principle is behind the capacitive liquid level transmitter. It varies the dielectric constant as a result of changes in the liquid level.

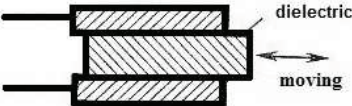


Fig. 2.21. Principle of operation of capacitive displacement transducer.  
*Source: built by the author.*

**Inductive displacement transducers.** The self-inductance of a coil changes as a magnetically permeable body approaches it, so the displacement of the body relative to the coil can be determined using a sensing coil with self-inductance. Measuring transducers that utilize this principle are usually non-contact (fig. 2.22.a). There are also coupled inductive displacement transducers (fig. 2.22.b), in which the coil core is mechanically coupled to the body whose displacement is being measured. Non-contact transducers of the described type are used as a base for construction of inductive proximity sensors and inductive proximity switches.

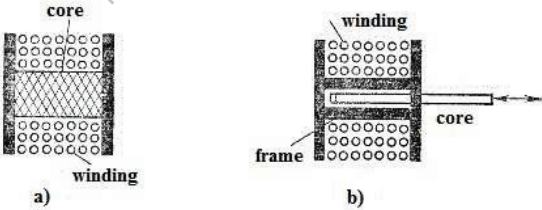


Fig. 2.22. Inductive transducers of displacement: a - non-contact; b – connected.  
*Source: built by the author based on [15].*

**Magnetic displacement transducers.** Transducers of this type are based on the use of the change in magnetic resistance between two or more magnetic coils, depending on the displacement of the body. The displacement causes a change in the output voltage of the transducer. Constant or alternating magnetic fields, whose

magnitude varies linearly, can also be used. In this case, a magnetic field sensor placed on the body being moved will track the displacement.

**Inductive displacement transducers.** The principle of operation of inductive transducers is based on the dependence of inductance or mutual inductance of windings on the position, geometric dimensions and magnetic state of the constituent elements of their magnetic circuit.

It follows from the theory (and mathematical formulas) that inductance and mutual inductance can be changed by influencing the geometrical dimensions (length, cross-sectional area) of the air section of the magnetic circuit, the magnetic permeability, and the losses in the magnetic core.

Alternating current flowing through the coil creates an alternating magnetic field. When an electrically conducting material (metal, etc.) is placed in it, some of the energy of the magnetic field is transferred to the metal object. This transferred energy induces eddy currents (Foucault currents) on the surface of the object. Their magnitude depends on the size, composition of the metal, and location of the object relative to the magnetic field. Eddy currents in the object create its own magnetic field, which interacts with the primary field generated by the coil. Due to the effect, the effective inductance of the coil decreases and, as a result, the resonant frequency of the circuit in which the inductance is included changes.

## 2.19. Flow measurement instruments. Flow meters

**Mechanical.** In practice, quite a few methods of flow determination are known. The simplest and therefore most common methods of flow measurement are those using mechanical sensing elements, in which the flow moves or rotates a solid body. This displacement or rotation of the solid is thus found to be proportional to the flow rate.

Figure 2.23 shows a schematic of one of the mechanical flow measurement methods. It shows a spring-loaded, pivot-suspended paddle that deflects to open an orifice as fluid passes through the transducer. The greater the flow rate, the more the blade deflects.

There are other varieties of mechanical methods of flow measurement. In a flow transducer, the method of a propeller rotating when a substance is flowing can be realized. And the speed of rotation of the propeller is proportional to the flow rate of this substance. The most common mechanical flow transducer is a turbine flow meter with a rotating propeller (or in this case a turbine). The turbine is mounted in the flow of the substance by means of bearings. In general, the turbine blades are made of ferromagnetic material. Therefore, a coil mounted on the flowmeter body is used to determine the turbine speed. The electromagnetic sensing element of the flow

transmitter creates a turbine braking effect, which can affect the angular speed of the turbine at low flow rates. Other designs of sensing elements, such as electro-optical ones, are used for low flow rate measurements.

For accurate measurements, it is important that there is no swirling of the flowing substance, as this directly affects the turbine speed. For this reason, flow straightening vanes are usually installed at the inlet of the flow meter. These blades also form one of the reference points of the turbine. Of course, considerably simpler flowmeter designs are also possible when the accuracy of measurement is not essential, i.e. when flow braking and swirling can be ignored.

One of the advantages of turbine flowmeters compared to other types of flowmeters is the linear dependence of their output signal on the flow velocity in the range set for the device.



Fig. 2.23. One example of a mechanical flow measurement device design.

Source: built by the author.

Flow measurement based on thermal phenomena. Thermal flow meters operate on the principle that the heat carried by a substance from one point to another is proportional to the mass flow rate of that substance. For example, fig. 2.24.a shows how two temperature transducers (T) determine the temperature of a substance before and after heating, which is carried out by a heating element located between these transducers.

Figure 2.24.b shows a thermoanemometer that measures the flow of a substance by means of a single heating element located in its flow. The cooling effect of the substance flowing through this element characterizes the mass flow rate, i.e., cooling is monitored due to the change in resistance of the heating element wires. Often a metal or semiconductor film is used instead of a wire element in the transducer. With the thermoanemometer it is possible to measure extremely fast fluctuations in the flow rate of substances.

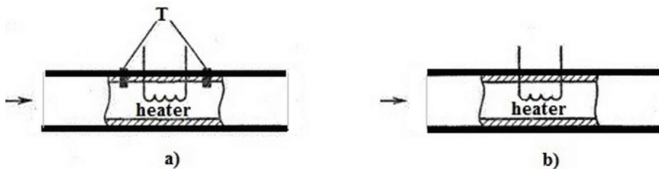


Fig. 2.24. Methods of realization of the thermal principle of flow measurement using a heating element.

Source: built by the author.

**Thermoanemometric method of flow determination. Principle of measurement.** The method provides determination of flow rate by temperature change of electrically heated metal wire or film (flow transducer) placed in the controlled gas flow. Cooling of the transducer depends on the velocity of the flowing stream, physical properties of the gas (thermal conductivity, temperature and density) and on the temperature difference between the transducer and the gas.

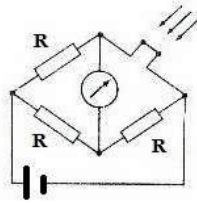


Fig. 2.25. Thermoanemometer powered by direct voltage.

*Source: built by the author.*

**Two methods are known:**

**A. Constant current method.** The current (or voltage) heating the wire is kept constant and measured by the change in resistance caused by its cooling:  $R = f(V)$ . The parameters and power supply of the bridge circuit (fig. 2.25) are selected so that it is in equilibrium at zero velocity  $V$  of the gas. The deviation of the galvanometer arrow serves as a measure of the flow velocity.

The method has sufficient sensitivity only at low velocities of controlled flows and is unsuitable for measuring high velocities ( $V > 0.5$  cm/s).

**B. Constant temperature method.** The resistance of the flow-cooled transducer is kept constant by adjusting the heating voltage (bridge supply voltage). This bridge supply voltage or current serves as a measure of the velocity of the monitored flow. As in the previous case, the sensitivity of the thermoanemometer decreases as the velocity of the monitored flow increases, but this decrease is substantially less than with a constant heating voltage thermoanemometer circuit.

**Evaluation of the thermoanemometric method.** The thermoanemometric method has a number of advantages:

- high sensitivity;
- miniaturized dimensions of the sensing element;
- simple schemes and devices are applicable for measurements.

The disadvantages of the method include:

- decreasing sensitivity with increasing flow velocity;
- necessity of individual calibration of primary transducers;

- instability of the calibration characteristic.

The use of annealed wire reduces the aging rate. The low operating temperature of the wire increases the influence of gas temperature. This influence can be eliminated by temperature compensation. Self-convective gas flows around the heated wire (at zero velocity of the monitored flow) also distort the readings, which is especially important for low velocity measurements. Due to low inertia wire thermoanemometers are used in studies of turbulent flows.

**Magneto induction method of flow measurement.** When a conductor moves in a magnetic field, according to the law of electromagnetic induction, an electromotive force is generated in the conductor and an electric current is induced. This effect is used in the induction flow meter to determine the flow rate. The flowing liquid must have a certain minimum conductivity. According to Faraday's law, an electric field is generated in an electrically conductive fluid flowing through a magnetic field. The controlled flow flows through an insulator-covered pipe, in the walls of which two diametrically located electrodes are installed perpendicular to the direction of the magnetic field and the fluid (medium) flow, from which the voltage is removed. The voltage value is proportional to the average velocity of the medium flow. This voltage, generated by a high impedance source (liquid), is brought by means of a cable to the measuring transducer, which amplifies it and carries out further processing. The signal value is usually a few millivolts.

The theory of the induction flow meter is based on Maxwell's equations. A conductive flowing liquid has a certain number (concentration) of electric charges. The Lorentz force acts on the moving charges and deflects them in perpendicular direction, which causes the occurrence of electric potential difference (electric voltage). The voltage value is proportional to the flow velocity and electrophysical properties of the fluid (flow).

The output useful signal of such a flowmeter is small. At such scheme of flow measurement there are significant interferences. To eliminate these disadvantages in the industry in flow meters of this type use a variable or switchable magnetic field. This technique allows to isolate the useful signal and achieve acceptable measurement accuracy.

## **2.20. Switches and sensors for proximity detection (motion sensors)**

Proximity sensors have no physical connection with objects. They judge the presence of a body by means of some physical detection principle implemented in the respective transducers,

**An inductive proximity sensor** uses a tuned oscillator. When a conducting body approaches the sensor, there is a damping of oscillations sensed by the coupling

circuitry. More general and simple devices are inductive proximity switches, in which an interface circuitry is used to turn them on or off when a conductive body approaches them.

**Capacitive proximity sensors** are either in the form of measuring transducers or switches. Their principle of operation is that a nearby body changes the dielectric constant of a capacitor, which unbalances the bridge in one of the arms of which the capacitor is placed. Capacitive sensors are capable of sensing the proximity of bodies made of different materials in a wide range of distances.

There are also a large number of **optical sensors** for proximity sensing. They consist of a basic sensing element and a scheme for its connection to the measuring system. The following methods of proximity detection can work in the devices under consideration (fig. 2.26). The sensors may be of the design (fig. 2.26.a) where the light source and sensing element are placed together and the emitted light is reflected back and travels along the same path as the incident light. In other devices (fig. 2.26.b), the beam from the source and the reflected light beam are at some angle to each other and are reflected from the body surface as from a mirror. Sensors, in which the passage of light through the body surface is also used, are possible.

**Magnetic proximity sensors** are very common devices and include reed relays or Hall sensors.

**Radar proximity sensors** consist of a radar signal generator and a mixer where the reflected and probe signals interact. Using the Doppler effect (the frequency of the reflected signal differs from the frequency of the probing signal when the body is moving), the frequency of the mixer output is zero when the body is not moving and different from zero when it is moving. Most of these proximity sensors operate in the X-ray range.

The application of these devices (proximity sensors) is not limited only to the measurement of displacement. The sensors can also record distance, hence speed, by determining the time between the transmitted and reflected pulses and performing the necessary calculations with the results of these measurements.

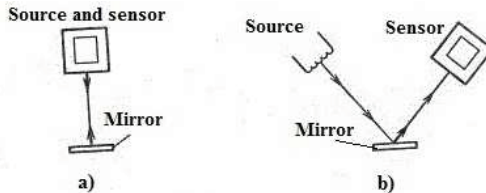


Fig. 2.26. Principles of operation of some optical devices (sensors, transducers) for proximity detection.

*Source: built by the author based on [25].*

## 2.21. Weight sensors. Methods and means of conversion

### **Electromechanical weight sensors. Weight sensors with strain gauges.**

Weight sensors with strain gauges are among the most accurate force-measuring devices used for weighing. Along with strain gauges in the weight sensors are built in resistors designed to adjust the bridge circuit, which provides interchangeability of sensors, as well as the ability to include several sensors in a common circuit if necessary. The characteristic of the strain gauge weight sensor indicates the value of the output voltage in millivolts at rated load, referred to 1 V supply voltage. Typically, this value is 1-2 mV/V. Overloads greater than 150% nominal do not cause a zero offset. Overloads up to 500 % of the nominal value also do not cause mechanical damage.

**Weighing sensors with vibrating string.** The principle of operation provides excitation of constant frequency vibration of a pre-tensioned string by means of an electromagnetic system and transfer to the string of the force developed by the load in the weighing scale. This force increases the tension of the string and, as a consequence, the frequency of its vibration. The change in frequency is a measure of the determined mass of the load. High accuracy of weight measurement can be achieved with such sensors.

**Magnetoelastic weight sensors.** The magnetoelastic effect causes some materials (e.g. permalloy) subjected to a load to change their magnetic susceptibility. Such a material is used as the core of a winding whose total resistance decreases with increasing load due to a decrease in magnetic susceptibility. Such sensing elements have relatively high output power, which allows their output signal to be used without amplification. However, the small linearity range of the characteristic is insufficient for accurate measurements.

**Inductive weight sensors.** In inductive weight sensors, the change in winding inductance is caused by the displacement of the iron core by the measured force.

Of particular importance in the field of weight measuring technology are the following devices:

- a) With two or four variable inductances (twin inductor with pull-in or cross armature);
- b) with variable mutual inductance (differential transformer with pull-in armature).

Compared to strain gauges, inductive weight sensors have higher output voltages, lower sensitivity to temperature and humidity, and larger armature displacements. These properties allow the use of soft springs, which in turn enables the measurement of small forces. However, the accuracy of inductive weight sensors is lower than that of strain gauges.

**Weight sensors with electromagnetic force compensation device.** In this device, the scale bowl is connected by a lever to a compensation coil, which is in the field of a permanent magnet. The current in the winding of this coil is controlled by a position sensor connected to an amplifier. The change of current in the winding of the compensation coil takes place until the balance is reached. As the load changes in the scale, the current in the coil, which is a measure of the weight of the load, changes accordingly.

**Hydraulic weight sensors.** Force is determined by measuring the pressure developed by the load on the piston or diaphragm of the hydraulic system. The fluid pressure is measured by a pressure gauge. The rubber diaphragm output design eliminates friction. In addition, sensors of this type allow deviations of the direction of the acting force up to a few degrees from vertical without additional errors. The error is estimated at  $\pm 0.2\%$  within the weighing range. The largest weighing limits are from 50 kg to 500 tons.

**Weight sensors using ionization measurement methods.** Weighing with radioactive isotopes can be carried out by two methods: the transmission method and the scattering method.

When using the transmission method, the absorption of radiation by the weight being weighed is measured. The use of hard radiation allows the value of the mass attenuation coefficient to be considered independent of the chemical composition of the material. In the scattering method, the direct radiation is shielded. Lateral radiation is scattered by the material and directed to the detector. The weighing method allows this type of scales to be used as conveyor scales or truck scales operating in harsh environmental conditions where scales with conventional measuring systems wear out quickly. The error ranges can reach several percent.

## **2.22. Fill level sensors. Fill level measurement**

Depending on the industry and the conditions in which the level sensors are to be used, different requirements are placed on them. When planning to use a level gauge, it is necessary to know the physical and chemical properties of the filling materials (viscosity, electrical conductivity, radioactivity, abrasiveness, etc.), external measurement conditions - temperature, pressure, aggressiveness of the environment, etc.

There are quite a lot of physical effects and material properties, on the basis of which sensors (measuring transducers) of filling level can be designed and manufactured.

**Measurement with float.** A float is used as the sensing element of a liquid level sensor. As a rule, spherical bodies with a density lower than the density of the

liquid are used as a float. Transmission of information from the sensor about the level of filling can be carried out mechanically with the help of various rollers, gears, cables or use electrical data transmission systems (connecting the movement with a variable resistor, etc.). For data transmission can also be used step switches, sending pulses, magnetic transmission of float movement, inductive displacement sensors.

Measurement errors in such devices are mainly due to changes in the density of the liquid to be filled or changes in the data transmission conditions (friction, backlashes, etc.).

**Capacitive method of level measurement. Capacitive level sensors.** The capacitive method of level measurement makes it possible to measure the filling of powdery, viscous, granular materials. Capacitive method measures the levels of powdered food, grain, washing powder, cement, sand, coal dust, fuel oil, fuel oil, water, acids, alkalis, etc. The capacitive method allows for continuous measurement of the level of powdered food, grain, washing powder, cement, sand, coal dust, fuel oil, fuel oil, water, acids, alkalis, etc. Capacitive method allows for continuous measurements. The method of operation of sensors is based on the measurement of electrical capacitance (the principle of capacitor operation). The capacitor is formed by the tank wall and a probe that is immersed in the tank contents. Capacitance is usually measured by applying an electrical voltage of high frequency. Capacitance varies with fill level. The capacitance is equal to the sum of the capacitances of the immersed section and the section in the air. The two capacitances are connected in parallel and the total capacitance is summed. The accuracy depends on the probe design. The probe consists of a cable, rod or tube. If necessary, an insulating coating is applied.

If the tank is made of dielectric material, a separate opposite electrode must be provided. Sometimes a cylindrical condenser is used in the design of level gauges, with the open end immersed in the medium.

**Fill level measurement based on conductivity.** Sensors and the conductivity-based level measurement method can only be used for level measurement of conductive liquid materials.

The measuring principle is based on the change in electrical resistance between two electrodes when they are immersed in the fill material. The resistance decreases with immersion. This method and sensors have found application for filling level measurement in steam boilers. The disadvantage of the method is that it can only be used to measure the level of electrically conductive liquid materials.

**Hydrostatic and pneumatic methods of level measurement.** These methods can be used to measure the level of any liquid. The hydrostatic method utilizes the pressure of the liquid at the bottom of the vessel and its change as the level changes. The pressure at the bottom of a liquid vessel can be measured in open tanks using a

conventional or differential pressure gauge. In closed tanks, where the liquid may be pressurized, only by a differential manometer. The pressure depends on the height of the liquid column and its density. If the manometer is not installed at the level of the bottom, a correction must be made.

In the pneumatic method of level measurement, air or protective gas must be forced into the tank. The method is used in steam boilers, reactors, etc.

The pneumatic method of level measurement consists in immersing a tube to a certain level in the liquid, the level of which is to be measured. Air (or any gas) is fed into the tube through a special throttle. The pressure in the tube and, respectively, above the throttle is equal to the pressure of the liquid column (and depends, respectively, on the liquid level) relative to the lower edge of the tube.

The advantages of these considered methods and level sensors are their rather high degree of reliability.

**Ultrasonic level measurement method.** The ultrasonic filling measurement method can be used for liquids and bulk solids. It cannot be used only if the liquid contains solid particles, which can lead to large measurement errors. This measurement method allows easy automation of the measurement process.

To realize the ultrasonic method of filling level measurement it is necessary to have a source of ultrasonic waves (transmitter) and a receiver. Typically, frequencies from 20 kHz to several megahertz are used. There are two ways to produce ultrasonic vibrations: piezoelectric and magnetostrictive.

A measure of level can be, for example, the transit time of an ultrasonic beam. The velocity of the beam depends on the propagation medium. This way of level measurement can serve for signaling of fill level limits (see fig. 2.27). When a certain space is filled, the ultrasonic device sends a signal.

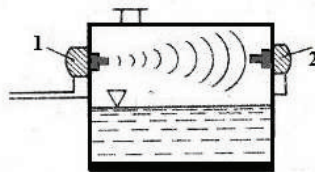


Fig. 2.27. Design of ultrasonic level meter. 1 - emitter, 2 – receiver.

*Source: built by the author based on [25].*

But for liquids, the ultrasonic level measurement method based on the echo sounder principle is more convenient and accurate. Ultrasound propagates in the space above the liquid, is reflected from the surface (air-liquid interface) and by the time of return to the receiver the level is determined.

One of the main advantages of the ultrasonic level sensor is the possibility of its application in hard-to-reach places.

**Level gauges based on radioactive isotopes. Measurement method.** Level sensors based on radioactive isotopes are used where it is impossible to make measurements with conventional sensors. Most often the method of level measurement based on radioactive isotopes is used to measure the level of aggressive materials, in tanks with high temperature, in metallurgical plants, materials such as coal, ore, etc. The most common application of radioactive isotope-based level sensors is for measuring the level of aggressive materials.

The operation of the sensors is based on the phenomenon of absorption of radioactive radiation by the materials contained in the tank. In practice, thick layers of materials are usually measured, so  $\gamma$ -rays are most often used in such sensors. The beam of  $\gamma$ -rays passes through the tank in a straight line. A radiation receiver is located on the opposite wall of the tank. The intensity of the rays hitting the receiver depends on the degree of absorption by the material. The design of sensors and level measurement systems using radioactive isotopes can vary depending on the technical conditions and requirements.

If a level sensor working on the principle of a signaling device is required, its design is approximately the same as on the basis of ultrasonic radiation (see fig. 2.27). When the level changes and the material overlaps the beam, the sensor and the measuring system are triggered.

If continuous level measurement is required, other sensor designs are used. For example, when several emitters are placed on the tank wall, the beams from which are directed to the receiver on the other side. When the level of the material changes, part of the beams overlap and the intensity of the radiation reaching the receiver changes.

Advantages of the considered method of level measurement are: absence of contacts, possibility of measurement in especially difficult conditions, operational reliability.

**Other methods and sensors for level measurement.** Level measurement using temperature sensors - thermocouples, thermistors. This method of measurement is possible for liquid materials that are not aggressive. The principle of measurement is based on the difference between the temperature of the material in the tank and the external temperature. The design of such measuring transducers depends on the requirements and measurement conditions.

**Measurements with dynamometers.** Essentially, the tank and the material in it are weighed. The method is suitable for measuring the filling level of bulk materials, aggressive materials. The designs of measuring systems can be different and are developed according to the technical requirements.

Fill level measurement can also be carried out by means of limit switches with vibrating sensing elements, etc. There are level sensors based on the interferometric method.

**Mechanical methods of measuring the fill level. Measurement of liquid filling level by means of a float.** The physical principle of measurement can be explained using fig. 2.28. Three forces act on the float - weight  $P$ , pushing force (Archimedes' force)  $F_a$  and reaction force of the readout transmission system  $F_r$ . The magnitudes of the forces depend mainly on the air density, the liquid density, and the type of communication system between the float and the measuring device. In the state of equilibrium the sum of these forces is equal to 0. When the liquid level changes, the equilibrium of forces is broken and the float moves up or down. The displacement determines the height of the liquid relative to the initial position.

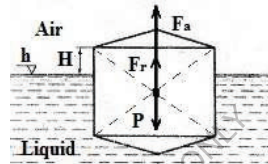


Fig. 2.28. Float method of liquid level measurement.

*Source: built by the author.*

As floats in sensors are used mainly hollow spherical or spherical-cylindrical bodies, the density of which is less than the density of the liquid, so they can float on its surface. Changing the density of the liquid or the friction conditions in the sensor transmission system leads to a distortion of the measurement result. This effect is less pronounced with respect to lift height the flatter the sensor float is.

In the simplest case, the sensor float is attached to a rope or chain, which is passed over a roller or gear wheel. In this case, the measured value is transmitted mechanically. To ensure continuous operation of the sensor, a counterweight is attached to the other end of the cable or chain.

In this method of liquid level measurement, the angle of rotation of the roller corresponds to the change in liquid level. The axis of the guide roller can be connected to the slider of the sensor potentiometer in order to realize the electrical transmission of the measured value.

It is quite simple to mechanically transmit level data in open tanks by means of a cable system or, in closed tanks, by means of a gland entry if the distances for data transmission are short.

However, in most cases, both in open and closed tanks, electrical data transmission systems are used in level sensors, especially if the measurement result is fed to a calculating device.

**An example of a float level sensor is an automobile fuel level sensor (fig. 2.29).** Here the so-called potentiometric method of transferring information about liquid level is used (potentiometric level sensor). Float 1 is mechanically connected with rheostat 2. The float, moving accordingly to the liquid level, mechanically moves the slide of potentiometer (rheostat) 2. Thus, the output electrical resistance of the potentiometer (rheostat) changes, which is processed and output by the sensor to the appropriate fuel level indicator.

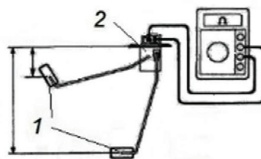


Fig. 2.29. Schematic diagram of automobile fuel level sensor operation.

*Source: built by the author.*

The advantages of potentiometric fuel level sensors include simplicity of the device and low cost. The disadvantage is the wear of moving electrical contacts of the sensor. This is especially true in vehicles that use aggressive fuels such as ethanol, methanol and biodiesel. In such conditions, a non-contact fuel level sensor design that utilizes the interaction of magnetic elements is used.

### 2.23. Speed measurement. Tachometers

Transducers of this type are used to measure linear or angular speed. Angular speed meters are usually electromagnetic devices and are called tachometers. Tachometers of the electron-optical type, are called stroboscopes. Linear speed is usually determined indirectly by converting the linear speed of the flywheel or gear rotation. The angular velocity is then measured using an angular encoder (tachometer). Direct determination of linear speed is provided by electromagnetic transducers, non-contact Doppler microwave radar transducer, etc.

**Pulse tachometers.** The most common method of conversion is the one in which the receiving coil of known design allows to determine the speed of rotation of the shaft. As a rule, such a shaft is made with recesses or protrusions, thus forming a gear wheel (fig. 2.30). When the protrusion or notch passes through the coil, the

output current voltage changes. Calculation of the change in output voltage over a certain time interval, and gives the value of angular velocity.

In pulse tachometers it is possible to use, for example, the Hall effect, inductive eddy currents, optical phenomena (in non-contact transducers), but the most common in tachometers is the electromagnetic principle.

The ferromagnetic rotor with a sensing element is made here in the form of a permanent magnet or coil. The magnet creates a magnetic field around the sensing element. When the rotor tooth crosses the field, the magnetic flux changes and EMF is induced in the tachometer coil. The advantage of this conversion principle is the dependence of the output signal on the rotor tooth configuration. Some known types of output pulses for different shapes of tachometer rotor teeth are shown in fig.2.30.

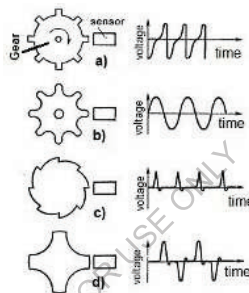


Fig. 2.30. Dependence of the output signal of the electromagnetic pulse tachometer on the configuration of the rotor teeth: a-rough teeth, b-precisely machined rotor tachometer teeth, c- and d-special shape of teeth.

*Source: built by the author based on [25].*

**Tachometer generators.** When speed measurement concerns a particular oscillator, the angular velocity can be judged from the amplitude or frequency of its output voltage. Generators used for this purpose are called tachometers.

Such a small energy should be selected from the moving body for the measuring transducer as to eliminate the influence of the tachogenerator on the angular velocity of the shaft.

**Stroboscopes.** Stroboscopes are special type electro-optical tachometers in which the rotating shaft is illuminated by flashes of light. The speed of the flashes is manually adjusted as long as the image of the shaft is stationary. This occurs when each flash falls one revolution of the tachometer shaft.

## Bibliography

1. Klokova N.P. *Tenzorezistory* [Strain gauges]. -M.Mashinostroenie, 1990.-224p.
2. Daychik M.L., Prigorovskiy N.I., Khurshudov G.Kh. *Metody i sredstva naturnoy tenzometrii. Spravochnik* [Methods and means of full-scale strain gauging. Directory] M. Mashinostroenie, 1989.-240p.
3. Vaganov V. I. *Integral'nye tenzopreobrazovateli* [Integral strain gauges]. – M.: Energoatomizdat, 1983. – 136 p.
4. Gridchin V.M., Lyubimsky V.M. *P'ezosoprotivlenie v plenkakh polikristallicheskogo kremniya p-tipa* [Piezoresistance in p-type polycrystalline silicon films]. *FTP*, 2004, v.38, №.8, 38-46p.
5. Klokova N.P. *Tenzorezistory* [Strain gauges]. *Datchiki i sistemy* [Sensors and systems] 2004, №3, p.10-12.
6. Nikolay Gorbachuk, Mikhail Larionov, Aleksey Firsov, Nikolay Shatil. *Semiconductor Sensors for a Wide Temperature Range. Sensors & Transducers Journal and Magazine*, Vol. 162, Issue 1, January 2014, pp.1-4
7. Gorbachuk N.T., Didenko P.I. *Issledovanie nekotorykh elektrofizicheskikh svoystv plenok n-Si, legirovannykh ionnoy implantatsiyey* [Study of some electrophysical properties of n-Si films doped by ion implantation]. *Poverkhnost'. Rentgenovskie, sinkhrotronnye i neytronnye issledovaniya*, 2006, №4, p.104-106
8. Druzhinin A.A., Mar'yamova I.I., Kubrakov A.P., Pavlovskiy I.V. *Tenzorezistory dlya nizkikh temperatur na osnove nitevidnykh kristallov kremniya* [Strain gauges for low temperatures based on silicon whiskers]. *Tekhnologiya i konstruirovaniye v elektronnoy apparature*. 2008, №4, s. 26-30.
9. Terston R. *Primeneniye poluprovodnikovyykh preobrazovateley dlya izmereniya deformatsiy, uskoreniy i smeshcheniy* [Application of semiconductor transducers to measure deformations, accelerations and displacements]. –V kn.: *Fizicheskaya akustika/ Pod red. U. Mezona, t.1, chast' B –Metody i pribory ul'trazvukovykh issledovaniy. Per. s angl.* – M.: Mir, 1967, p.187–209.
10. Mykola Gorbachuk. *ELECTROTECHNICAL MATERIALS*. LAP LAMBERT Academic Publishing. 120 High Road, East Finchley, London, N2 9ED, United Kingdom, 2024, 112p. ISBN: 978-620-3-46212-8.
11. Zeeger K. *Fizika poluprovodnikov* [Semiconductor physics]. *Per. s angl. pod red. Yu.K. Pozhely.* –M.: Mir, 1977, p. 615.
12. Smith C.S. Piezoresistance effect in germanium and silicon. - *Phys. Rev.* 1954, v. 94, 1, p. 42-49.

13. Tufte O.N., Stelzer E.L. Piezoresistive properties of silicon diffused lauers. – J. Appl. Phys., 1963, v. 34, 9, p. 313–318.
14. Patent RF 2043671. *Poluprovodnikovyy tenzorezistor* [Semiconductor strain gauge]. Avt. Gorbachuk N.T. / B.I. 1995, №25.
15. A.B.Renskiy and etc. *Tenzometrirovaniye stroitel'nykh konstruksiy i materialov* [Strain measuring of building structures and materials]. M.- Stroyizdat, 1977, 239p.
16. Gorbachuk N.T., Mitin V.V. Thorik Yu.A. Schwartz Yu.M. Piezo-Hall effect in p-germanium. Phys. Stat. Sol.(c) 100. 1980, p.309.
17. Gorbachuk N.T., Mitin V.V. Thorik Yu.A. Schwartz Yu.M. On determining the deformation potential constants of semiconductors of the p-germanium type from the temperature dependence of the piezoresistance. FTP, vol. 15, v. 14, p. 649, 1981.
18. Gorbachuk N.T., Shvarts Yu.M. *Vliyanie deformatsii na velichinu magnitosoprotivleniya v ob'emnom p-Ge i plenkakh p-Ge na arsenide galliya* [Effect of deformation on the magnitude of magnetoresistance in bulk p-Ge and p-Ge films on gallium arsenide]. OPT, 1984, №6, s.88.
19. Gorbachuk N.T., Mitin V.V. Thorik Yu.A. Schwartz Yu.M. *Poluprovodnikovyy termostenzodatchik* [Semiconductor thermal strain gauge]. PSU, 1984, No. 9, p. 21.
20. Gorbachuk N.T., Mitin V.V. Thorik Yu.A. Schwartz Yu.M. *P'ezogal'vanomagnitnye svoystva plenok germaniya na arsenide galliya i perspektivy ispol'zovaniya ikh v kachestve tenzorezistorov* [Piezogalvanomagnetic properties of germanium films on gallium arsenide and prospects for their use as strain gauges]. UFZh, 1984, No. 12, p. 1850.
21. Gorbachuk N.T., Mitin V.V. Thorik Yu.A. Schwartz Yu.M. *Sposob opredeleniya temperatury i deformiruyushego usiliya*. [Method for determining temperature and deforming force]. A.s. No. 932282, 05/30/82 Bulletin. No. 20.
22. Gorbachuk N.T., Sakidon P.A., Thorik Yu.A., Shvarts Yu.M. *Poluprovodnikovyy tenzorezistor* [Semiconductor strain gauge]. A.s. No. 11 16305 1984.
23. Gorbachuk N.T., Didenko P.I. *Izmeritel'nye preobrazovateli na osnove GaAs, polikremniya i dispersnogo germaniya i perspektivy ikh ispol'zovaniya* [Measuring transducers based on GaAs, polysilicon and dispersed germanium and prospects for their use]. *Perspektivnye materialy*, 2004, N 5, p.93-97.
24. Gorbachuk N.T., Didenko P.I. *Vliyanie neytronnogo oblucheniya na kharakteristiki poluprovodnikovykh izmeritel'nykh preobrazovateley temperatury, deformatsii, magnitnogo polya* [The influence of neutron irradiation on the

characteristics of semiconductor measuring transducers of temperature, strain, and magnetic field]. *Poverkhnost'*, 2005, 4, pp.57-58.

25. P. Profos. *Spravochnik «Izmereniya v promyshlennosti»* [Directory "Measurements in Industry"] 1-3 volumes. M.: *Metallurgiya*, 1990.

26. Kiknadze G.I., Plesh A.G., Safronov A.N., Gorbachuk N.T. and others. *Rezultaty eksperimental'nogo issledovaniya protsessa okhlazhdeniya model'noy seksii i eksperimental'nogo bloka sverkhprovodyashchey obmotki toroidal'nogo polya ustanovki T-15 na komplekse SIMS* [Results of an experimental study of the cooling process of the model section and the experimental block of the superconducting winding of the toroidal field of the T-15 installation on the SIMS complex]. *Preprint IAE-4320/10*, M., 1986, 24 p.

27. Belyakov V.A., Gorbachuk N.T., Didenko P.I., Filatov O.G., Sychevskiy S.E., Firsov A.A. etc. *Poluprovodnikovye izmeritel'ne preobrazovateli deformatsii, temperatury i magnitnogo polya dlya primeneniya v usloviyakh radiatsionnogo vozdeystviya, shirokom diapazone temperatur i magnitnykh poley* [Semiconductor measuring transducers of deformation, temperature and magnetic field for use in conditions of radiation exposure, a wide range of temperatures and magnetic fields]. *Voprosy atomnoy nauki i tekhniki», Seriya: Elektrofizicheskaya apparatura*, v.3(29), 2005, p.46-54.

21. Kucheruk I.M., Gorbachuk N.T., Lutsik P.P. *Zagal'niy kurs fiziki: Navchal'niy posibnik* [General course of physics: Study guide], T. 1-3. – K.: Tekhnika, 2001.

## Chapter 3. Magnetic Fields. Transducers, sensors, measurement

### 3.1. Hall sensors. Principle of operation, description, device

A Hall sensor is a device that measures the magnitude of a magnetic field using the Hall effect. Hall sensor consists of a semiconductor rectangular plate to which four electrical leads are connected. Schematically, the sensing element of a Hall sensor is shown in fig. 3.1.

Hall effect. Let the sample has the form of a rectangular plate of length  $l$ , width  $d$ , thickness  $b$  (see fig.3.1).

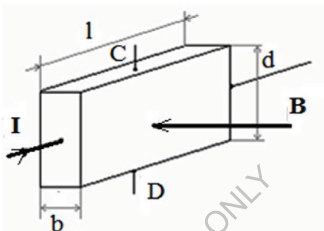


Fig. 3.1 Hall effect in a plate with a longitudinal current  $I$  and a magnetic field  $B$  perpendicular to the plate plane.

Source: built by the author.

If an electric current  $I$  is passed along the sample and a magnetic field  $B$  is created perpendicular to the plate plane, an electric field, which is called the Hall field, will appear on the side planes of the plate in the CD direction. In practice, as a rule, the Hall field is characterized by a potential difference, which is measured between symmetric points C and D on the lateral surface of the sample. This potential difference is called the Hall potential difference  $U_{hal}$  or Hall EMF  $\varepsilon_{hal}$ .

In the classical theory of conduction, the Hall effect is explained by the fact that in a magnetic field the Lorentz force acts on moving electric charges, the magnitude and direction of which are determined by the vector equation:

$$F = e [\mathbf{VB}] \quad (3.1),$$

where  $\mathbf{B}$  is the vector of magnetic field induction,  $\mathbf{V}$  is the vector of charge velocity,  $e$  is the charge of current carriers taking into account the sign.

Due to this force in the CD direction, there is a difference in the concentration of current carriers and, accordingly, an electric field. In our case,  $\mathbf{V}$  is perpendicular to  $\mathbf{B}$  and, based on the known laws of electrophysics, the Hall electric field is defined:

$$E_{hal} = F/e = VB \quad (3.2),$$

The field is related to the Hall EMF  $\varepsilon_{hal}$ , or the Hall potential difference  $U_{hal}$ , as follows:

$$\varepsilon_{hal} \approx U_{hal} = E_{hal} d = VBd \quad (3.3).$$

The force of current that flows through a unit cross-sectional area of the sample is equal to the current density:

$$J = I/S = enV \quad (3.4),$$

where  $n$  is the number of current carriers in a unit volume of the sample (concentration of current carriers).

Hence the current strength:

$$I = jbd = enVbd \quad (3.5).$$

Which makes it possible to write:

$$V = I/enbd \quad (3.6).$$

Hence:

$$\varepsilon_{hal} = IB/enb \quad (3.7).$$

Thus, the Hall EMF (or  $U_{hal}$ ) is proportional to the current strength, the induction of the magnetic field, and inversely proportional to the thickness of the sample and the concentration of current carriers in it.

It is often written:

$$\varepsilon_{hal} = R \cdot IB/b \quad (3.8).$$

Where the coefficient  $R = 1/ne$  is the Hall constant, which, for example, for semiconductors has a value from 10 to  $10^5 \text{ cm}^3/\text{Kl}$ .

### 3.2. Principle of operation of a Hall sensor

Figure 3.2 shows a typical shape of the sensing element of a Hall sensor. This type of sensing element can be made either from bulk material or based on materials in film form.

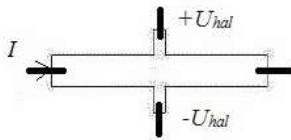


Fig. 3.2 Schematic representation of the shape of the sensing element of the Hall sensor.

Source: built by the author.

Fig. 3.3 shows the characteristic dependence of  $U_{hal}$  (potential difference in the direction of contacts CD - fig. 3.1) on the magnetic field at constant supply current.

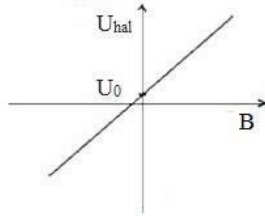


Fig. 3.3. Dependence of electric voltage on Hall contacts  $U_{hal}$  on the value of magnetic field induction  $B$ .

Source: built by the author.

In the absence of a magnetic field, the Hall EMF (potential difference) should be equal to zero. But as a result of various side phenomena (for example, insufficiently symmetrical placement of the measuring electrodes of the sensor), the measuring device can show some potential difference  $U_o$  at the output of the Hall sensor even in the absence of a magnetic field. In order to eliminate the associated errors, the value of  $U_o$  should be subtracted from the measured potential difference in the magnetic field.

One of the main characteristics of a Hall sensor is its sensitivity:

$$\gamma = \Delta U_{hal} / \Delta B \quad (3.9).$$

The sensitivity of the Hall sensor, specified in its data sheet, is used to determine the magnitude of the induction of the measured magnetic field:

$$B = U_{hal} / \gamma \quad (3.10).$$

Note that the Hall sensor measures the perpendicular (to the sensor plane) component of the magnetic field vector. Therefore, if the maximum value of the magnetic field is to be measured, the Hall sensor must be oriented accordingly.

Semiconductors InP, InSb, GaAs, Ge, Si are most often used for manufacturing Hall sensors. The use of semiconductors is due to the fact that due to the high mobility of current carriers they have a high sensitivity to the influence of the magnetic field. The sensing element of the Hall sensor can be made either of bulk material or on the basis of semiconductor films on insulating substrates. Hall sensor can have a different shape, which affects the linearity of the dependence of the output signal on the magnetic field, sensitivity. Dimensions of modern Hall sensors may not exceed 1x1x0.5 mm, supply currents are usually 1- 100 mA (depends on the input resistance of the sensor), sensitivity may reach 1000 mV/T and more, operating temperature range from -270 °C to 200 °C. In addition to sensitivity, one of the main parameters of Hall sensors are temperature dependence of sensitivity, input resistance, initial output signal  $U_o$ . In good Hall sensors they should be insignificant.

### 3.3. Modern Hall Effect Sensors

Hall sensors are produced by many companies in the world, for example, by Honeywell. DHC-0.5A sensors are known in Russia.

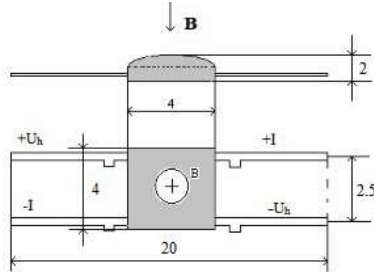


Fig. 3.4. Schematic representation of one of the sensors DHC-0.5A.

*Source: built by the author.*

Hall sensor DHC-0.5A is designed to measure the magnetic induction value on the basis of magnetic induction conversion into output voltage. The sensor is made on the basis of a planar topological structure formed on the surface of a silicon crystal.

**Main technical characteristics:**

Nominal control current is 3 mA;

Hall voltage at magnetic induction 0.25 T and rated control current - 70 mV (sensitivity  $\gamma = 280$  mV/T);

Residual voltage at rated control current - not more than 7 mV

Input resistance - 1.8 ... 3 kOhm (resistance between pins I);

Output resistance - not more than 3 kOhm (resistance between  $U_h$  pins);

Weight - not more than 2.5 g.

- $I_h$  and + $I_h$  - pins for connection of the control current source (current pins);

- $U_h$  and + $U_h$  are output signal pins (Hall pins); the resistance between the current pins is smaller than between the Hall pins.

The DHC-0.5A sensor is familiar-sensitive both in relation to the direction of magnetic induction and to the polarity of the control current.

**Magnetic field sensors (Hall sensors) based on GaAs films.** Technical characteristics of magnetic field sensors based on the Hall effect (Hall sensors) depend both on the material used and on the geometric dimensions and shape of the sensing element. The most common materials used for sensitive elements of Hall sensors are InSb and GaAs, the main advantages of which are high mobility of charge carriers, resulting in high sensitivity of sensors.

The results of the development and experimental study of metrological characteristics of magnetic field transducers (sensors) and the effect of neutron irradiation on the main parameters are presented below.

GaAs films on semi-insulating gallium arsenide were used to create sensors. The purpose of development was to create sensors with low noise levels, high linearity of dependence of the useful signal on the magnetic field, weak dependence of parameters on temperature, as well as miniaturization of the working area. Fig. 3.2 shows an approximate scheme of the sensor sensing element.

The thickness of the CaAs films varied between 0.1-5  $\mu\text{m}$ , and the current carrier concentration  $\cong 5 \cdot 10^{18} \text{ cm}^{-3}$ . The size of the working area was  $100 \times 100 \mu\text{m}$ . Depending on the thickness of the films and the concentration of current carriers, the input and output electrical resistances of the sensors varied in the range of 15 - 1500 ohms. The supply currents were 3 - 150 mA. The initial output signal  $U_o$  was within 0.01 - 5 mV, temperature dependence of  $U_o$  was less than 0.1 %/K,  $R \sim 0.08 \text{ %/K}$ , sensitivity to magnetic field was within 80 - 500 mV/T. Linearity of the output signal in the field up to 2 Tesla is not worse than 0.1%.

The sensors can operate in the temperature range of 4.2 - 400 K.

It is known, for example, that the resistance of semiconductor devices to radiation irradiation depends on the level of doping, defectivity of semiconductor material, etc. The electrophysical properties of semiconductors are most affected by neutron irradiation. Neutron irradiation has the greatest impact on the electrophysical properties of semiconductors. And the mechanism of influence is mainly in the formation of structural defects and radioactive transformation of atoms. With increasing doping level the influence of irradiation is weakened.

The characteristics of the sensors were measured at a temperature of 300 K before irradiation and after irradiation with neutron fluxes  $\Phi$  from  $8 \cdot 10^{14} \text{ cm}^{-2}$  to  $1 \cdot 10^{17} \text{ cm}^{-2}$ . The temperature during the measurements was stabilized to an accuracy of 0.1 K. The neutron energy was 1 MeV, the flux intensity was  $(2-4) \cdot 10^8 \text{ fl/s}$ .

Fig. 3.5 shows the dependence of relative change of input resistance of magnetic field measuring transducers (Hall sensors) on the value of neutron flux  $\Phi$ . Input resistance of the sensors is 1.1 kOhm, initial output signal is not more than 4.5 mV, sensitivity is 350 mV/T.

The resistance changes begin at fluxes of  $1 \cdot 10^{15} \text{ cm}^{-2}$  and amount to 15-20 %, and at  $1 \cdot 10^{16} \text{ cm}^{-2}$  the resistance increases 3.3 times. At the same time, the initial output signal at a constant supply voltage of 4.5 V changed by no more than 15%, which is equivalent to the effect of a magnetic field of up to 1 mT. At constant supply voltage the sensitivity after irradiation decreased approximately 1.4 times. After irradiation with fluxes of  $1 \cdot 10^{17} \text{ cm}^{-2}$  the resistance of sensors grows to infinity.

Thus, the magnetic field sensors are operable in a wide temperature range, have a weak temperature dependence of sensitivity and initial output signal (less than 0.1%). Nonlinearity of the output signal does not exceed 0.1% in the field up to 2T, sensitivity can reach 500 mV/T.

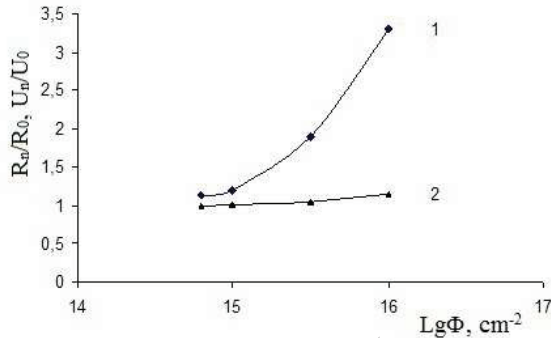


Fig. 3.5. Dependence of relative change of input resistance  $R_n/R_0$  (1) (where  $R_n$  - value of resistance after irradiation,  $R_0$  - initial resistance) and initial output signal  $U_n/U_0$  (2) (where  $U_n$  - value of output signal after irradiation,  $U_0$  - initial output signal) of magnetic field measuring transducer on the value of neutron flux irradiation.

Source: built by the author based on [7].

The studies have shown that at 300 K the developed transducers are operable up to neutron irradiation levels of  $10^{15} cm^{-2}$ . The resulting changes in the characteristics of the transducers up to levels of  $1 \cdot 10^{16} cm^{-2}$  can be accounted for to some extent, due to the fact that good repeatability of the results was observed. The transducers can be used both for diagnostics of technical devices of nuclear power engineering, cryogenic equipment, and, due to high sensitivity, in ecology for control of environmental parameters, such as electromagnetic fields, etc.

***Some characteristics of experimental magnetic field sensors (Hall sensors) based on GaAs films for cryogenic temperatures and climatic range:***

- material - GaAs
- operating temperature range 4.2 - 400 K
- supply current 1 - 100 mA
- sensitivity 60 - 500 mV/T
- initial signal within 0.010 - 5 mV
- active area of the sensor  $100 \times 100 \mu m$
- overall dimensions - at least  $1 \times 1 \times 0.4 mm$

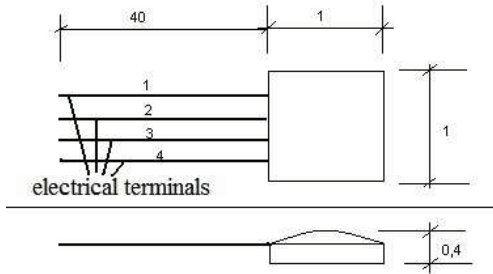


Fig. 3.6: Schematic representation of the Hall sensor. Outputs: 1,4 - supply voltage(current); 2,3 - output voltage ( $U_H$ ).

*Source: built by the author.*

### 3.4. A series of precision Hall EMF generators (Hall sensors)

The results of research and characteristics of high-precision Hall sensors based on InSb and GaAs are presented here (Zhelamsky M.V., Gorbachuk N.T. et al.). Magnetic measurements are one of the main ones in the development of electrophysical equipment utilizing magnetic fields. The small size of Hall e.m.f. generators (HGs) is an undeniable advantage among other magnetometer devices, which determines their wide application for magnetic measurements in electrophysics.

When measuring strong fields, one of the main sources of error is the influence of temperature on the HG output signal, which is insignificant against the background of a relatively large output signal. For example, in a 2 Tesla field, the HG output signal can reach 200 mV, whereas a 1°C change in temperature changes the output signal by a few microvolts. Besides, at such level of signals the temperature influence is additive with the main signal and can be compensated methodically, especially in the cryogenic region, where liquid helium is an ideal temperature stabilizer and the fields are high enough. When measuring strong fields, special attention should be paid to minimizing the planar and gradient components of the HG output signal.

In weak magnetic fields, at the level of small HG output signals, additional sources of error, such as thermoelectric (Seebeck, Peltier) effects, eigenfield effects, properties and homogeneity of the applied material are more pronounced. Therefore, for example, special measures are required to measure the magnetic field distribution in the center zone of a quadrupole magnet.

In both cases, minimization of error, calibration, directionality is also important.

The goal of the work was both to obtain the ultimate absolute sensitivity of Hall generators in measuring weak magnetic fields and to maximize the accuracy and stability of measuring strong fields.

The results of the development of magnetometer devices based on Hall generators for measuring weak magnetic fields at the level of the Earth's field are described, including both optimization of the design, manufacturing technology and electrophysical properties of HGs, and a set of circuitry, design, methodological measures aimed at achieving high accuracy and absolute sensitivity of measurements.

The developed three-component magnetic field sensors are also described.

**The main properties and features of the developed devices are analyzed.**

Two semiconductor materials were used - doped gallium arsenide (GaAs) and indium antimonide (InSb). The first one is used to obtain maximum temperature stability and linearity, the second one - for maximum sensitivity of measurements.

To improve the measurement accuracy, an optimal cross-shaped crystal shape is chosen, shown in fig. 3.7.



Fig. 3.7. Crystal (chip) of the Hall oscillator.

*Source: built by the author based on [12].*

The dimensions of the active zone of the generator are  $100 \times 100 \mu\text{m}$  and can be further reduced if necessary. Determination of the center position of the working area is performed on special equipment with accuracy not worse than  $\pm 0.5 \mu\text{m}$ , determination of the angular position of the normal to the HG plane - with accuracy not worse than  $\pm 0.1^\circ$ .

A wide range of input resistance variation (5-1500 ohm) provides the possibility of selecting the nominal current value within 1-200 mA with unchanged magnetic sensitivity to obtain the required resolution and speed of magnetic field measurements.

The value of the initial HG offset determined by the technology is - 500  $\mu\text{V}$ . Reduction of the offset to the value  $< 100 \mu\text{V}$  is provided by additional adjustment. The variation of parameters in a batch does not exceed 10%. The temperature coefficient of the initial offset voltage is determined by the HG design and can be brought to a value of less than 1-2  $\mu\text{V}/^\circ\text{C}$ .

Active thermostabilization of the HG provides stability of results at  $\pm 0.05 \text{Gs}$  over 8 h of operation. The operating temperature range is 4.2-450 K.

For precision HGs magnetic sensitivity at rated supply current is  $8 \pm 2 \mu\text{V/Gs}$  for GaAs and  $25 \pm 3 \mu\text{V/Gs}$  for InSb. High absolute sensitivity of measurements is provided due to minimization of HG and equipment noise, adopted circuitry and design measures, as well as a special algorithm.

Three-component thermostabilized assemblies were created on the basis of the described HGs. Each assembly consists of three one-component HGs assembled on the orthogonal planes of the supporting copper cube. A thermometer and heater are mounted on the free planes and used to stabilize the temperature of the assembly. The support cube on the PCB is covered with external thermal insulation and mounted on a heat-insulating stand. The main parameters of three-component HG assemblies are given in table 3.1.

Table 3.1. Basic parameters of three-component HG assemblies.  
Source: built by the author based on [12].

Parameter	Value
Assembly size	Cube with a side of 7 mm
Accuracy of determining the spatial and angular coordinates of single-component GH	$0.5 \mu\text{m}$ , 0.1 corner radius
Rated supply current	30 mA
Assembly stabilization accuracy in the range $\pm 60$	No worse $0,05 \text{ }^\circ\text{C}$
Absolute sensitivity with special equipment	$<1 \text{ mGs}$
Assembly dimensions without equipment	$20 \times 20 \times 15 \text{ mm}$

### 3.5. Estimated measurements of alternating magnetic fields in the environment

Many works are devoted to the problems of measuring magnetic and alternating electromagnetic fields. Analyzing the literature we can say that the most common methods used to measure magnetic fields are based on the phenomenon of electromagnetic induction and the Hall effect.

The induction method of measurement is based on the phenomenon of electromagnetic induction, which consists in the fact that in a conducting circuit placed in a magnetic field, under certain conditions, an electromotive force (EMF) arises, which is determined by the known expression:

$$\varepsilon_i = -N d\Phi/dt \quad (3.11),$$

where  $N$  is the number of turns in the circuit,  $\Phi$  is the magnetic flux penetrating the circuit,  $t$  is time.

The induction method can be used to measure both variable and constant magnetic fields.

To measure permanent magnetic fields, it is necessary to change one or more parameters of the induction coil (circuit) directly over time: the angle  $\alpha$  between the normal to the plane of the circuit and the vector of magnetic induction, the area of the circuit  $S$ , the relative magnetic permeability of the core  $\mu_c$ , the core demagnetization coefficient  $k$ . The value of EMF induction for these conditions can be determined by the expression

$$\varepsilon_i = -N \left( X \frac{dB}{dt} + B \frac{dX}{dt} \right) \quad (3.12),$$

where  $X = S \cdot \mu \cdot \cos \alpha / [1 + N(\mu_c - 1)]$  is the so-called generalized parameter of the induction coil, the details of which are not important for this work.

The accuracy of measuring magnetic fields using an induction sensor depends both on the design features of the sensor itself and to a large extent on the measurement scheme and the secondary equipment that determines the magnitude of the output signal.

Here it should be noted that in practice the measured signal, as a rule, does not have a correct sinusoidal form, often in the form of separate pulses, etc.

The essence of the method of measurement with the help of Hall transducers (sensors) consists in the use of the Hall effect, which consists in the occurrence of EMF  $\varepsilon_{hal}$  in the direction perpendicular to the current  $I$  in the conductor plate placed in the magnetic field  $B$ . At a constant value of current in the plate, the value of EMF is determined by the expression:

$$\varepsilon_{hal} = A \cdot I \cdot B / n \cdot e \cdot d \quad (3.13),$$

where  $A$  is a constant varying within 1...2 depending on the mechanisms of current carriers scattering,  $n$  is the concentration of current carriers in the plate material,  $e$  is the electron charge,  $d$  is the plate thickness.

Semiconductor materials are used for manufacturing Hall converters, as in them the considered effect is of the greatest importance. And recently semiconductors in the form of films on insulating substrates have been used, which simplifies the manufacturing technology, enables miniaturization, etc.

Hall transducers based on InSb, GaAs have the highest sensitivity. In addition, various technological methods are used to increase sensitivity: integrated design, use of ferromagnetic concentrators and others.

Experimental evaluation of the values of alternating magnetic fields in the environment arising during the operation of various household and industrial equipment was carried out using a manufactured induction coil and in some cases a Hall transducer based on InSb.

Measurements with the help of the induction coil were carried out after its calibration according to the simplified connection scheme. During calibration, the coil was placed in an alternating magnetic field created by a sinusoidal current  $I$  in the conductor. An alternating current generator was used for this purpose. The output signal from the coil was measured using an AC voltage voltmeter.

The magnitude of the magnetic field at a certain distance  $r$  from the conductor was calculated on the basis of the Bio-Savard-Laplace law:

$$B = -N\mu\mu_0 I / 2\pi r \quad (3.14),$$

where  $\mu$  is the relative magnetic permeability of the medium,  $\mu_0 = 4\pi \cdot 10^{-7}$  Gn/m is the magnetic constant.

The distance from the conductor, the magnitude of the current and its frequency were varied during calibration. The results were then averaged and plotted.

Fig. 3.8 shows the dependence of the resulting electromotive force in the coil (voltage  $U$  measured by a voltmeter) on the frequency of the alternating magnetic field (current in the conductor). The graph shows the recalculation of  $U$  in sensitivity to the magnetic field.

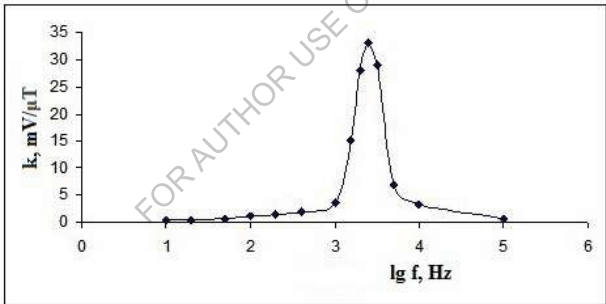


Fig. 3.8. Dependence of sensitivity  $k = \Delta U / \Delta B$  of the manufactured induction coil on the frequency of the magnetic field  $f$ .

Source: built by the author based on [16].

In the subsequent practical application of the coil, the output signal and its frequency were measured. The same voltmeter was used for the graduations and practical measurements, since its technical characteristics may influence the obtained results. According to the obtained data and the calibration curve, the value of the alternating magnetic field was determined.

A ferromagnetic concentrator was used for measurements with the InSb-based Hall transducer. As a result, the sensitivity was approximately  $1 \cdot 10^4$  mV/T and can be

increased with design improvements. The data obtained with the Hall transducers matched the induction coil measurements with an accuracy of 20%.

The determined values of alternating magnetic fields emitted by various electrical devices are summarized in Table 3.2.

Table 3.2. Results of measurements of magnetic fields of different radiation sources.

*Source: built by the author based on [16].*

<b>Object</b>	<b>Distance</b>	<b>Magnetic field value, <math>\mu\text{T}</math></b>
Supra TV	1.5 m from the screen	1-2
	3.5 m from the screen	0.03
	1.5 m from the side	5
TV Slavutich (big screen)	3 m from the screen	4
	0,2 m from the side	50
computer monitor	0,1-0,2 m from the screen	3-5
high-voltage power line (110 kV)	70-100	2-5
in - off household appliances (iron, lamp)	0.1-1.0	up to 2 (pulses)

The existing sanitary norms for permissible levels of magnetic fields, taken from various sources, are values of 0,2-0,5  $\mu\text{T}$ . It may be noted here that in the known literature the frequencies of radiation are not given, although from the physical point of view they may not affect biological objects in the same way.

Despite the rather simplified approach, the results obtained agree quite well with other known literature data. This allows us to speak about the possibility of using the described methods for indication and assessment of electromagnetic radiation levels, creation of inexpensive (household) indicators of electromagnetic radiation, as well as creation of high-precision measuring devices based on Hall transducers.

### **3.6. Automotive Hall Sensor. Hall sensor in the ignition system**

Currently, Hall sensors are widely used in the automotive industry. They are used to control the movement and rotation of various components of the car, engine vibrations, in the ignition system and others.

Probably the most famous is the automotive Hall sensor used to control and ensure the operation of the car ignition system. The scheme of its device is shown in fig. 3.9.

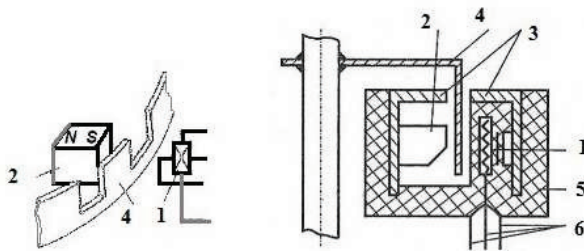


Fig. 3.9. Schematic representation of the device of the automobile Hall sensor. 1- sensitive element of the Hall sensor, from which leads to the output signal processing chip go, 2 - permanent magnet, 3 - magnetic conductors, 4 - rotor blades, 5 - plastic housing, 6 - leads from the sensor.

*Source: built by the author based on Transducer instructions.*

The sensor consists of a sensing element 1 (Hall sensor directly) and a microcontroller 1 integrated with it (microcircuit for processing the output signal from the Hall sensor). As a result, the automotive Hall sensor has three contacts 6 (terminals) for connection into the electrical circuit (circuit) of the vehicle. The automotive Hall sensor for the ignition system also has a permanent magnet 2, which is separated by a gap from the sensing element of the Hall sensor, and magnetic wires. The magnetic field of the permanent magnet is able to induce an output signal from the Hall sensor, and the metal blades 4 of the rotating shaft, overlapping (shunting) the magnetic flux will lead to a corresponding change (oscillation) of the output signal. Further, the output signal is connected with the system of ignition spark supply at the desired moment of the shaft position.

#### **How do I check the Hall sensor?**

There are several ways to check if your car's Hall sensor is working properly. One of the simplest is the following. Connect the automotive Hall sensor according to the diagram as shown in fig. 3.10. The removed Hall sensor can be powered by a Krona battery (9 V). To measure the output signal (voltage)  $V$ , it is best to use a compact digital multimeter. If the magnetic flux through the sensing element of the Hall sensor changes (e.g., by rotating the rotor shaft or simply by bridging the gap with a metal plate), the output signal from the sensor will also change, which will indicate its operability. The output signal may vary depending on the sensor model, but is typically between 0.5 and 1.0 V.

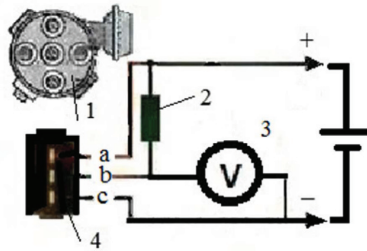


Fig. 3.10. Checking the Hall sensor. General chem. 1 - distributor sensor, 2 - resistor of 2 kOhm, 3 - voltmeter (digital multimeter), 4 - connector of distributor sensor (Hall sensor).

Source: built by the author.

### 3.7. Magneto-resistive transducers. Magneto-resistive effect

The change in the magnetic field resistance of a conductor (semiconductor) in which an electric current flows is called the magneto-resistive effect. The increase in electrical resistance under the action of a magnetic field occurs both in the case of perpendicularity of the magnetic induction vector to the surface of semiconductor plates (transverse magneto-resistance) and in the case of parallel (longitudinal magneto-resistance). However, the resistance changes in the second case, as a rule, insignificantly.

The change in the semiconductor resistance in a magnetic field  $B$  is proportional to the square of the mobility  $\mu$  of current carriers:

$$\Delta\rho/\rho = c \mu^2 \cdot B^2 \quad (3.15),$$

where  $c$  is the proportionality coefficient related to the scattering of charge carriers.

In a semiconductor plate placed in a magnetic field, a Lorentz force proportional to the electric Hall field acts on the moving charge carriers. However, the Hall field equilibrates only those carriers traveling at medium velocities. In slower media the Hall field is greater, in fast media the Lorentz force is greater. The trajectory bends and the effective free path length decreases, resulting in increased drag. Obviously, the smaller the Hall effect in a semiconductor, the greater the resistance. In a semiconductor with two types of carriers, the Hall field is smaller, so the current lines are not parallel to the faces, and the magneto-resistance effect is correspondingly larger.

To eliminate the influence of the Hall effect, it is possible to use special geometrical shapes of samples in a semiconductor with a predominance of one type of carriers. The most obvious example of the influence of the structure on the

magnetoresistance effect is the Corbino disk, which is a semiconductor plate with a concentric arrangement of contacts: one in the center and the second on the circumference at equal distances from the first. If voltage is applied to the electrodes of such a disk, the trajectories of electrons will look like radial rays coming from the center. When placed in a magnetic field perpendicular to the plane of the plate, the carriers are deflected along the surface, the current lines are elongated, but the accumulation of charges does not occur, and the Hall EMF does not arise. In this structure, the maximum magnetoresistance effect is observed, but due to technical difficulties, the practical application of the Corbino disk is very difficult.

### 3.8. Magnetoresistor designs

The effect of increasing magnetoresistance due to resistor geometry can also be achieved in a semiconductor wafer whose length  $L$  is much smaller than its width  $W$ . When the plate is subjected to a magnetic field whose direction is perpendicular to the plate plane, the Hall voltage is attenuated due to the shunt effect of the current electrodes. Geometrically, the magnetoresistance effect in this case is stronger the smaller the  $L/W$  ratio. To further increase the effect, resistors with a small  $L/W$  ratio are connected.

The basis of the magnetoresistor material is usually indium antimonide, which has a high mobility of current carriers, to which 1.8% NiSb is added. After melting and subsequent cooling, nickel antimonide crystallizes into indium antimonide in the form of needles with a thickness of  $1\ \mu\text{m}$  and a length of about  $50\ \mu\text{m}$ , arranged parallel to each other and perpendicular to the current direction. The conductivity of the NiSb needle is about  $10^4\ \text{ohm}^{-1}\cdot\text{cm}^{-1}$ , while that of InSb is two orders of magnitude smaller.

Thus, the needles play the role of good conducting electrodes dividing the bulk of the semiconductor into separate regions with a small  $L/W$  ratio. This leads to a sharp suppression of the Hall field and, consequently, to the curvature of electron trajectories under the action of the magnetic field, i.e., to an increase in the magnetoresistance effect.

Another way to realize this principle on the basis of microelectronic technology. Its essence lies in the formation of magnetoresistors based on silicon epitaxial film containing low-resistance shunt sections of polycrystalline silicon (PS) located perpendicular to the current direction.

The fabrication technology of such a magnetoresistive material is based on the simultaneous growth of mono- and polycrystalline silicon (PS) films. By means of oxidation and photolithography processes, local  $\text{SiO}_2$  regions are formed in which PC films grow during epitaxial film growth.

To close the Hall EMF, the PS regions are doped with phosphorus atoms up to the concentration of  $10^{21} \text{ cm}^{-3}$ , and, taking into account the higher diffusion rate of the dopant atoms in PS compared to single-crystal silicon, doping is carried out simultaneously with the process of film creation in single-crystal n+ - regions under ohmic contacts.

FOR AUTHOR USE ONLY

## Bibliography

1. O.K.Homeriki. *Poluprovodnikovye preobrazovateli magnitnogo polya* [Semiconductor transducers of magnetic field]. M.- *Energoatomizdat*, 1986, 136 pp.
2. Vikulin I.M., Stafeev V.I. *Fizika poluprovodnikovyykh priborov* [Physics of semiconductor devices]. M.: *Radio i svyaz'*, 1990. 264 p.
3. Belyakov V.A., Gorbachuk N.T., Didenko P.I., Filatov O.G., Sychevskiy S.E., Firsov A.A. etc. Poluprovodnikovye izmeritel'ne preobrazovateli deformatsii, temperatury i magnitnogo polya dlya primeneniya v usloviyakh radiatsionnogo vozdeystviya, shirokom diapazone temperatur i magnitnykh poley [Semiconductor measuring transducers of deformation, temperature and magnetic field for use in conditions of radiation exposure, a wide range of temperatures and magnetic fields]. *Voprosy atomnoy nauki i tekhniki*, Seriya: Elektrofizicheskaya apparatura, v.3(29), 2005, p.46-54.
4. N.Gorbachuk, M.Larionov, A.Firsov, N.Shatil Semiconductor Sensors for a Wide Temperature Range. *Sensors & Transducers Journal and Magazine*, Vol. 162, Issue 1, January 2014, pp.1-4.
5. Kulakov V.M., Ladygin E.A., Shekhovtsov V.I. et al. *Deystvie pronikayushchey radiatsii na izdeliya elektronnoy tekhniki*. Moskva [Action of Penetrating Radiation on Electronic Equipment Products]. Moscow: *Sov. radio*, 1980. 224 p.
6. Gorbachuk N.T., Didenko P.I. *Izmeritel'nye preobrazovateli na osnove GaAs, polikremniya i dispersnogo germaniya i perspektivy ikh ispol'zovaniya* [Measuring transducers based on GaAs, polysilicon and dispersed germanium and prospects for their use]. *Perspektivnye materialy*, 2004, N 5, p.93-97.
7. Gorbachuk N.T., Didenko P.I. *Vliyanie neytronnogo oblucheniya na kharakteristiki poluprovodnikovyykh izmeritel'nykh preobrazovateley temperatury, deformatsii, magnitnogo polya* [The influence of neutron irradiation on the characteristics of semiconductor measuring transducers of temperature, strain, and magnetic field]. *Poverkhnost'*, 2005, 4, pp.57-58.
8. Henrichsen K. N. Classification of magnetic measurement methods //CERN acceleration schol. Magnetic measurement and alignment. Montreux. Switzerland. March, 1992 , p.70-83.
9. Berkes B. Hall generators //CERN acceleration schol. Magnetic measurement and alignment. Montreux. Switzerland. March, 1992 , p.167-192.
10. Afanasyev Yu V., Sludentsov N. V., Shchelkin A. P. *Magnitometricheskie preobrazovateli, pribory, ustanovki*. L.: [Magnetometric transducers, devices, installations]. L.: *Energiya. Leningradskiy filial*. 1972.- 272p.

11. Knoopers H. G. et al. Third round of the ITER strand bench mark test // Proceedings of EUCAS-97. P. 1271-1274.

12. Zhelamskii M.V., Sychevskii S.E., Filatov O.G., Gorbachuk N.T. et al. *Ryad pretsizionnykh generatorov E.D.S. Kholla* [A Range of Precision E.D.S. Hall Oscillators]. *Voprosy atomnoy nauki i tekhniki. Seriya: Elektrofizicheskaya apparatura*, v. 1(27), 2002, pp.9-14.

13. V.V.Panin, B.M.Stepanov. *Izmerenie impul'snykh magnitnykh i elektricheskikh poley* [Measurement of Pulsed Magnetic and Electric Fields]. – *Moskva: Energoatomizdat*, 1987. - 120 p.

14. I.A.Bolshakova, M.R.Gladun, R.L.Golyaka and others. *Mikroelektronnyye sensornyye ustroystva magnitnogo polya: Monografiya / Pod red. Z.Ya. Gotri* [Microelectronic sensor devices of the magnetic field: Monograph / Edited by Z.Y. Gotri]. – *L'vov: Izdatel'stvo Natsional'nogo universiteta «L'vovskaya politekhnika»*, 2001. - 412 p.

15. Gorbachuk N.T., Firsov A.A.. *Datchiki magnitnogo polya (datchiki Kholla) na osnove plenok GaAs* [Magnetic field sensors (Hall sensors) based on GaAs films]. *Mezhdunarodnaya nauchno-prakticheskaya konferentsiya «Perspektivnyye innovatsii v nauke, obrazovanii, proizvodstve i transporte '2010»* [International Scientific and Practical Conference "Perspective Innovations in Science, Education, Production and Transportation '2010"]. *Sbornik nauchnykh trudov*, vol.6, pp.24-25, June 21-30, 2010, Odessa.

16. N.T. Gorbachuk, P.I. Didenko. *Otsenochnyye izmereniya peremennykh magnitnykh poley v okruzhayushchey srede* [Estimated measurements of alternating magnetic fields in the environment]. *Mezhdunarodnaya nauchno-prakticheskaya konferentsiya «Nauchnyye issledovaniya i ikh prakticheskoe primeneniye. Sovremennoye sostoyaniye i puti razvitiya '2010»* [International Scientific and Practical Conference "Scientific Research and its Practical Application. Modern state and ways of development '2010"]. *Sbornik nauchnykh trudov*, vol.3,p.40-41, October 4-15, 2010, Odessa.

17. Amoskov V.M., Vasiliev V.N., Gorbachuk N.T., Sychevsky S.E. et al. 16. *Pretsiionnyy trekhkomponentnyy magnetometr na generatorakh e.d.s. Kholla dlya izmereniya slabnykh magnitnykh poley* [Precision three-component magnetometer on Hall e.d.s. generators for measurement of weak magnetic fields] // *Giroskopiya i navigatsiya* [Gyroscopy and Navigation], No. 4(31), 2000. p. 56.

18. Filatov, O.G.; Soldatenkov, V.A.; Sychevskiy, S.E.; Gorbachuk, N.T., et al. *Sistema elektromagnitnogo pozitsionirovaniya dlya sistemy pritselivaniya i indikatsii, ustanovlennoy na shleme* [Electromagnetic Positioning System for Helmet Mounted Targeting and Indication System]. *Elektronika: Nauka, tekhnologii, biznes*. [Electronics: Science, Technology, Business]. 5/2003, p.62-67.

19. Filatov O.G., Sychevskiy S.E., Gorbachuk N.T., et al. *Razrabotka pretsizionnykh datchikov fizicheskikh velichin na osnove optimizirovannykh magnitnykh tsepey* [Development of precision sensors of physical quantities on the basis of optimized magnetic circuits]. *Nauchno-tekhnicheskiy zhurnal «Aviakosmicheskoe priborostroenie»* [Scientific and Technical Journal "Aviakosmicheskoe Instrument Engineering"], 2004, N 5, pp. 7-13.

20. Zhelamskiy M.V., Konstantinov A.B., Sychevskiy S.E., Gorbachuk N.T., et al. *Odnokomponentnyy pervichnyy preobrazovatel', odnokomponentnyy datchik, trekhkomponentnyy pervichnyy preobrazovatel' i trekhkomponentnyy datchik magnitnogo polya, rabotayushchie na effekte Kholla*. [One-component primary transducer, one-component sensor, three-component primary transducer and three-component magnetic field sensor operating on the Hall effect]. Russian Federation patent №2001115570.

21. Gorbachuk N.T., Mitin V.V. Thorik Yu.A. Schwartz Yu.M. Piezo-Hall effect in p-germanium. *Phys. Stat. Sol.(c)* 100. 1980, p.309.

22. Gorbachuk N.T. *Chuvstvitel'nost' magnitosoprotivleniya i khollovskoy podvizhnosti v slabolegirovannom p-Ge k izmeneniyu kontsentratsii primesi* [Sensitivity of magnetoresistance and Hall mobility in lightly doped p-Ge to changes in impurity concentration]. *UFZh*, 1984, No. 6, P.92.

23. Gorbachuk N.T., Shvarts Yu.M. *Vliyanie deformatsii na velichinu magnitosoprotivleniya v ob'emnom p-Ge i plenkakh p-Ge na arsenide galliya* [Effect of deformation on the magnitude of magnetoresistance in bulk p-Ge and p-Ge films on gallium arsenide]. *OPT*, 1984, No. 6, p. 88.

24. Mykola Gorbachuk. ELECTROTECHNICAL MATERIALS. LAP LAMBERT Academic Publishing. 120 High Road, East Finchley, London, N2 9ED, United Kingdom, 2024, 112p. ISBN: 978-620-3-46212-8.

25. Sominskiy M.S. *Poluprovodniki* [Semiconductors].- L. Nauka 1967. 439p.

26. Kucheruk I.M., Gorbachuk I.T., Lutsik P.P. *Zagal'niy kurs fiziki: Navchal'niy posibnik* [General course of physics: Study guide], T. 1-3. – K.: Tekhnika, 2001.

27. Baranochnikov M.L. *Mikromagnitoelektronika* [Micromagneto-electronics]. Tom 1. DMK.-M.:2001.

## Chapter 4. Humidity, gases. Methods of measuring humidity.

### Hygrometer

The air around us contains some amount of water vapor (water molecules). The maximum possible amount of water vapor in the air (air saturation with water vapor) depends on temperature. The number of molecules in saturating water vapor increases with increasing temperature. Saturation water vapor is formed, for example, at the surface of water when the temperatures of water and air are equal - equilibrium occurs: the number of evaporating water molecules equals the number of condensing molecules.

In general, normal air at a given temperature does not contain saturating water vapor. But when the air temperature changes (drops, e.g. at night), unsaturating water vapor can change to saturating water vapor - the dew point. The dew point is the temperature at which the water vapor in the air becomes saturating.

According to the level of water vapor content, air is characterized by humidity. Absolute humidity  $\rho$  is the amount of water vapor contained in 1 cubic meter at a given temperature. Relative air humidity  $f$  is the ratio of absolute humidity to the amount of vapor  $\rho_o$ , which is necessary to saturate 1 cubic meter of air at a given temperature (i.e. the amount corresponding to the dew point condition for a given temperature. the value of  $\rho_o$  can be found in the relevant tables):

$$f = (\rho/\rho_o)100\% \quad (4.1).$$

Instruments for measuring humidity are called hygrometers. Currently, the following methods and instruments for measuring air humidity are mainly used.

#### 4.1. Hygrometers

**Dew point hygrometers.** A small mirror cooled (e.g. by means of a Peltier element) is placed in the flow of the gas under investigation. With the help of a photocell, which detects the formation of dew on the mirror, its temperature is regulated. Having measured the temperature, the dew point is determined. There are hygrometers that use electrodes instead of a mirror, the conductivity of which changes as a result of misting.

**Psychrometer.** An instrument consisting of two thermometers, one humidified and one ordinary. By analyzing the difference in the thermometer readings, the dew point is determined. The lower the saturation of air with water vapor, the more intensively water will evaporate from the surface of the humidified thermometer and the lower its temperature and the greater the difference between the readings of the two thermometers.

**Electrolysis hygrometer.** A measured stream of air (gas) is passed near platinum electrodes with phosphorus pentoxide, which absorbs water. When a voltage is applied to the electrodes, the water decomposes into hydrogen and oxygen. The electrolysis current is proportional to the amount of water absorbed, i.e. absolute humidity.

**Infrared hygrometer.** By measuring the absorption of infrared radiation, absolute humidity is determined.

**Electric hygrometers with a conductive film.** Depending on the amount of absorbed water vapor, the electrical resistance of the conductive film changes. Having calibrated the film it is possible to determine the absolute humidity of the gas under study.

**Hair hygrometers.** In such hygrometers the elongation of defatted human hair is measured and air humidity is determined. Elongation under the influence of humidity can reach up to 2.5%.

**Hygrometers with a bimorph element.** The basis of such a hygrometer is a metal coil spring, covered on one side with a moisture-absorbing substance. Under the influence of absorbed water, the substance expands and changes the geometric parameters of the spring. By calibrating it is possible to determine the humidity of air (gas).

**Conductive film hygrometer.** Water absorbed by certain materials can affect the electrophysical properties of these materials. This phenomenon is the basis of the conductive film hygrometer. Depending on the level of humidity of air (gas) in hygrometers with a conductive film, the electrical resistance of the film - the sensitive element of the hygrometer - changes.

This type of hygrometer measures the relative humidity of the air, which is one of the main advantages, since relative humidity depends very little on temperature. The disadvantage is the need to calibrate each hygrometer and not high stability of such calibration. The calibration may shift as a result of ion deposits on the film when it comes into contact with dust and other gas constituents. In addition, the hygrometer does not have a high output signal power, which is also a disadvantage. The signal power of the hygrometer can be increased by increasing the size of the sensing element, but at the same time it loses speed and hysteresis appears.

A conductive film hygrometer consists of a sensing element - a layer of hygroscopic substance applied to an insulating substrate. Oxides of some metals and other materials are often used as hygroscopic substance (hygrometer sensing element). Electrical contacts are made, as a rule, in the form of comb. As the humidity of the gas and, accordingly, of the sensing film increases, its electrical resistance decreases. The dependence in most cases is exponential.

A hygrometer with a conductive film has a sufficiently low inertia and is often used to determine small values of air (gas) humidity.

#### **4.2. Resistive gas analysis. Gas concentration transducer**

A **resistive oxygen concentration transducer**, such as a titanium oxide-based transducer, can serve as the basis for an exhaust gas analyzer (sensor). Titanium oxide is a substance whose resistance varies according to the number of oxygen molecules adsorbed on its surface.

The transducer is made, for example, of platinum wire or a thin film resistor, the surface of which is coated with titanium oxide. Depending on the oxygen content of the exhaust gas, the titanium oxide layer changes its resistance and therefore the overall resistance of the device.

Other substances are used in resistive gas analyzers to determine the content of other gases. There are also resistive transducers for the detection of propane and methane. Resistive transducers usually have two sensing elements, one coated with a substance and the other uncoated. This is used as a temperature compensating element when measurements are made with the transducer included in a bridge circuit.

There are resistive gas analyzers and gas sensing elements based on their sensitivity to changes in the thermophysical characteristics of the surrounding gases.

For example, a sensing element based on the change in electrical resistance of metals with temperature. The sensitive element of such a transducer (catarometer) is made of a sufficiently long metal wire connected to a source of electric voltage. The wire is in the flow of the analyzed gas. The amount of current flowing and heating the wire is controlled with high accuracy. As the concentration of the surrounding gas changes, the thermal conductivity of the gas changes accordingly. As a result, the heat transfer between the wire and the surrounding gas changes. Accordingly, the temperature of the wire and its electrical resistance change. This leads to a change in the value of the electric current, which is detected by the measuring device.

## Bibliography

1. Jan F.Kreider. Handbook of Heating, Ventilation, and Air Conditioning. - Taylor & Francis, 2019, 680p.
2. Kucheruk I.M., Gorbachuk I.T., Lutsik P.P. Zagal'niy kurs fiziki: Navchal'niy posibnik [General course of physics: Study guide],T. 1-3. – K.: Tekhnika, 2001.
3. Sominskiy M.S. *Poluprovodniki* [Semiconductors].- *L. Nauka* 1967. 439p.
4. P. Profos. *Spravochnik «Izmereniya v promyshlennosti»* [Directory “Measurements in Industry”] 1-3 volumes. M.: *Metallurgiya*, 1990.

FOR AUTHOR USE ONLY

## Chapter 5. Light. Transducers, photocells

### 5.1. Photoconductivity

While in metals - conduction is observed at various temperatures, the conductivity of semiconductors under ordinary conditions arises only through thermal motion. However, it is possible to create conditions that ensure the appearance of conductivity in a semiconductor and without increasing its temperature. Since the electrical conductivity of the semiconductor arises only due to the fact that the electrons fall into the conduction zone, it is enough to give the electrons the energy needed to throw them into the free zone to appear conductivity. This energy in normal conditions electrons receive from other particles involved in thermal motion, but the energy can also come from outside, in particular, for example, in the form of radiation.

As early as last century, it was discovered that the resistance of a selenium stick changes dramatically depending on its illumination. Careful studies have shown that the resistance of selenium decreases with illumination.

Later it was established that this property is possessed not only by selenium, but also by some other semiconductors. The emergence of quantum mechanical concepts made it possible to explain this phenomenon, which was named photoconductivity or internal photoeffect in science.

The physical nature of photoconductivity is as follows. At a certain temperature in a darkened semiconductor some number of electrons  $n$  is in the free zone. These electrons account for the normal electrical conductivity of the substance, otherwise called dark conductivity. If the semiconductor is then exposed to light, then in the free zone, in addition to the previously existing there dark electrons, a new number  $n_l$  of light electrons will appear and the total number of electrons in the zone will become equal to  $n + n_l$ . The electrical conductivity in this connection will increase and become equal to:

$$\sigma = neU + n_l eU_l, \quad (5.1)$$

where the first summand corresponds to dark conduction, and the second - to photoconductivity,  $e$  - electron charge,  $U$  - mobility of current carriers (electrons).

From the general ideas about the nature of semiconductors, the reason for the appearance of photoelectrons in the free zone becomes clear. There is no doubt that the supplier of both dark and light electrons in an impurity-free semiconductor is a filled zone. It is clear that both those and other electrons got into the free zone only because they received the energy necessary for them to overcome the forbidden zone

"with a width of  $\Delta E$ . Consequently, photoconductivity has arisen due to the fact that the photons falling on the surface of the semiconductor and absorbed by it have given all their energy to the photoelectrons. Each photon carries an energy  $h\nu$ . If this energy is greater than the energy  $\Delta E$  or at least equal to it, then the electron from the filled zone can move to the conduction zone. From this follows an indispensable consequence: photoconductivity is possible when  $h\nu > \Delta E$ . Thus, for each photosensitive substance there is a different limit of photoconductivity, corresponding to the following condition:

$$h\nu_0 = \Delta E \quad (5.2).$$

If the frequency  $\nu$  of radiation incident on the semiconductor is less than  $\nu_0$ , photoconductivity does not occur.

Only radiation with frequency  $\nu > \nu_0$  can create photoconductivity.

The limit of the photoeffect (red limit), i.e. the value of  $\nu_0$ , depends on the semiconductor itself, in which the photoeffect is observed, whether it is impurity-free or not.

Photoconductivity, or internal photoeffect, does not occur in all semiconductors. Regardless of this indispensable condition for the emergence of photoconductivity is the absorption of matter incident on it radiation. Only in this case, in principle, can the photoeffect arise.

Experiments of physicists have established that in their behavior photoelectrons do not differ from thermal electrons up to almost complete coincidence of their mobility.

A careful study of the internal photoeffect has shown that the change in resistance in different substances occurs under the action of radiation of different spectral composition: in some substances it is observed when the substance is illuminated by ultraviolet rays, in others - when illuminated by visible or infrared rays.

The electrons released by light are in the free zone for a very short period of time. During this time they wander in the interatomic gaps and in the presence of a potential difference between two points of the semiconductor move mainly in one direction, thus forming an electric current. The photoelectrons then move to lower impurity levels or to the filled zone. However, with continuous illumination of the semiconductor, more and more photoelectrons appear, and during the same time some number of them return back. As a result, a dynamic equilibrium is established, i.e. the number of emerging photoelectrons becomes equal to the number of electrons returning back.

In the free state, photoelectrons are in the free state for a very short time (on the order of  $10^{-3}$  to  $10^{-7}$  seconds). But during this short period of life they are full-fledged conduction electrons. Semiconductor substances significantly increase their

electrical conductivity not only under the action of radiation. Any other particle entering the atom and giving all its energy to the electron, in principle is able to transfer the electron into a free state. And indeed, numerous, repeated experiments have shown that conduction also occurs when the surface of a substance is bombarded by fast electrons, alpha-particles, protons and other particles. It is clear that for this purpose the energy of the bombarding particle must be greater than the energy of transfer of the electron to the free state.

In semiconductors, the concentration of conduction electrons at room temperature is much smaller than in metals, and the number of photoelectrons appearing under the influence of light is relatively large. Under appropriate illumination in some substances, such as cadmium sulfide (CdS), the number of photoelectrons can exceed the number of dark conduction electrons by four orders of magnitude. In other less photosensitive substances, the number of photoelectrons, even if not under too intense irradiation, can reach 20-30% of the total number of conduction electrons. This property of some semiconductors makes them important and necessary in various conversion technologies.

## **5.2. The photoeffect of the confinement layer**

In Section 5.1 it was shown that under the action of absorbed light, electrons can move from the filled zone to the free zone, thus creating photoconductivity. In this case, only additional conduction occurs in the semiconductor, but no intrinsic electromotive forces are generated. However, another phenomenon is open and known - the appearance of electromotive forces as a result of illumination of the semiconductor. For example, if we subject the semiconductor to uneven illumination so that some parts of the sample illuminated much stronger, and others much weaker, it is possible in some cases to detect some potential difference between light and dark areas. This phenomenon is explained by the fact that at the moment of illumination the electrons begin to diffuse from the illuminated parts to the dark parts in greater numbers than in the opposite direction. Such preferential diffusion leads to the fact that the dark areas in the case of the electronic conduction mechanism are gradually charged negatively, while the light areas are positively charged. As a consequence, a gradually increasing electric field is formed inside the semiconductor, which will eventually establish an equilibrium state characterized by the fact that the electronic fluxes in both directions are equal.

When the equilibrium occurs, between the light and dark parts of the semiconductor will exist a certain potential difference, up to tenths of a volt.

**In addition, the manifestation of the effect of light on the semiconductor exists in the so-called locking layer photoeffect.**

If we create the structure shown in fig. 5.1, it is possible to observe experimentally the photoeffect of the locking layer.

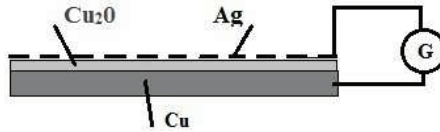


Fig. 5.1. Photo effect of the barrier layer. Schematic of the material structure.

*Source: built by the author.*

If we oxidize a copper plate Cu and form a layer of copper oxide  $\text{Cu}_2\text{O}$  on it, we get a classical semiconductor. Then let's put a thin layer of silver on top of the  $\text{Cu}_2\text{O}$  semiconductor. The thin silver layer will be transparent to light. If we connect a galvanometer between the silver layer and a copper plate (see fig. 5.1), a current will flow in the circuit when the silvered surface is illuminated. This phenomenon is explained by the existence of a so-called barrier layer in the metal-semiconductor system.

In this case, under the influence of light, electrons pass from the copper oxide through the barrier layer into the copper. As a result, the copper plate is negatively charged and the transparent silver electrode is positively charged. When the circuit is closed, a current is induced in the circuit. A similar phenomenon can be observed in other semiconductors. This effect is particularly pronounced in systems containing such semiconductors as sulfur-thallium, sulfur-silver, selenium, germanium, silicon, and others.

The valve photoeffect (blocking layer photoeffect) refers to the appearance of electromotive force at light absorption in a system containing the contact of two impurity semiconductors of different conductivity or in the semiconductor-metal system (fig. 5.2).

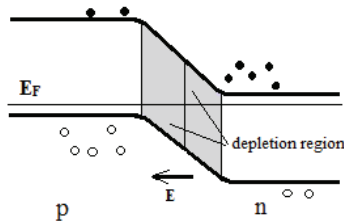


Fig. 5.2. General energy diagram of a  $p$ - $n$  junction (locking layer).

*Source: built by the author.*

When such a system is illuminated, the absorbed light transfers electrons from the valence band to the conduction band. At that, holes are formed in the valence zone, i.e. electron-hole pairs are generated. The behavior of nonequilibrium carriers depends on the region of the system in which the radiation is absorbed. If the radiation is absorbed in the  $p$ -region, the electrons near the  $p$ - $n$  junction can reach it and under the action of the contact electric field will move to the  $n$ -region.

If radiation is absorbed in the  $n$ -region, only holes are ejected through the  $p$ - $n$  junction into the  $p$ -region.

If the pairs are generated in the bulk charge region ( $p$ - $n$  junction), the field "distributes" the charge carriers in such a way that they end up in the region where they are basic.

In this case, electrons are concentrated in the  $n$ -semiconductor, while holes are concentrated in the  $p$ -semiconductor.

The electric field created by them grows, which prevents further transition of non-basic carriers through the confinement layer.

There comes a dynamic equilibrium, in which the number of non-basic carriers moving per unit time through the locking layer is equal to the number of the same carriers moving for the same period of time in the opposite direction.

With the onset of equilibrium, a potential difference is established between the  $p$ - and  $n$ -semiconductors, representing the photoelectromotive force.

The phenomenon of the emergence of valve photo-EMF at illumination of the  $p$ - $n$  junction is used to create photodetectors and photovoltaic energy converters - solar batteries.

This is the mechanism of the photoelectromotive force in a system consisting of  $p$  and  $n$  semiconductors and a locking layer between them.

The valve photoeffect is especially active in semiconductor systems with a large diffusion length of "non-main" current carriers and, accordingly, a large time of their life.

From the consideration of the mechanism of occurrence of the valve photoelectromotive force it is clear that the electrode directly contacting the electron semiconductor is always negatively charged, while the electrode directly contacting the hole semiconductor is positively charged. Therefore, in different types of valve cells, the top translucent electrode can be positively or negatively charged.

The discovery of the locking layer photoeffect expanded the possibilities of practical use of semiconductors and formed the basis for the device of valve photovoltaic cells - devices that convert the energy of light into electrical energy.

### 5.3. Solar battery

The solar cell was the name given to the first silicon-based photovoltaic cell. The photocell is a converter of solar (light) energy into electrical energy.

The electrical conductivity of silicon, depending on the grade and the number of impurities introduced into it, varies within a fairly wide range. For many years silicon has been the object of comprehensive physical research. As a result of many years of research work have been obtained results of great value for both theory and practice.

An important result should be considered the development of technology for introducing impurities of foreign atoms into single crystals of silicon, allowing to obtain in one crystal  $p-n$  - junction, on the basis of which was created a silicon photocell with a locking layer. A solar battery was created on the basis of such photocells.

The technology of silicon photocell manufacturing is rather complicated. Nowadays, modern planar microelectronics technologies are used for this purpose.

Individual photovoltaic cells can be connected with each other in series and in parallel, thus obtaining a photovoltaic (solar) battery. Such a solar battery can be used to power household appliances, portable electronics, etc. The first solar cells have already been created.

Practically already the first created silicon photovoltaic cells had an efficiency of about 6%. For comparison it is possible to bring that steam engines have efficiency of about 6-8%. In addition, it should be borne in mind that, unlike other energy converters, the service life of semiconductor cells can be very long.



Fig. 5.3. Modern portable solar battery - battery (solar charger).  
*Source: built by the author based on Transducer instructions.*

### 5.4. Bolometers

A bolometer is a device by means of which radiation energy can be measured with a high degree of accuracy. Most bolometers are based on the principle of converting radiant energy into heat energy. With the discovery of the electrophysical

properties of semiconductors, they were utilized for bolometer technology and greatly increased the sensitivity limit of bolometers.

Bolometers are widely used for a wide variety of purposes. Bolometers are of exceptional value when it is necessary to perform any spectrometric studies.

The principle circuit of an ordinary bolometer is a bridge, one arm of which includes a sensitive thermal resistor. When some thermal radiation falls on the thermistor, it raises its temperature, as a result of which the equilibrium of the bridge is disturbed and the arrow of the measuring instrument, pre-programmed in the appropriate units, will deviate by the appropriate number of divisions. The thermistor is often placed in a metal or glass vacuum cylinder with a window made of some transparent material. On the outer part of the cylinder leads from the thermistor to include it in the circuit.

The sensitivity of modern bolometers is  $10^1\text{-}5\cdot 10^3$  V/W. Bolometers are used to record optical radiation of the infrared range. They are very sensitive to thermal radiation and are mainly used for recording IR radiation with wavelengths from 10 to 5000  $\mu\text{m}$ .

### 5.5. Selenium photocells

The first photocell was made of copper oxide and was in use for a number of years. Almost at the same time, the selenium cell was discovered, which was much more widespread and has not lost its importance today.

The technology of manufacturing a selenium photocell has undergone significant changes.

Any photocell with a locking layer is a system consisting of a metal substrate, a semiconductor layer and a top metal semitransparent electrode.

The substrate of the future photocell performs two functions. On the one hand, it is a holder of the fragile selenium layer, protecting it from mechanical damage, and on the other hand, it is used to make a reliable electrical contact. The disk-shaped side of the substrate on which the selenium layer is applied is ground so that the selenium layer adheres well to the steel disk. The ground substrate is suspended inside the vacuum unit.

The selenium layer is applied by vacuum evaporation.

To obtain photovoltaic cells with good parameters it is necessary that the thickness of the semiconductor layer is equal to 0.1 mm.

The deposited selenium is in amorphous modification, has a very high resistivity and does not yet have the required photovoltaic properties. Therefore, at the next stage of the technological process selenium is converted from amorphous to crystalline modification, which has a high photosensitivity. For this purpose, a disk

with selenium deposited on it is removed from under the hood and placed in a special furnace. With the help of a certain technological process in the furnace, amorphous selenium is transformed into crystalline selenium.

The top translucent metal electrode is usually applied by cathode sputtering.

Finished disks of the photocell are assembled in an ebonite or plastic mandrel with two clamps led outside.

## 5.6. Selenium photoresistors

The electrical resistance of a sample of semiconductor material decreases under the influence of light radiation, but no EMF or electric current is generated in it.

Thus, photoresistance is a semiconductor device that changes its electrical resistance under the action of light.

From the previous consideration of the physical essence of the internal photoeffect, the fundamental structure of the photo-resistance becomes clear. A photoresistance is a plate (in most cases a thin layer of semiconductor), on the edge areas of which metal electrodes are applied to ensure reliable electrical contact. Such a photoresistance is included in a circuit in series with the power supply.

When the photoresistance is darkened, an electric current flows in the whole circuit, and therefore in the photoresistance itself, the value of which is determined by the ohmic resistance of the photoresistance and the potential difference applied to it. Such current is called dark current. At illumination of photoresistance, the current increases and this increase is the greater, the greater the light flux. The difference between light and dark currents gives us the value of photocurrent.

Depending on their purpose, photo resistors are made of different semiconductor materials. The sensitivity of photo resistors is much higher than the sensitivity of vacuum photocells with external photoeffect. It means that at the same illumination photo-resistance provides several times more increase of current in the circuit in comparison with a photocell with external photoeffect. The essential disadvantage of the majority of the first created photo resistors was a significant inertia, while the vacuum photoelectric cell with external photoeffect is practically inertia-free device.

The second significant disadvantage of photoresistors is the nonlinear dependence of photocurrent increase on the increase of light flux intensity. Fig. 5.4 shows the dependence of photocurrent on light flux.

Nowadays, new semiconductor materials, which are largely deprived of these disadvantages, are obtained, new types of photoresistors with improved parameters are designed. Most recently, physicists have succeeded in resolving many difficulties

and obtaining photoresistors largely free from the disadvantages inherent in their predecessors.

Depending on the substance from which photoresistors are made, they have different spectral characteristics and different integral sensitivity. Spectral sensitivity characterizes the amount of photocurrent arising from the action of a unit of light energy flux of a certain wavelength. Thus, if the integral sensitivity of a photocell can be determined by one number - the value of photocurrent attributed to the unit of incident energy, the spectral sensitivity of each photocell is usually depicted in the form of a graph. The first photoresistance was made of selenium, which played a major role in the history of science and technology.

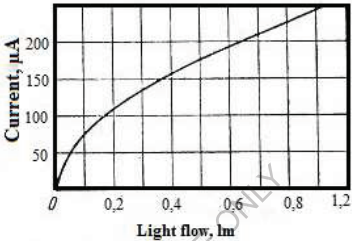


Fig. 5.4. Dependence of photocurrent on light flux. Example of light characteristic of selenium photoresistance.

Source: built by the author based on [6].

**5.7. Photoelectric transducers. General principles of operation**

Photoelectric transducers are such primary measuring transducers that react to electromagnetic radiation falling on the surface of the converting element. Radiation can be visible, i.e. light, as well as having a longer or shorter wavelength and being invisible.

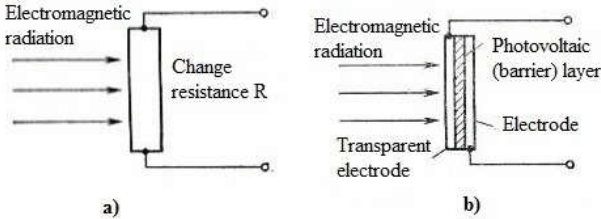


Fig. 5.5. Examples of photoconverters. a) - photoconductive conversion, b) - solar cell as an example of photovoltaic conversion.

Source: built by the author based on [7].

**Photoconductive converters.** These converters turn the change of the measured quantity into the change of resistance of the used material (fig. 5.5.a). Such converters are called passive converters, i.e., they require external power. Often their name characterizes the type of conversion used, such as light-sensitive resistors.

The resistance of a material is a function of the density of basic charge carriers, and since the density increases with increasing radiation intensity, the conductivity increases. Since conductivity is inversely proportional to resistance, it can be concluded that resistance is an inverse function of irradiation intensity. The value of resistance at full irradiation is generally 100- 200 ohms, and in total darkness this resistance is megaohms. Cadmium sulfide, cadmium selenide, etc. are used in the design of light-dependent resistors.

**Solar cells.** Solar cells are photovoltaic converters that convert electromagnetic energy into electrical energy (fig. 5.5.b).

The converter design includes a layer of photosensitive high resistivity material placed between two conducting electrodes. One of the electrodes is made of a transparent material through which radiation passes and hits the photosensitive material. When fully illuminated, a single cell produces an output voltage of about 0.5 V between the electrodes.

As a rule, semiconductor valve photovoltaic cells (photovoltaic cells with a locking layer) are used as a photovoltaic layer (fig. 5.5.b).

One of the most important parameters of a photovoltaic cell used as a source of electrical energy is the efficiency factor (EF). The efficiency of a solar cell is the ratio of the maximum power of electric current that can be obtained from the cell to the power of light radiation falling on the cell. The efficiency will be the greater the greater the part of the spectrum of light radiation is involved in the generation of current carriers. One of the ways to increase the efficiency of solar cells is to create photocells with the widest possible spectral characteristics. Photocells made of silicon have efficiency up to 12%. Photocells based on gallium arsenide compounds have efficiency up to 20%.

**Photodetectors.** Semiconductor transducers designed to measure changes in the parameters of light radiation are called photodetectors. A photoelectric transducer, which is the simplest type of photodetectors, is a semiconductor diode. One of the main among such transducers is the photodiode, which utilizes the effect of irradiating a negatively biased *p-n* junction with light (visible or other wavelengths). In the presence of irradiation, the current flowing through the junction changes. The response time of such a photodiode is only a few nanoseconds.

To provide a faster response to changes in radiation parameters, PIN-diodes have been developed in which there is a layer of impurity-free semiconductor between the *p*- and *n*-type layers.

**Phototransistors.** In a number of devices photodiodes are used together with amplifiers to increase sensitivity. But there are devices that combine these properties - phototransistors. They are made in a transparent housing that allows light radiation to pass through. Light falling on the collector-base junction of the phototransistor ( $p$ - $n$  junction with negative bias) causes a photocurrent in the base, which is amplified with the gain of the transistor, resulting in a very large emitter current.

Since photodetectors are semiconductor devices, their saturation current is temperature dependent. In the absence of light radiation, a dark current flows in them, which limits measurements of low levels of light radiation.

**Photoresistors. Characteristics of photoresistor.** The value of dark resistance depends on the shape, size, temperature and physicochemical nature of the photosensitive layer of the photoresistor. Very high dark resistance (from  $10^4$  to  $10^9$  Ohm at  $25^\circ\text{C}$ ) possesses photoresistors based on PbS, CdS, CdSe. The dark resistance of InSb, InAs, CdHgTe ( $10$  to  $10^3$  Ohm at  $25^\circ\text{C}$ ) is not very high. The irradiated photoresistor resistance decreases rapidly with increasing irradiation (fig. 5.6).

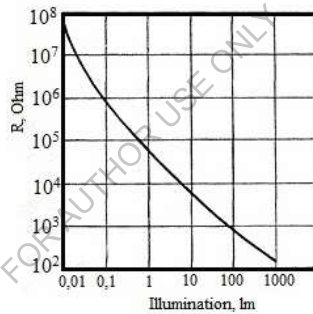


Fig. 5.6. Example of dependence of photoresistor resistance on illumination.

Source: built by the author based on [6].

## 5.8. Valve photocells. Designs

The construction of all photocells with a locking layer is practically the same. There can be some differences, but they do not change the general character of photocell construction. The shape of the photocell, its dimensions, methods of application of the upper electrode, the output of such electrodes, etc. may vary.

Usually manufacturing of the valve photocell (fig. 5.7) begins with the so-called lower electrode - a metal plate 1-2 mm thick, on which a thin layer of semiconductor is applied. The semiconductor layer is then treated to create a  $p$ - $n$  junction in its thickness. After that, a top metal electrode, which is a thin translucent layer of metal that transmits light, is applied to the outer surface in most cases.

A valve photocell includes a lower metal electrode, an electron (or hole) semiconductor layer, a locking layer, a hole (or electron) layer, and an upper metal semitransparent electrode (fig. 5.7).

The photocell is placed in a plastic case with electrical leads and a window for light.

The radiant flux falling on the surface of the photocell is partially reflected from the semitransparent metal electrode and partially absorbed in it. Part of the flux that has passed through the electrode is absorbed in the semiconductor layer adjacent to it. As a result, electron-hole pairs arise in this layer. Electrons are concentrated at the electrode covering the semiconductor layer, which has an electronic conduction mechanism, and holes are concentrated at the electrode of the hole semiconductor.

Between the lower and upper electrode there appears a potential difference, the value of which up to a certain limit will be the greater, the greater the intensity of the radiant flux. By closing the electrodes of the photocell by an external circuit, we create conditions for the flow of electric current in it. This will be the case while the photocell is illuminated, and in the range of small light fluxes with a limit value of 1 lumen, the short-circuit current of the photocell depends almost linearly on the intensity of the light flux. When an external resistance is included in the circuit of the photocell, this linearity is broken.

Scientists are constantly researching and making efforts to obtain photocells from new materials with significant integral sensitivity and to make the photocell sense not only the entire visible part of the spectrum, but also possibly more invisible - infrared and ultraviolet.

Photovoltaic processes occurring in valve photocells have a noticeable inertia, which affects the shape of their frequency characteristics. The strong decrease in the yield of most valve cells with increasing frequency limits their use in cases of variable light fluxes of relatively high frequency.

Valve photovoltaic cells are made of different photosensitive semiconductor materials. Selenium photocells are widely used. The spectral characteristic of selenium photocell is close to the sensitivity of human eye, the maximum of spectral sensitivity is in the region of 5500-6000 Å (0,55 - 0,6 μm), i.e. lies in the visible part of the spectrum (fig. 5.8). The integral sensitivity of the selenium photocell reaches 600 μA/lm, i.e. exceeds the sensitivity of photocells with external photoeffect.

Silver sulfide (Ag<sub>2</sub>S) photocells - PCSS - are even more widespread. Integral sensitivity of PCSS reaches 9000 μA/lm, rather wide spectral characteristic (from 0.4 to 1.4 μm) with maximum sensitivity in the near infrared region (0.8 - 0.9 μm). Sulfur-silver photocells have high stability in operation.

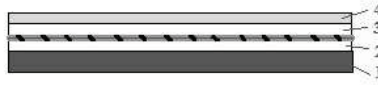


Fig. 5.7. Schematic structure of a valve photocell: 1 - lower metal electrode; 2 - electron (hole) semiconductor layer; 3 - hole (electron) semiconductor layer; 4 - upper metal semiconductor electrode. The area with dashes is the locking layer.

Source: built by the author.

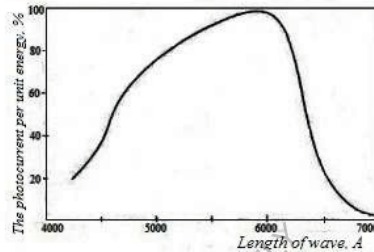


Fig. 5.8. Spectral characteristic of a selenium photocell. Pure selenium.

Source: built by the author based on [7].

## 5.9. LEDs

Emission in LEDs is due to recombination of injected carriers in one part of the  $p$ - $n$  junction. Recombination occurs when carriers move from upper levels to lower levels. Interzone transitions between the minimum of the conduction band and the maximum of the valence band are accompanied by effective emission if the transitions are direct, i.e., the minimum and maximum are located at the same value of the wave vector  $k$ . Such transitions are realized, for example, in gallium arsenide at  $k = 0$ .

The main characteristic of LEDs is internal quantum efficiency  $\eta_{iqe}$  (the ratio of the number of photons generated to the number of carriers injected into the base) and external  $\eta_{eqe}$  (the ratio of the number of photons leaving the LED to the total number of charge carriers flowing through it).

The decrease in  $\eta_{eqe}$  is caused by radiation-free recombination at defects in the structure and photon absorption in the semiconductor itself (self-absorption), since the photon energy is close to  $E_g$ .

Significant  $\eta_{vnt}$  (up to 20-28%) are possessed by the most widespread nowadays LEDs created by epitaxial build-up of gallium arsenide doped with silicon ( $p$ -type) on  $n$ -GaAs. This is due to both the greater perfection of the crystal structure and the fact that the region of the highly silicon-compensated semiconductor emits

light quanta with energies of 1.31 ... 1.34 eV, lower than  $E_g$  of uncompensated gallium arsenide, which reduces self-absorption when radiation is emitted through the  $n$ -region.

Many problems of LEDs are also solved by the use of modern heterojunctions.

Table 1 summarizes the main materials currently used to create LEDs with the best performance in the corresponding spectral regions. Parameter  $\eta_{\text{leqe}}$  significantly depends on the technology and with the growth of its level can be significantly increased.

LEDs are widely used in digital indicators and light displays for measuring instruments and computer output devices, as well as in optoelectronics devices. Compared to conventional light sources, LEDs have small overall dimensions, low operating voltages, high speed (up to  $10^{-9}$  s) and long service life.

Table 5.1. Some materials used to create LEDs.

Source: built by the author based on [6,7,5].

Material	Impurity or composition	Glow color	$\lambda_{\text{max}}$ , nm	$\eta_{\text{leqe}}$
GaAs	Si, Zn	IR	950 900	12-50
GaP	Zn, O, N	Red green	690 550	7 0,7
GaAs <sub>1-x</sub> P <sub>x</sub>	x=0,39 x=0,5-0,75	Red amber	660 610	0,5 0,04
Ga <sub>1-x</sub> Al <sub>x</sub> As	x=0,05-0,1 x=0,3	IR red	800 675	12 1,3
In <sub>1-x</sub> Ga <sub>x</sub> P	x=0,58  x=0,6	Red Amber yellow-green	659 617 570	0,2 0,1 0,02

### 5.10. Semiconductor lasers. $P$ - $n$ -junction laser

The principle of operation of a semiconductor laser is as follows. In an intrinsic semiconductor, there are always electrons thermally abandoned from the valence band in the conduction band. When light passes through the semiconductor, the electrons in the valence band absorb quanta of light and can move to the conduction band if the frequency of the incident light is:

$$\nu \geq E_g/h \quad (5.3),$$

where  $E_g$  is the width of the forbidden zone,  $h$  is Planck's constant. Therefore, the intensity of light will decrease after passing through the semiconductor.

Simultaneously, the radiation incident on the semiconductor stimulates the transitions of excited electrons from the conduction band to the valence band and the emission of light quanta (fig. 5.9.a). These quanta are added to the external radiation as it passes through the semiconductor, i.e. light amplification occurs.

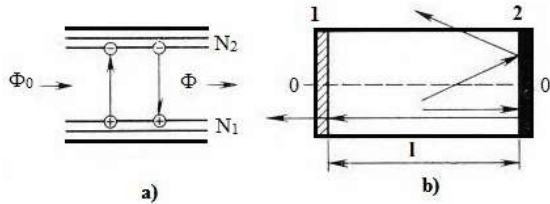


Fig. 5.9. Interzone transitions under the action of radiation on a semiconductor - a, diagram of a semiconductor laser - b.

Source: built by the author based on [5].

Transitions occurring under the influence of external radiation are called induced in contrast to spontaneous transitions occurring independently of external radiation. In a state of thermodynamic equilibrium, the number of electrons in the valence band is many times greater than in the conduction band. Hence, absorption of light dominates over amplification. For light amplification, it is necessary to create such conditions in which the concentration of electrons near the bottom of the conduction zone will be greater than their concentration near the ceiling of the valence zone ( $N_2 > N_1$ ). Such a state of the semiconductor is called a state with level population inversion.

The light amplification factor  $\alpha$  when light passes through a semiconductor depends on the difference between the populations of the upper and lower levels. Since the probabilities of upward and downward electron transitions are equal, the amplification occurs when the population difference between the upper and lower levels  $N_2 - N_1 > 0$ .

The attenuation of light passing through a semiconductor is caused not only by electron transitions from the valence band to the conduction band, but also by scattering of light on various inhomogeneities of the crystal. As a result, the intensity of light changes with distance  $x$  inside the semiconductor according to the law:

$$\Phi = \Phi_0 \exp(\alpha - \chi_l)x \quad (5.4),$$

where  $\alpha$  is the gain coefficient, the coefficient  $\chi_l$  characterizes losses,  $x$  is the distance.

Thus, a semiconductor crystal amplifies external radiation if there is a level population inversion in it and the gain exceeds the loss coefficient ( $\alpha > \chi_l$ ).

In order to turn an amplifier into a radiation generator, it is necessary to introduce positive feedback, i.e., to feed a part of the radiation from the output to the input. In lasers, to create feedback, the working crystal is placed between two parallel mirrors (1 and 2 in fig. 5.9.b). The light passing through the crystal will be amplified  $\exp(\alpha - \chi_{ls})^l$  times, then reflected from the mirror, passed through the crystal again and amplified again by the same factor, etc. The primary quanta of light arise due to spontaneous transitions, and then there is amplification of light during its propagation in the crystal due to induced transitions.

Population inversion of semiconductor levels can be created by several methods. One of them is to irradiate the semiconductor itself with intense light (optical pumping). Electrons from the valence band move to the conduction band and accumulate there. If the pumping intensity is sufficiently high, level population inversion can occur. Another method is the transfer of electrons from the valence band to the conduction band by bombarding the semiconductor with fast electrons. With both methods it is possible to obtain high emission powers, but in general the efficiency of the devices is low.

The *p-n* junction laser has the highest efficiency and simplicity of design. The laser action is based on the fact that at direct bias electrons are injected into the *p*-region, where their radiative recombination with the holes present there takes place. To create a state with population inversion, a large concentration of holes in the valence band is required, which is achieved by increasing the concentration of doping acceptor impurity. In order that the injection of electrons into the *p*-region exceeded the injection of holes into the *n*-region (where the recombination is radiationless), it is necessary that the concentration of donor impurity in the *n*-region was higher than the concentration of acceptor impurity in the *p*-region, i.e.,  $n_n > p_p$ .

Thus, to obtain a state with population inversion in the *p*-region, a high degree of doping of both regions of the *p-n* junction with impurities is required.

The best material for laser diodes is gallium arsenide. The thickness of the emitting part of the *p*-region is of the order of 2  $\mu\text{m}$ . Laser diode is the first laser in which it was possible to realize direct conversion of electrical energy into energy of coherent light radiation. It also has the highest efficiency and high speed performance.

Basically, the main reason for the decrease in efficiency of the laser diode is the need for strong doping of the *p*- and *n*-regions of the transition. Simultaneously with the introduction of impurities in the semiconductor, a large number of defects are formed in the active region, which leads to significant radiation losses. In addition, defects can form energy levels in the forbidden zone of the semiconductor. Since the concentration of impurities in both parts of the *p-n* junction is large, the width of the *p-n* junction is small, and consequently, current carriers can move from

the conduction band to these levels and then tunnel into the valence band of the  $p$ -region. The tunneling current is not coupled to radiation and this also degrades the efficiency.

Laser diodes can be used in light locators for observation and photography in the dark, in range finders, and for communications, among others.

FOR AUTHOR USE ONLY

## Bibliography

1. John Kimbala, Mehmet Kanoglu. Fundamentals and Applications of Renewable Energy. - McGraw-Hill, 2019, 416p.
2. David L. Greenaway, Gunter Harbeke. Optical properties and band structure of semiconductors. Pergamon Press Ltd., Headington Hill Hall, Oxford 4&5 Fitzroy Square, London W.I. 1968, 172p.
3. Paul Holmes, Shalve Mohile, Shantanu Mohile. Solar Power for Beginners: How to Design and Install the Best Solar Power System for Your Home (DIY Solar Power) Kindle Edition. 2020, 179p, ISBN-13 979-8642013625
4. Nsakalagos L., Balch J., Fronheiser J., Korevaar B.A., Sulima O., Rand J. Silicon nanowire solar cells//Appl. Phys. Lett. – 2007. – Vol. 91. – P. 233117(1)-233117(3).
5. Vikulin I.M., Stafeev V.I. *Fizika poluprovodnikovyykh priborov* [Physics of semiconductor devices]. M.: *Radio i svyaz'*, 1990. 264 p.
6. Sominskiy M.S. *Poluprovodniki* [Semiconductors].- *L. Nauka* 1967. 439p.
7. P. Profos. *Spravochnik «Izmereniya v promyshlennosti»* [Directory "Measurements in Industry"] 1-3 volumes. M.: *Metallurgiya*, 1990.
8. Mykola Gorbachuk. ELECTROTECHNICAL MATERIALS. LAP LAMBERT Academic Publishing. 120 High Road, East Finchley, London, N2 9ED, United Kingdom, 2024, 112p. ISBN: 978-620-3-46212-8.
9. Kucheruk I.M., Gorbachuk I.T., Lutsik P.P. *Zagal'niy kurs fiziki: Navchal'niy posibnik* [General course of physics: Study guide], T. 1-3. – K.: *Tekhnika*, 2001.

## Chapter 6. Ionization transducers. Sensors

### 6.1. pH transducers

Ionization transducers convert a change in a measured quantity into a change in, for example, an ionization current that flows through a liquid placed between two electrodes (fig. 6.1). A typical example of the use of the ionization principle is an instrument for measuring the acidity of a solution. The degree of acidity of a solution is determined by the concentration of positively charged hydrogen ions in it, called the hydrogen potential (better known by the abbreviation  $pH$ ). Moreover:

$$pH = -\log[H^+], \quad (1)$$

where  $H^+$  is the concentration of hydrogen ions in grams per liter.

The  $pH$  value is 0 for a purely acidic solution, 7 for a neutral solution (such as pure water), and 14 for a purely alkaline solution.

A typical  $pH$  probe has electrodes in gelatin with a known value of hydrogen potential. They are formed by a special glass membrane which, is in contact with the solution whose  $pH$  value is being measured. The potential difference between the two electrodes reflects the  $pH$  value of the solution (about 59 mV per  $pH$  unit).

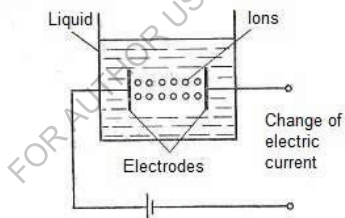


Fig. 6.1 Ionization transformation, in which ions migrate in liquids to electrodes and act as charge carriers, creating an electric current.

*Source: built by the author.*

### 6.2. Ionization chambers. General principles of operation

An instrument (sensor) with an ionization chamber consists of a chamber  $K$  with one inner and one outer electrode, a voltage source, an indication system (indicating device)  $G$  and a measuring resistor  $R$  or measuring capacitor  $C$  (fig.6.2). The ionization current (flux density or dose rate) is measured by the value of the voltage drop across the high-resistance resistor  $R$ . The charge measurement as an integral of current over time (flux or dose measurement) is determined by the charging of capacitor  $C$ .

Depending on the required sensitivity and geometric fit to the measurement task at hand, various ionization chambers are used. The measurement range of detectors based on the ionization chamber principle covers values from fractions of micrograys to thousands of grays ( $\mu\text{Gy/h}$  to  $\text{kGy/h}$ ).

When filled with air, ionization chambers are suitable by definition for ion dose measurement. However, for this purpose it is necessary to use special constructions excluding or compensating the influence of ionization chamber walls limiting the air volume. Many measuring chambers have been developed for practical measurements. When using them, along with sensitivity, measurement range and reproducibility of the obtained results, the following considerations should be taken into account:

1. The energy dependence of sensitivity shows to what extent the measured value depends on the radiation energy. Typical examples of this energy dependence for different types of radiation detectors are shown in Fig. 6.3.

2. The dependence of sensitivity on the direction of flight of particles (rays) is due to the detector design itself. Depending on the direction of incidence of rays it is necessary to introduce corrections, which in turn may depend on the energy of radiation.

3. Dependence of sensitivity on temperature and pressure is manifested in the fact that in case of unsealed ionization chamber systems, the calculated mass changes with air temperature and pressure. This also necessitates a correction factor by which the reading must be multiplied to obtain the correct value of the measured quantity, if the sensitivity of the measuring system has not been adjusted in advance using a reference current.

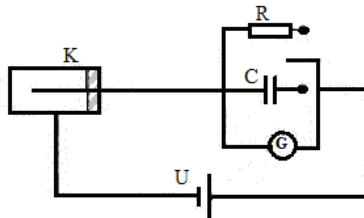


Fig. 6.2. Principle scheme of ionization chamber for measuring dose rate or absorbed dose.

*Source: built by the author.*

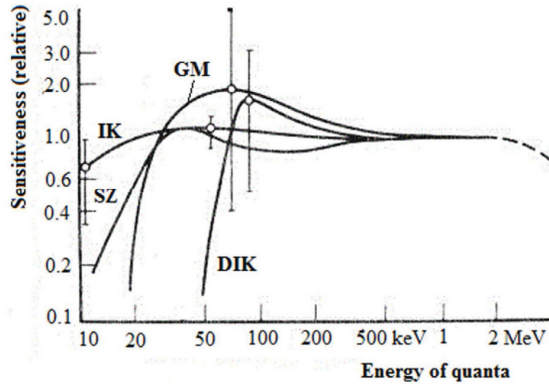


Fig. 6.3. Typical dependences of sensitivity of different radiation detectors on energy level (average values for a large number of individual detectors) and maximum spreads in the critical region. GM - Geiger-Muller counter; IK - ionization chamber; SZ - scintillation counter; DIK - high-pressure ionization chamber.

Source: built by the author based on [7].

### 6.3. Ionization measuring transducers

Fig. 6.4 shows the structural diagram of one of the ionization transducers with radioactive isotope. The device is designed for continuous thickness measurement of a moving belt or, for example, rolled steel.

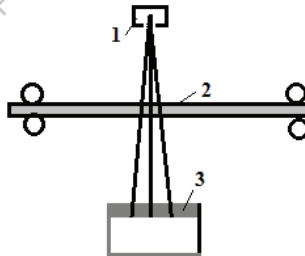


Fig. 6.4. Schematic of the ionization transducer for tape thickness measurement.

Source: built by the author.

The principle of operation of the device is as follows. Radioactive radiation of isotope 1 is partially absorbed by the product 2. The amount of energy received by the indicator 3 depends on the material and thickness of the product. Indicator 3

through an amplifier is connected to the measuring system calibrated in values of the measured value.

Fig. 6.5 shows schematics of devices of level gauge and gas pressure meter working on the ionization principle.

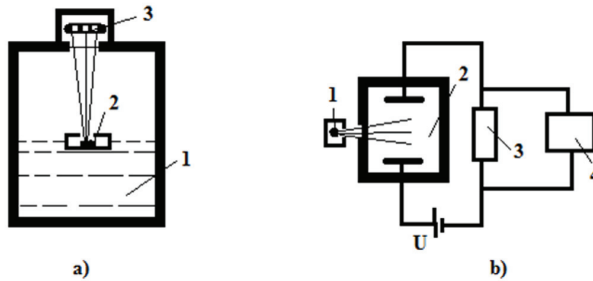


Fig. 6.5. a - scheme of ionization level gauge, b - scheme of gas pressure measuring device.

*Source: built by the author.*

Float 2 with radioactive isotope floats on the surface of liquid 1 (fig. 6.5.a). The indicator 3, perceiving radiation, is located above the float. When the liquid level changes, the distance from the radiation source to the indicator and, consequently, the amount of energy received by the indicator change. Thus, the liquid level is monitored.

Fig. 6.5.b shows the structural diagram of the ionization gas pressure meter. Under the influence of radioactive radiation of isotope 1, gas ionization occurs in vessel 2. Depending on the gas pressure, the ionization intensity changes. Consequently, the ionization current flowing through the circuit under the action of the applied voltage  $U$  changes. The measuring device is connected to the resistance 3, the voltage drop on which is created by the ionization current.

Ionization gas analyzers have a similar device.

#### 6.4. Ionization chamber. Radioactive radiation. Counters

In the simplest case, the ionization chamber is a device consisting of two metal plates insulated from each other and separated by a gas gap (fig. 6.6).

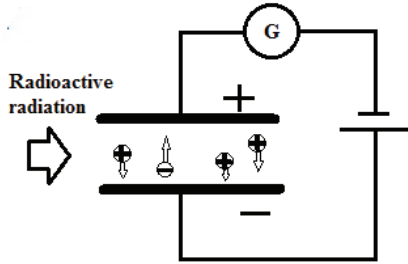


Fig. 6.6. Schematic and principle of operation of an ionization chamber.

*Source: built by the author.*

Any air condenser can act as ionization chambers. The space between the plates is called the working volume of the chamber. If a constant voltage is applied to a plate, a space with an electric field is formed, the lines of force of which are directed from the positive plate to the negative plate. A force will act on an electrically charged particle placed in the electric field and it will move along a trajectory that coincides with the direction of the electric field lines. The direction of motion of positively charged particles coincides with the direction of the field lines. Negative particles move in the opposite direction.

Let us consider the processes occurring in the working volume of the ionization chamber. In the absence of voltage on the electrodes of the chamber, ions and electrons formed in the working volume as a result of radioactive radiation move randomly together with neutral atoms, some of which will reach the electrodes. If a small constant voltage is now applied to the electrodes, under the influence of the electric field the ions and electrons acquire a directed motion corresponding to the field lines (fig. 6.6). The electrons move toward the positively charged anode plate and the positive ions toward the negatively charged cathode plate. The speed of motion of heavy positive ions is thousands and tens of thousands times less than the speed of light electrons.

At low voltage, the electrode field is weak and the particles move slowly. Therefore, most of them recombine and do not reach the electrodes. They turn into neutral gas particles. As a result, the current in the external circuit will be very small.

The strength of the ionization current is equal to the total electric charge contributed by charged particles to the electrode surface during one second. The more ions going to the electrode, the greater the current. This current is recorded using any electrical instrument connected to the chamber circuit.

As the voltage applied to the plates increases, the electric field strength increases, and an increasing number of charged particles, which have not had time to

recombine, fall on the electrodes. The current strength in the external circuit increases (fig. 6.7, from O to A).

Then at some voltage  $U_1$  the electric field strength increases, so that all charged particles formed by the external ionizer in the working volume of the chamber will fall on the electrodes. In this case, the current in the external circuit is determined only by the ionization capacity of the radiation. If the ionization capacity of the radiation does not change, the current in the chamber does not change (curve A-B). This current is called the saturation current of the chamber.

When the voltage is further increased to  $U_2$ , the current flowing in the chamber circuit begins to increase again, slowly at first and then faster and faster (part of the curve above the dot). This is due to the fact that at voltages above  $U_2$  the electric field strength inside the chamber increases so that the electrons gain velocities sufficient to ionize the neutral gas atoms when they meet. Therefore, the current in the external circuit is determined by the total amount of charges formed under the influence of the external ionizer and under the action of ionizing electrons trapped inside the working volume of the chamber.

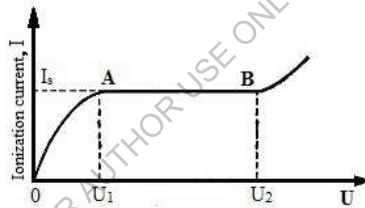


Fig. 6.7. Volt-ampere characteristic of an ionization chamber.

*Source: built by the author.*

The curve of dependence of the ionization current of the chamber on the magnitude of the applied voltage is called the volt-ampere characteristic.

Ionization chambers usually operate in the saturation region of the current. Since the magnitude of this current is proportional to the number of ions produced, it can serve as a measure of the ionization capacity of the radiation.

Depending on their use, ionization chambers are of two types:

- A chamber used to measure the total ionization caused by the passage through it of a significant number of ionizing particles is called an integrating ionization chamber. The magnitude of the saturation current is equal to the product of the number of pairs of ions produced per second per cubic centimeter of the chamber, its bias, and the charge of each ion. Consequently, the saturation current value can serve as a measure of radiation dose.

- The second type is counting ionization chambers, which can be used to test and determine the ionization capacity of any single ionizing particle (e.g. an  $\alpha$ -particle) captured in the working volume of the chamber.

**Geiger-Muller ionization chamber.** Figure 6.8 shows a device consisting of a metal cylinder, on the axis of which a wire filament is stretched on insulators. Such a device is called a gas-discharge counter. Figure 6.8 shows the cross section of the counter. The cylinder is connected to the negative terminal of the battery and it is called the cathode. The anode is connected through the load resistance.

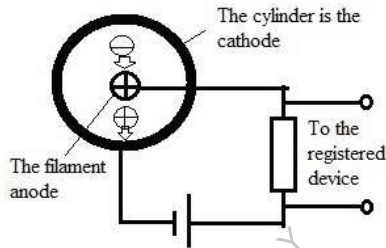


Fig. 6.8. Schematic and operation of the ionization counter.

*Source: built by the author.*

If an ionizing particle passes through the working volume of the counter, positive ions and electrons will appear in the chamber, which under the action of the electric field move to the electrodes: electrons to the filament, ions to the cylinder. A current pulse will flow in the external circuit, which forms a voltage drop pulse on the load resistance. This voltage pulse can be recorded with a recording device.

The amount of electricity in the current pulse depends on the magnitude of the applied voltage. In general, this dependence is shown in fig. 6.7, and the physical principles of operation of the meter are similar to those of the ionization chamber (fig. 6.6).

Depending on the applied voltage, the counter can operate as an ionization chamber, a proportional counter, and a gas-discharge Geiger-Muller counter. However, in practice they are three types of different devices with different designs and depending on the intended use apply one or another device.

**Meter designs. Gamma counter design.** The designs of gas-discharge counters are constantly being improved and changed. The counters can be divided into several groups: gamma counters, so-called beta-gamma counters, counters for soft  $\beta$ -particles, which in their design should have a window for the passage of soft  $\beta$ -particles, counters of photons (quanta of light) and others.

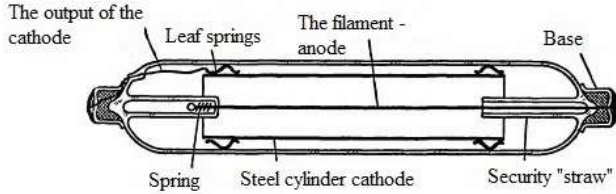


Fig. 6.9. Schematic view of gamma counter in section.

*Source: built by the author based on Sensor instructions.*

The gamma counter device is quite simple. A gamma counter with argon content is shown in fig. 6.9. Here a thin-walled cylinder - stainless steel cathode is inserted into a glass cylinder. The contact is led out of the cylinder with a molybdenum wire. A metal filament (anode) is attached to the axle. The meter is filled with a mixture of halogens (neon-argon-bromine) and can be used in both pulse (counting) and current modes. This meter belongs to the STM (steel meter) series.

In pulse mode, the meter has a very long service life. STM series counters will allow counting rates of one hundred thousand pulses per minute and above; this maintains the proportionality between irradiation intensity and counting rate up to two hundred thousand pulses per minute.

This count rate characteristic corresponds to a dose of about 0.25 (R / h). The dose rate up to which the count rate remains directly proportional to it, as well as the value of the maximum dose of the counter operation in the current mode, depend on the geometrical dimensions. The smaller the cathode diameter and operating length, the larger the dose limit and the longer the proportionality between the count rate and the radiation dose rate is maintained.

When selecting the working length, the working length ratios are adjusted in the meter to be at least twice the cathode diameter. With a smaller working length, the meter also works, but the potential spark discharge value increases dramatically.

For example, for a counter with a cathode diameter of 10 mm at a working length equal to 5 diameters (50 mm), at a certain gas filling, the starting voltage is 400 V, at a working length equal to two cathode diameters - 405, at a working length equal to one cathode diameter - 450 V, and at a working length equal to 0.5 cathode diameter, the ignition potential increases to 500 V.

As the working length of the filament decreases, both the counting plateau length and the characteristics decrease.

## Bibliography

1. Radiation Technologies and Applications in Materials Science. Edited by Subhendu Ray Chowdhuru. -Taylor & Francis, 2022, 396p. ISBN 9781032343945
2. Mykola Gorbachuk. ELECTROTECHNICAL MATERIALS. LAP LAMBERT Academic Publishing, 120 High Road, East Finchley, London, N2 9ED, United Kingdom, 2024, 112p. ISBN: 978-620-3-46212-8.
3. Kucheruk I.M., Gorbachuk I.T., Lutsik P.P. *Zagal'niy kurs fiziki: Navchal'niy posibnik* [General course of physics: Study guide],T. 1-3. – K.: *Tekhnika*, 2001.
4. Vikulin I.M., Stafeev V.I. *Fizika poluprovodnikovoykh priborov* [Physics of semiconductor devices]. M.: *Radio i svyaz'*, 1990. 264 p.
5. Sominskiy M.S. *Poluprovodniki* [Semiconductors].- L. *Nauka* 1967. 439p.
6. P. Profos. *Spravochnik «Izmereniya v promyshlennosti»* [Directory “Measurements in Industry”] 1-3 volumes. M.: *Metallurgiya*, 1990.

FOR AUTHOR USE ONLY

## Appendix

**Table 1.** Dependence of the EMF of a differential chromel-coppel (Тун L) thermocouple on the temperature of the working junction (calibration table).  
Temperature range from -20 °C ° to +200 °C  
*Source: built by the author based on [21], chapter 1.*

<b>t, °C</b>	0	1	2	3	4	5	6	7	8	9
	<b>EMF, mV</b>									
-20	-1,27	-1,35	-1,39	-1,46	-1,52	-1,58	-1,64	-1,70	-1,77	-1,83
-10	-0,64	-0,70	-0,77	-0,83	-0,89	-0,96	-1,02	-1,08	-1,14	-1,21
-0	0	-0,06	-0,13	-0,19	0,26	-0,32	-0,38	0,45	-0,51	-0,58
+0	0	0,07	0,13	0,20	0,26	0,33	0,39	0,46	0,52	0,59
10	0,65	0,72	0,78	0,85	0,91	0,98	1,05	1,11	1,18	1,24
20	1,31	1,38	1,44	1,51	1,57	1,64	1,70	1,77	1,84	1,91
30	1,98	2,05	2,12	2,18	2,25	2,32	2,38	2,45	2,52	2,59
40	2,66	2,73	2,80	2,87	2,94	3,00	3,07	3,14	3,21	3,28
50	3,35	3,42	3,49	3,56	3,63	3,70	3,77	3,84	3,91	3,98
60	4,05	4,12	4,19	4,26	4,33	4,41	4,48	4,55	4,62	4,69
70	4,76	4,83	4,90	4,98	5,05	5,12	5,20	5,27	5,34	5,41
80	5,48	5,56	5,63	5,70	5,78	5,85	5,92	5,99	6,07	6,14
90	6,21	6,29	6,36	6,43	6,51	6,58	6,65	6,73	6,80	6,87
100	6,95	7,03	7,10	7,17	7,25	7,32	7,40	7,47	7,54	7,62
110	7,69	7,77	7,84	7,91	7,99	8,06	8,13	8,21	8,28	8,35
120	8,43	8,50	8,58	8,65	8,73	8,80	8,88	8,95	9,03	9,10
130	9,18	9,25	9,33	9,40	9,48	9,55	9,63	9,70	9,78	9,85
140	9,93	10,00	10,08	10,16	10,23	10,31	10,38	10,46	10,54	10,61
150	10,69	10,77	10,85	10,92	11,00	11,08	11,15	11,23	11,31	11,38
160	11,46	11,54	11,62	11,69	11,77	11,85	11,93	12,00	12,08	12,16
170	12,24	12,32	12,40	12,48	12,55	12,63	12,71	12,79	12,87	12,93
180	13,03	13,11	13,19	13,27	13,36	13,44	13,52	13,60	13,68	13,76
190	13,84	13,92	14,00	14,08	14,16	14,23	14,33	14,42	14,50	14,58
200	14,66	14,74	14,82	14,90	14,98	15,06	15,14	15,22	15,30	15,38

**Table 2.** Dependence of the EMF of a differential chromel-alumel (Type K) thermocouple on the temperature of the working junction (calibration table).

Temperature range from -270 °C to 1370 °C.

Source: built by the author based on [21], chapter 1.

t, °C	EMF, mV										
	0	1	2	3	4	5	6	7	8	9	0
-270	-6.458										
-260	-6.441	-6.444	-6.446	-6.448	-6.450	-6.452	-6.453	-6.455	-6.456	-6.457	-6.458
-250	-6.404	-6.408	-6.413	-6.417	-6.421	-6.425	-6.429	-6.432	-6.435	-6.438	-6.441
-240	-6.344	-6.351	-6.358	-6.364	-6.370	-6.377	-6.382	-6.388	-6.393	-6.399	-6.404
-230	-6.262	-6.271	-6.280	-6.289	-6.297	-6.306	-6.314	-6.322	-6.329	-6.337	-6.344
-220	-6.158	-6.170	-6.181	-6.192	-6.202	-6.213	-6.223	-6.233	-6.243	-6.252	-6.262
-210	-6.035	-6.048	-6.061	-6.074	-6.087	-6.099	-6.111	-6.123	-6.135	-6.147	-6.158
-200	-5.891	-5.907	-5.922	-5.936	-5.951	-5.965	-5.980	-5.994	-6.007	-6.021	-6.035
-190	-5.730	-5.747	-5.763	-5.780	-5.797	-5.813	-5.829	-5.845	-5.861	-5.876	-5.891
-180	-5.550	-5.569	-5.588	-5.606	-5.624	-5.642	-5.660	-5.678	-5.695	-5.713	-5.730
-170	-5.354	-5.374	-5.395	-5.415	-5.435	-5.454	-5.474	-5.493	-5.512	-5.531	-5.550
-160	-5.141	-5.163	-5.185	-5.207	-5.228	-5.250	-5.271	-5.292	-5.313	-5.333	-5.354
-150	-4.913	-4.936	-4.960	-4.983	-5.006	-5.029	-5.052	-5.074	-5.097	-5.119	-5.141
-140	-4.669	-4.694	-4.719	-4.744	-4.768	-4.793	-4.817	-4.841	-4.865	-4.889	-4.913
-130	-4.411	-4.437	-4.463	-4.489	-4.515	-4.542	-4.567	-4.593	-4.618	-4.644	-4.669
-120	-4.138	-4.166	-4.194	-4.221	-4.249	-4.276	-4.303	-4.330	-4.357	-4.384	-4.411
-110	-3.852	-3.882	-3.911	-3.939	-3.968	-3.997	-4.025	-4.054	-4.082	-4.110	-4.138
-100	-3.554	-3.584	-3.614	-3.645	-3.675	-3.705	-3.734	-3.764	-3.794	-3.823	-3.852
-90	-3.243	-3.274	-3.306	-3.337	-3.368	-3.400	-3.431	-3.462	-3.492	-3.523	-3.554
-80	-2.920	-2.953	-2.986	-3.018	-3.050	-3.083	-3.115	-3.147	-3.179	-3.211	-3.243
-70	-2.587	-2.620	-2.654	-2.688	-2.721	-2.755	-2.788	-2.821	-2.854	-2.887	-2.920
-60	-2.243	-2.278	-2.312	-2.347	-2.382	-2.416	-2.450	-2.485	-2.519	-2.553	-2.587
-50	-1.889	-1.925	-1.961	-1.996	-2.032	-2.067	-2.103	-2.138	-2.173	-2.208	-2.243
-40	-1.527	-1.564	-1.600	-1.637	-1.673	-1.709	-1.745	-1.782	-1.818	-1.854	-1.889
-30	-1.156	-1.194	-1.231	-1.268	-1.305	-1.343	-1.380	-1.417	-1.453	-1.490	-1.527
-20	-0.778	-0.816	-0.854	-0.892	-0.930	-0.968	-1.006	-1.043	-1.081	-1.119	-1.156
-10	-0.392	-0.431	-0.470	-0.508	-0.547	-0.586	-0.624	-0.663	-0.701	-0.739	-0.778
0	0.000	-0.039	-0.079	-0.118	-0.157	-0.197	-0.236	-0.275	-0.314	-0.353	-0.392
0	0.000	0.039	0.079	0.119	0.158	0.198	0.238	0.277	0.317	0.357	0.397
10	0.397	0.437	0.477	0.517	0.557	0.597	0.637	0.677	0.718	0.758	0.798
20	0.796	0.838	0.879	0.919	0.960	1.000	1.041	1.081	1.122	1.163	1.203
30	1.203	1.244	1.285	1.326	1.366	1.407	1.448	1.489	1.530	1.571	1.612
40	1.612	1.653	1.694	1.735	1.776	1.817	1.858	1.899	1.941	1.982	2.023
50	2.023	2.064	2.106	2.147	2.188	2.230	2.271	2.312	2.354	2.395	2.436
60	2.436	2.478	2.519	2.561	2.602	2.644	2.685	2.727	2.768	2.810	2.851
70	2.851	2.893	2.934	2.976	3.017	3.059	3.100	3.142	3.184	3.225	3.267
80	3.267	3.308	3.350	3.391	3.433	3.474	3.516	3.557	3.599	3.640	3.682
90	3.682	3.723	3.765	3.806	3.848	3.889	3.931	3.972	4.013	4.055	4.096
100	4.096	4.138	4.179	4.220	4.262	4.303	4.344	4.385	4.427	4.468	4.509
110	4.509	4.550	4.591	4.633	4.674	4.715	4.756	4.797	4.838	4.879	4.920
120	4.920	4.961	5.002	5.043	5.084	5.124	5.165	5.206	5.247	5.288	5.328
130	5.328	5.369	5.410	5.450	5.491	5.532	5.572	5.613	5.653	5.694	5.735
140	5.735	5.775	5.815	5.856	5.896	5.937	5.977	6.017	6.058	6.098	6.138
150	6.138	6.179	6.219	6.259	6.299	6.339	6.380	6.420	6.460	6.500	6.540
160	6.540	6.580	6.620	6.660	6.701	6.741	6.781	6.821	6.861	6.901	6.941
170	6.941	6.981	7.021	7.060	7.100	7.140	7.180	7.220	7.260	7.300	7.340
180	7.340	7.380	7.420	7.460	7.500	7.540	7.579	7.619	7.659	7.699	7.739
190	7.739	7.779	7.819	7.859	7.899	7.939	7.979	8.019	8.059	8.099	8.139

## Continuation of Table 2

200	8.138	8.178	8.218	8.258	8.298	8.338	8.378	8.418	8.458	8.499	8.539
210	8.439	8.479	8.519	8.559	8.599	8.639	8.679	8.719	8.759	8.800	8.840
220	8.940	8.980	9.020	9.061	9.101	9.141	9.181	9.222	9.262	9.302	9.343
230	9.343	9.383	9.423	9.464	9.504	9.545	9.585	9.626	9.666	9.707	9.747
240	9.747	9.788	9.828	9.869	9.909	9.950	9.991	10.031	10.072	10.113	10.153
250	10.153	10.194	10.235	10.276	10.316	10.357	10.398	10.439	10.480	10.520	10.561
260	10.561	10.602	10.643	10.684	10.725	10.766	10.807	10.848	10.889	10.930	10.971
270	10.971	11.012	11.053	11.094	11.135	11.176	11.217	11.259	11.300	11.341	11.382
280	11.382	11.423	11.465	11.506	11.547	11.588	11.630	11.671	11.712	11.753	11.795
290	11.795	11.836	11.877	11.919	11.960	12.001	12.043	12.084	12.126	12.167	12.209
300	12.209	12.250	12.291	12.333	12.374	12.416	12.457	12.499	12.540	12.582	12.624
310	12.624	12.665	12.707	12.748	12.790	12.831	12.873	12.915	12.956	12.998	13.040
320	13.040	13.081	13.123	13.165	13.206	13.248	13.290	13.331	13.373	13.415	13.457
330	13.457	13.498	13.540	13.582	13.624	13.665	13.707	13.749	13.791	13.833	13.874
340	13.874	13.916	13.958	14.000	14.042	14.084	14.126	14.167	14.209	14.251	14.293
350	14.293	14.335	14.377	14.419	14.461	14.503	14.545	14.587	14.629	14.671	14.713
360	14.713	14.755	14.797	14.839	14.881	14.923	14.965	15.007	15.049	15.091	15.133
370	15.133	15.175	15.217	15.259	15.301	15.343	15.385	15.427	15.469	15.511	15.554
380	15.554	15.596	15.638	15.680	15.722	15.764	15.806	15.849	15.891	15.933	15.975
390	15.975	16.017	16.059	16.102	16.144	16.186	16.228	16.270	16.313	16.355	16.397
400	16.397	16.439	16.482	16.524	16.566	16.608	16.651	16.693	16.735	16.778	16.820
410	16.820	16.862	16.904	16.947	16.989	17.031	17.074	17.116	17.158	17.201	17.243
420	17.243	17.285	17.328	17.370	17.413	17.455	17.497	17.540	17.582	17.624	17.667
430	17.667	17.709	17.752	17.794	17.837	17.879	17.921	17.964	18.006	18.049	18.091
440	18.091	18.134	18.176	18.218	18.261	18.303	18.346	18.388	18.431	18.473	18.516
450	18.516	18.558	18.601	18.643	18.686	18.728	18.771	18.813	18.856	18.898	18.941
460	18.941	18.983	19.026	19.068	19.111	19.154	19.196	19.239	19.281	19.324	19.366
470	19.366	19.409	19.451	19.494	19.537	19.579	19.622	19.664	19.707	19.750	19.792
480	19.792	19.835	19.877	19.920	19.962	20.005	20.048	20.090	20.133	20.175	20.218
490	20.218	20.261	20.303	20.346	20.389	20.431	20.474	20.516	20.559	20.602	20.644
500	20.644	20.687	20.730	20.772	20.815	20.857	20.900	20.943	20.985	21.028	21.071
510	21.071	21.113	21.156	21.199	21.241	21.284	21.326	21.369	21.412	21.454	21.497
520	21.497	21.540	21.582	21.625	21.668	21.710	21.753	21.796	21.838	21.881	21.924
530	21.924	21.966	22.009	22.052	22.094	22.137	22.179	22.222	22.265	22.307	22.350
540	22.350	22.393	22.435	22.478	22.521	22.563	22.606	22.649	22.691	22.734	22.776
550	22.776	22.819	22.862	22.904	22.947	22.990	23.032	23.075	23.117	23.160	23.203
560	23.203	23.245	23.288	23.331	23.373	23.416	23.458	23.501	23.544	23.586	23.629
570	23.629	23.671	23.714	23.757	23.799	23.842	23.884	23.927	23.970	24.012	24.055
580	24.055	24.097	24.140	24.182	24.225	24.267	24.310	24.353	24.395	24.438	24.480
590	24.480	24.523	24.565	24.608	24.650	24.693	24.735	24.778	24.820	24.863	24.905
600	24.905	24.948	24.990	25.033	25.075	25.118	25.160	25.203	25.245	25.288	25.330
610	25.330	25.373	25.415	25.458	25.500	25.543	25.585	25.627	25.670	25.712	25.755
620	25.755	25.797	25.840	25.882	25.924	25.967	26.009	26.052	26.094	26.136	26.179
630	26.179	26.221	26.263	26.306	26.348	26.390	26.433	26.475	26.517	26.560	26.602
640	26.602	26.644	26.687	26.729	26.771	26.814	26.856	26.898	26.940	26.983	27.025
650	27.025	27.067	27.109	27.152	27.194	27.236	27.278	27.320	27.363	27.405	27.447
660	27.447	27.489	27.531	27.574	27.616	27.658	27.700	27.742	27.784	27.826	27.869
670	27.869	27.911	27.953	27.995	28.037	28.079	28.121	28.163	28.205	28.247	28.289
680	28.289	28.332	28.374	28.416	28.458	28.500	28.542	28.584	28.626	28.668	28.710
690	28.710	28.752	28.794	28.836	28.877	28.919	28.961	29.003	29.045	29.087	29.129

## Continuation of Table 2

700	29.129	29.171	29.213	29.255	29.297	29.338	29.380	29.422	29.464	29.506	29.548
710	29.546	29.589	29.631	29.673	29.715	29.757	29.798	29.840	29.882	29.924	29.965
720	29.965	30.007	30.049	30.090	30.132	30.174	30.216	30.257	30.299	30.341	30.382
730	30.382	30.424	30.466	30.507	30.549	30.590	30.632	30.674	30.715	30.757	30.798
740	30.798	30.840	30.881	30.923	30.964	31.006	31.047	31.089	31.130	31.172	31.213
750	31.213	31.255	31.296	31.338	31.379	31.421	31.462	31.504	31.545	31.586	31.628
760	31.628	31.669	31.710	31.752	31.793	31.834	31.876	31.917	31.958	32.000	32.041
770	32.041	32.082	32.124	32.165	32.206	32.247	32.289	32.330	32.371	32.412	32.453
780	32.453	32.495	32.536	32.577	32.618	32.659	32.700	32.742	32.783	32.824	32.865
790	32.865	32.906	32.947	32.988	33.029	33.070	33.111	33.152	33.193	33.234	33.275
800	33.275	33.316	33.357	33.398	33.439	33.480	33.521	33.562	33.603	33.644	33.685
810	33.685	33.726	33.767	33.808	33.848	33.889	33.930	33.971	34.012	34.053	34.093
820	34.093	34.134	34.175	34.216	34.257	34.297	34.338	34.379	34.420	34.460	34.501
830	34.501	34.542	34.582	34.623	34.664	34.704	34.745	34.786	34.826	34.867	34.908
840	34.908	34.948	34.989	35.029	35.070	35.110	35.151	35.192	35.232	35.273	35.313
850	35.313	35.354	35.394	35.435	35.475	35.516	35.556	35.596	35.637	35.677	35.718
860	35.718	35.758	35.798	35.839	35.879	35.920	35.960	35.000	36.041	36.081	36.121
870	36.121	36.162	36.202	36.242	36.282	36.323	36.363	36.403	36.443	36.484	36.524
880	36.524	36.564	36.604	36.644	36.685	36.725	36.765	36.805	36.845	36.885	36.925
890	36.925	36.965	37.006	37.046	37.086	37.126	37.166	37.206	37.246	37.286	37.326
900	37.326	37.366	37.406	37.446	37.486	37.526	37.566	37.606	37.646	37.686	37.726
910	37.726	37.765	37.805	37.845	37.885	37.925	37.965	38.005	38.044	38.084	38.124
920	38.124	38.164	38.204	38.243	38.283	38.323	38.363	38.402	38.442	38.482	38.522
930	38.522	38.561	38.601	38.641	38.680	38.720	38.760	38.799	38.839	38.878	38.918
940	38.918	38.958	38.997	39.037	39.076	39.116	39.155	39.195	39.235	39.274	39.314
950	39.314	39.353	39.393	39.432	39.471	39.511	39.550	39.590	39.629	39.669	39.708
960	39.708	39.747	39.787	39.826	39.865	39.905	39.944	39.984	40.023	40.062	40.101
970	40.101	40.141	40.180	40.219	40.259	40.298	40.337	40.376	40.415	40.455	40.494
980	40.494	40.533	40.572	40.611	40.651	40.690	40.729	40.768	40.807	40.846	40.885
990	40.885	40.924	40.963	41.002	41.042	41.081	41.120	41.159	41.198	41.237	41.276
1000	41.276	41.315	41.354	41.393	41.431	41.470	41.509	41.548	41.587	41.626	41.665
1010	41.665	41.704	41.743	41.781	41.820	41.859	41.898	41.937	41.976	42.014	42.053
1020	42.053	42.092	42.131	42.169	42.208	42.247	42.286	42.324	42.363	42.402	42.440
1030	42.440	42.479	42.518	42.556	42.595	42.633	42.672	42.711	42.749	42.788	42.826
1040	42.826	42.865	42.903	42.942	42.980	43.019	43.057	43.096	43.134	43.173	43.211
1050	43.211	43.250	43.288	43.327	43.365	43.403	43.442	43.480	43.518	43.557	43.595
1060	43.595	43.633	43.672	43.710	43.748	43.787	43.825	43.863	43.901	43.940	43.978
1070	43.978	44.016	44.054	44.092	44.130	44.169	44.207	44.245	44.283	44.321	44.359
1080	44.359	44.397	44.435	44.473	44.512	44.550	44.588	44.626	44.664	44.702	44.740
1090	44.740	44.778	44.816	44.853	44.891	44.929	44.967	45.005	45.043	45.081	45.119
1100	45.119	45.157	45.194	45.232	45.270	45.308	45.346	45.383	45.421	45.459	45.497
1110	45.497	45.534	45.572	45.610	45.647	45.685	45.723	45.760	45.798	45.836	45.873
1120	45.873	45.911	45.948	45.986	46.024	46.061	46.099	46.136	46.174	46.211	46.249
1130	46.249	46.286	46.324	46.361	46.398	46.436	46.473	46.511	46.548	46.585	46.623
1140	46.623	46.660	46.697	46.735	46.772	46.809	46.847	46.884	46.921	46.958	46.995
1150	46.995	47.033	47.070	47.107	47.144	47.181	47.218	47.256	47.293	47.330	47.367
1160	47.367	47.404	47.441	47.478	47.515	47.552	47.589	47.626	47.663	47.700	47.737
1170	47.737	47.774	47.811	47.848	47.884	47.921	47.958	47.995	48.032	48.069	48.105
1180	48.105	48.142	48.179	48.216	48.252	48.289	48.326	48.363	48.399	48.436	48.473
1190	48.473	48.509	48.546	48.582	48.619	48.656	48.692	48.729	48.765	48.802	48.838
1200	48.838	48.875	48.911	48.948	48.984	49.021	49.057	49.093	49.130	49.166	49.202
1210	49.202	49.239	49.275	49.311	49.348	49.384	49.420	49.456	49.493	49.529	49.565
1220	49.565	49.601	49.637	49.674	49.710	49.746	49.782	49.818	49.854	49.890	49.926
1230	49.926	49.962	49.998	50.034	50.070	50.106	50.142	50.178	50.214	50.250	50.286
1240	50.286	50.322	50.358	50.393	50.429	50.465	50.501	50.537	50.572	50.608	50.644
1250	50.644	50.680	50.715	50.751	50.787	50.822	50.858	50.894	50.929	50.965	51.000
1260	51.000	51.036	51.071	51.107	51.142	51.178	51.213	51.249	51.284	51.320	51.355
1270	51.355	51.391	51.426	51.461	51.497	51.532	51.567	51.603	51.638	51.673	51.708
1280	51.708	51.744	51.779	51.814	51.849	51.885	51.920	51.955	51.990	52.025	52.060
1290	52.060	52.095	52.130	52.165	52.200	52.235	52.270	52.305	52.340	52.375	52.410
1300	52.410	52.445	52.480	52.515	52.550	52.585	52.620	52.654	52.689	52.724	52.759
1310	52.759	52.794	52.828	52.863	52.898	52.932	52.967	53.002	53.037	53.071	53.106
1320	53.106	53.140	53.175	53.210	53.244	53.279	53.313	53.348	53.382	53.417	53.451
1330	53.451	53.486	53.520	53.555	53.589	53.623	53.658	53.692	53.727	53.761	53.795
1340	53.795	53.830	53.864	53.898	53.932	53.967	54.001	54.035	54.069	54.104	54.138
1350	54.138	54.172	54.206	54.240	54.274	54.308	54.342	54.377	54.411	54.445	54.479
1360	54.479	54.513	54.547	54.581	54.615	54.649	54.683	54.717	54.751	54.785	54.819
1370	54.819	54.852	54.886								

**Table 3.** Dependence of the EMF of a differential copper - constantan (**Type T**) thermocouple on the temperature of the working junction (calibration table).

Temperature range from -270 °C to 400 °C.

Source: built by the author based on [21], chapter 1.

t, °C	EMF, mV										
	0	1	2	3	4	5	6	7	8	9	0
-270	-6.258										
-260	-6.232	-6.238	-6.239	-6.242	-6.245	-6.248	-6.251	-6.253	-6.255	-6.258	-6.258
-250	-6.180	-6.187	-6.193	-6.198	-6.204	-6.209	-6.214	-6.219	-6.223	-6.228	-6.232
-240	-6.105	-6.114	-6.122	-6.130	-6.138	-6.146	-6.153	-6.160	-6.167	-6.174	-6.180
-230	-6.007	-6.017	-6.028	-6.038	-6.049	-6.059	-6.068	-6.078	-6.087	-6.096	-6.105
-220	-5.888	-5.901	-5.914	-5.928	-5.938	-5.950	-5.962	-5.973	-5.985	-5.996	-6.007
-210	-5.753	-5.767	-5.782	-5.795	-5.809	-5.823	-5.836	-5.850	-5.863	-5.876	-5.888
-200	-5.603	-5.619	-5.634	-5.650	-5.666	-5.680	-5.695	-5.710	-5.724	-5.739	-5.753
-190	-5.439	-5.456	-5.473	-5.489	-5.506	-5.523	-5.539	-5.555	-5.571	-5.587	-5.603
-180	-5.281	-5.279	-5.297	-5.316	-5.334	-5.351	-5.369	-5.387	-5.404	-5.421	-5.439
-170	-5.070	-5.089	-5.109	-5.128	-5.148	-5.167	-5.186	-5.205	-5.224	-5.242	-5.261
-160	-4.885	-4.888	-4.907	-4.928	-4.949	-4.969	-4.989	-5.010	-5.030	-5.050	-5.070
-150	-4.648	-4.671	-4.693	-4.715	-4.737	-4.759	-4.780	-4.802	-4.823	-4.844	-4.865
-140	-4.419	-4.443	-4.466	-4.489	-4.512	-4.535	-4.558	-4.581	-4.604	-4.626	-4.648
-130	-4.177	-4.202	-4.226	-4.251	-4.275	-4.300	-4.324	-4.348	-4.372	-4.395	-4.419
-120	-3.923	-3.949	-3.975	-4.000	-4.026	-4.052	-4.077	-4.102	-4.127	-4.152	-4.177
-110	-3.657	-3.684	-3.711	-3.738	-3.766	-3.791	-3.818	-3.844	-3.871	-3.897	-3.923
-100	-3.379	-3.407	-3.435	-3.463	-3.491	-3.519	-3.547	-3.574	-3.602	-3.629	-3.657
-90	-3.089	-3.118	-3.148	-3.177	-3.206	-3.235	-3.264	-3.293	-3.322	-3.350	-3.379
-80	-2.788	-2.818	-2.849	-2.879	-2.910	-2.940	-2.970	-3.000	-3.030	-3.059	-3.089
-70	-2.476	-2.507	-2.539	-2.571	-2.602	-2.633	-2.664	-2.695	-2.726	-2.757	-2.788
-60	-2.153	-2.186	-2.218	-2.251	-2.283	-2.316	-2.348	-2.380	-2.412	-2.444	-2.476
-50	-1.819	-1.853	-1.887	-1.920	-1.954	-1.987	-2.021	-2.054	-2.087	-2.120	-2.153
-40	-1.475	-1.510	-1.545	-1.579	-1.614	-1.648	-1.683	-1.717	-1.751	-1.785	-1.819
-30	-1.121	-1.157	-1.192	-1.228	-1.264	-1.299	-1.335	-1.370	-1.405	-1.440	-1.475
-20	-0.757	-0.794	-0.830	-0.867	-0.904	-0.940	-0.976	-1.013	-1.049	-1.085	-1.121
-10	-0.383	-0.421	-0.459	-0.496	-0.534	-0.571	-0.608	-0.646	-0.683	-0.720	-0.757
0	0.000	-0.039	-0.077	-0.116	-0.154	-0.193	-0.231	-0.269	-0.307	-0.345	-0.383
0	0.000	0.039	0.078	0.117	0.156	0.195	0.234	0.273	0.312	0.352	0.391
10	0.391	0.431	0.470	0.510	0.549	0.589	0.629	0.669	0.709	0.749	0.790
20	0.790	0.830	0.870	0.911	0.951	0.992	1.033	1.074	1.114	1.155	1.196
30	1.196	1.238	1.279	1.320	1.362	1.403	1.445	1.486	1.528	1.570	1.612
40	1.612	1.654	1.696	1.738	1.780	1.823	1.865	1.908	1.950	1.993	2.036
50	2.036	2.079	2.122	2.165	2.208	2.251	2.294	2.338	2.381	2.425	2.468
60	2.468	2.512	2.556	2.600	2.643	2.687	2.732	2.776	2.820	2.864	2.909
70	2.909	2.953	2.998	3.043	3.087	3.132	3.177	3.222	3.267	3.312	3.358
80	3.358	3.403	3.448	3.494	3.539	3.585	3.631	3.677	3.722	3.768	3.814
90	3.814	3.860	3.907	3.953	3.999	4.046	4.092	4.138	4.185	4.232	4.279
100	4.279	4.325	4.372	4.419	4.466	4.513	4.561	4.608	4.655	4.702	4.750
110	4.750	4.798	4.845	4.893	4.941	4.988	5.036	5.084	5.132	5.180	5.228
120	5.228	5.277	5.325	5.373	5.422	5.470	5.519	5.567	5.616	5.665	5.714
130	5.714	5.763	5.812	5.861	5.910	5.959	6.008	6.057	6.107	6.156	6.206
140	6.206	6.255	6.305	6.355	6.404	6.454	6.504	6.554	6.604	6.654	6.704
150	6.704	6.754	6.805	6.855	6.905	6.956	7.006	7.057	7.107	7.158	7.209
160	7.209	7.260	7.310	7.361	7.412	7.463	7.515	7.566	7.617	7.668	7.720
170	7.720	7.771	7.823	7.874	7.926	7.977	8.029	8.081	8.133	8.185	8.237
180	8.237	8.289	8.341	8.393	8.445	8.497	8.550	8.602	8.654	8.707	8.759
190	8.759	8.812	8.865	8.917	8.970	9.023	9.076	9.129	9.182	9.235	9.288

## Continuation of Table 3

200	9.288	9.341	9.395	9.448	9.501	9.555	9.608	9.662	9.715	9.769	9.822
210	9.822	9.876	9.930	9.984	10.038	10.092	10.146	10.200	10.254	10.308	10.362
220	10.382	10.417	10.471	10.525	10.580	10.634	10.689	10.743	10.798	10.853	10.907
230	10.907	10.962	11.017	11.072	11.127	11.182	11.237	11.292	11.347	11.403	11.458
240	11.458	11.513	11.569	11.624	11.680	11.735	11.791	11.846	11.902	11.958	12.013
250	12.013	12.069	12.125	12.181	12.237	12.293	12.349	12.405	12.461	12.518	12.574
260	12.574	12.630	12.687	12.743	12.799	12.856	12.912	12.969	13.026	13.082	13.139
270	13.139	13.196	13.253	13.310	13.366	13.423	13.480	13.537	13.595	13.652	13.709
280	13.709	13.766	13.823	13.881	13.938	13.995	14.053	14.110	14.168	14.226	14.283
290	14.283	14.341	14.399	14.456	14.514	14.572	14.630	14.688	14.746	14.804	14.862
300	14.862	14.920	14.978	15.036	15.095	15.153	15.211	15.270	15.328	15.386	15.445
310	15.445	15.503	15.562	15.621	15.679	15.738	15.797	15.856	15.914	15.973	16.032
320	16.032	16.091	16.150	16.209	16.268	16.327	16.387	16.446	16.505	16.564	16.624
330	16.624	16.683	16.742	16.802	16.861	16.921	16.980	17.040	17.100	17.159	17.219
340	17.219	17.279	17.339	17.399	17.458	17.518	17.578	17.638	17.698	17.759	17.819
350	17.819	17.879	17.939	17.999	18.060	18.120	18.180	18.241	18.301	18.362	18.422
360	18.422	18.483	18.543	18.604	18.665	18.725	18.786	18.847	18.908	18.969	19.030
370	19.030	19.091	19.152	19.213	19.274	19.335	19.396	19.457	19.518	19.579	19.641
380	19.641	19.702	19.763	19.825	19.886	19.947	20.009	20.070	20.132	20.193	20.255
390	20.255	20.317	20.378	20.440	20.502	20.563	20.625	20.687	20.748	20.810	20.872
400	20.872										

FOR AUTHOR USE ONLY

**Table 4.** Dependence of the EMF of a differential c platinum-30% rhodium/platinum-6% rhodium (**Type B**) thermocouple on the temperature of the working junction (calibration table).

Temperature range from 0 °C to 1820 °C.

Source: built by the author based on [21], chapter 1.

t, °C	EMF, mV										
	0	1	2	3	4	5	6	7	8	9	0
0	0.000	0.000	0.000	-0.001	-0.001	-0.001	-0.001	-0.001	-0.002	-0.002	-0.002
10	-0.002	-0.002	-0.002	-0.002	-0.002	-0.002	-0.002	-0.002	-0.003	-0.003	-0.003
20	-0.003	-0.003	-0.003	-0.003	-0.003	-0.002	-0.002	-0.002	-0.002	-0.002	-0.002
30	-0.002	-0.002	-0.002	-0.002	-0.002	-0.001	-0.001	-0.001	-0.001	-0.001	0.000
40	0.000	0.000	0.000	0.000	0.000	0.001	0.001	0.001	0.001	0.002	0.002
50	0.002	0.003	0.003	0.003	0.004	0.004	0.004	0.005	0.005	0.006	0.006
60	0.006	0.007	0.007	0.008	0.008	0.009	0.009	0.010	0.010	0.011	0.011
70	0.011	0.012	0.012	0.013	0.014	0.014	0.015	0.015	0.016	0.017	0.017
80	0.017	0.018	0.019	0.020	0.020	0.021	0.022	0.022	0.023	0.024	0.025
90	0.025	0.026	0.026	0.027	0.028	0.029	0.030	0.031	0.031	0.032	0.033
100	0.033	0.034	0.035	0.036	0.037	0.038	0.039	0.040	0.041	0.042	0.043
110	0.043	0.044	0.045	0.046	0.047	0.048	0.049	0.050	0.051	0.052	0.053
120	0.053	0.055	0.056	0.057	0.058	0.059	0.060	0.062	0.063	0.064	0.065
130	0.065	0.066	0.068	0.069	0.070	0.072	0.073	0.074	0.075	0.077	0.078
140	0.078	0.079	0.081	0.082	0.084	0.085	0.086	0.088	0.089	0.091	0.092
150	0.092	0.094	0.095	0.096	0.096	0.099	0.101	0.102	0.104	0.105	0.107
160	0.107	0.109	0.110	0.112	0.113	0.115	0.117	0.118	0.120	0.122	0.123
170	0.123	0.125	0.127	0.128	0.130	0.132	0.134	0.135	0.137	0.139	0.141
180	0.141	0.142	0.144	0.146	0.148	0.150	0.151	0.153	0.155	0.157	0.159
190	0.159	0.161	0.163	0.165	0.166	0.168	0.170	0.172	0.174	0.176	0.178
200	0.178	0.180	0.182	0.184	0.186	0.188	0.190	0.192	0.195	0.197	0.199
210	0.199	0.201	0.203	0.205	0.207	0.209	0.212	0.214	0.216	0.218	0.220
220	0.220	0.222	0.225	0.227	0.229	0.231	0.234	0.236	0.238	0.241	0.243
230	0.243	0.245	0.248	0.250	0.252	0.255	0.257	0.259	0.262	0.264	0.267
240	0.267	0.269	0.271	0.274	0.276	0.279	0.281	0.284	0.286	0.289	0.291
250	0.291	0.294	0.296	0.299	0.301	0.304	0.307	0.309	0.312	0.314	0.317
260	0.317	0.320	0.322	0.325	0.328	0.330	0.333	0.336	0.338	0.341	0.344
270	0.344	0.347	0.349	0.352	0.355	0.358	0.360	0.363	0.366	0.369	0.372
280	0.372	0.375	0.377	0.380	0.383	0.386	0.389	0.392	0.395	0.398	0.401
290	0.401	0.404	0.407	0.410	0.413	0.416	0.419	0.422	0.425	0.428	0.431
300	0.431	0.434	0.437	0.440	0.443	0.446	0.449	0.452	0.455	0.458	0.462
310	0.462	0.465	0.468	0.471	0.474	0.478	0.481	0.484	0.487	0.490	0.494
320	0.494	0.497	0.500	0.503	0.507	0.510	0.513	0.517	0.520	0.523	0.527
330	0.527	0.530	0.533	0.537	0.540	0.544	0.547	0.550	0.554	0.557	0.561
340	0.561	0.564	0.568	0.571	0.575	0.578	0.582	0.586	0.589	0.592	0.596
350	0.596	0.599	0.603	0.607	0.610	0.614	0.617	0.621	0.625	0.628	0.632
360	0.632	0.636	0.639	0.643	0.647	0.650	0.654	0.658	0.662	0.665	0.669
370	0.669	0.673	0.677	0.680	0.684	0.688	0.692	0.696	0.700	0.703	0.707
380	0.707	0.711	0.715	0.719	0.723	0.727	0.731	0.735	0.738	0.742	0.746
390	0.746	0.750	0.754	0.758	0.762	0.766	0.770	0.774	0.778	0.782	0.787
400	0.787	0.791	0.795	0.799	0.803	0.807	0.811	0.815	0.819	0.824	0.828
410	0.828	0.832	0.836	0.840	0.844	0.849	0.853	0.857	0.861	0.866	0.870
420	0.870	0.874	0.878	0.883	0.887	0.891	0.896	0.900	0.904	0.909	0.913
430	0.913	0.917	0.922	0.926	0.930	0.935	0.939	0.944	0.948	0.953	0.957
440	0.957	0.961	0.966	0.970	0.975	0.979	0.984	0.988	0.993	0.997	1.002
450	1.002	1.007	1.011	1.016	1.020	1.025	1.030	1.034	1.039	1.043	1.048
460	1.048	1.053	1.057	1.062	1.067	1.071	1.076	1.081	1.086	1.090	1.095
470	1.095	1.100	1.105	1.109	1.114	1.119	1.124	1.129	1.133	1.138	1.143
480	1.143	1.148	1.153	1.158	1.163	1.167	1.172	1.177	1.182	1.187	1.192
490	1.192	1.197	1.202	1.207	1.212	1.217	1.222	1.227	1.232	1.237	1.242

Continuation of Table 4

500	1.242	1.247	1.252	1.257	1.262	1.267	1.272	1.277	1.282	1.288	1.293
510	1.293	1.298	1.303	1.308	1.313	1.318	1.324	1.329	1.334	1.339	1.344
520	1.344	1.350	1.355	1.360	1.365	1.371	1.376	1.381	1.387	1.392	1.397
530	1.397	1.402	1.408	1.413	1.418	1.424	1.429	1.435	1.440	1.445	1.451
540	1.451	1.456	1.462	1.467	1.472	1.478	1.483	1.489	1.494	1.500	1.505
550	1.505	1.511	1.516	1.522	1.527	1.533	1.539	1.544	1.550	1.555	1.561
560	1.561	1.566	1.572	1.578	1.583	1.589	1.595	1.600	1.606	1.612	1.617
570	1.617	1.623	1.629	1.634	1.640	1.646	1.652	1.657	1.663	1.669	1.675
580	1.675	1.680	1.686	1.692	1.698	1.704	1.709	1.715	1.721	1.727	1.733
590	1.733	1.739	1.745	1.750	1.756	1.762	1.768	1.774	1.780	1.786	1.792
600	1.792	1.798	1.804	1.810	1.816	1.822	1.828	1.834	1.840	1.846	1.852
610	1.852	1.858	1.864	1.870	1.876	1.882	1.888	1.894	1.901	1.907	1.913
620	1.913	1.919	1.925	1.931	1.937	1.944	1.950	1.956	1.962	1.968	1.975
630	1.975	1.981	1.987	1.993	1.999	2.006	2.012	2.018	2.025	2.031	2.037
640	2.037	2.043	2.050	2.056	2.062	2.069	2.075	2.082	2.088	2.094	2.101
650	2.101	2.107	2.113	2.120	2.126	2.133	2.139	2.146	2.152	2.158	2.165
660	2.165	2.171	2.178	2.184	2.191	2.197	2.204	2.210	2.217	2.224	2.230
670	2.230	2.237	2.243	2.250	2.256	2.263	2.270	2.276	2.283	2.289	2.296
680	2.296	2.303	2.309	2.316	2.323	2.329	2.336	2.343	2.350	2.356	2.363
690	2.363	2.370	2.376	2.383	2.390	2.397	2.403	2.410	2.417	2.424	2.431
700	2.431	2.437	2.444	2.451	2.458	2.465	2.472	2.479	2.485	2.492	2.499
710	2.499	2.506	2.513	2.520	2.527	2.534	2.541	2.548	2.555	2.562	2.569
720	2.569	2.576	2.583	2.590	2.597	2.604	2.611	2.618	2.625	2.632	2.639
730	2.639	2.646	2.653	2.660	2.667	2.674	2.681	2.688	2.695	2.703	2.710
740	2.710	2.717	2.724	2.731	2.738	2.745	2.753	2.760	2.767	2.775	2.782
750	2.782	2.789	2.796	2.803	2.811	2.818	2.825	2.833	2.840	2.847	2.854
760	2.854	2.862	2.869	2.876	2.884	2.891	2.898	2.906	2.913	2.921	2.928
770	2.928	2.935	2.943	2.950	2.958	2.965	2.973	2.980	2.987	2.995	3.002
780	3.002	3.010	3.017	3.025	3.032	3.040	3.047	3.055	3.062	3.070	3.078
790	3.078	3.085	3.093	3.100	3.108	3.116	3.123	3.131	3.138	3.146	3.154
800	3.154	3.161	3.169	3.177	3.184	3.192	3.200	3.207	3.215	3.223	3.230
810	3.230	3.238	3.246	3.254	3.261	3.269	3.277	3.285	3.292	3.300	3.308
820	3.308	3.316	3.324	3.331	3.339	3.347	3.355	3.363	3.371	3.379	3.386
830	3.386	3.394	3.402	3.410	3.418	3.426	3.434	3.442	3.450	3.458	3.466
840	3.466	3.474	3.482	3.490	3.498	3.506	3.514	3.522	3.530	3.538	3.546
850	3.546	3.554	3.562	3.570	3.578	3.586	3.594	3.602	3.610	3.618	3.626
860	3.626	3.634	3.643	3.651	3.659	3.667	3.675	3.683	3.692	3.700	3.708
870	3.708	3.716	3.724	3.732	3.741	3.749	3.757	3.765	3.774	3.782	3.790
880	3.790	3.798	3.807	3.815	3.823	3.832	3.840	3.848	3.857	3.865	3.873
890	3.873	3.882	3.890	3.898	3.907	3.915	3.923	3.932	3.940	3.949	3.957
900	3.957	3.965	3.974	3.982	3.991	3.999	4.008	4.016	4.024	4.033	4.041
910	4.041	4.050	4.058	4.067	4.075	4.084	4.093	4.101	4.110	4.118	4.127
920	4.127	4.135	4.144	4.152	4.161	4.170	4.178	4.187	4.195	4.204	4.213
930	4.213	4.221	4.230	4.239	4.247	4.256	4.265	4.273	4.282	4.291	4.299
940	4.299	4.308	4.317	4.326	4.334	4.343	4.352	4.360	4.369	4.378	4.387
950	4.387	4.396	4.404	4.413	4.422	4.431	4.440	4.448	4.457	4.466	4.475
960	4.475	4.484	4.493	4.501	4.510	4.519	4.528	4.537	4.546	4.555	4.564
970	4.564	4.573	4.582	4.591	4.599	4.608	4.617	4.626	4.635	4.644	4.653
980	4.653	4.662	4.671	4.680	4.689	4.698	4.707	4.716	4.725	4.734	4.743
990	4.743	4.753	4.762	4.771	4.780	4.789	4.798	4.807	4.816	4.825	4.834

Continuation of Table 4

1000	4.834	4.843	4.853	4.862	4.871	4.880	4.889	4.898	4.908	4.917	4.926
1010	4.926	4.935	4.944	4.954	4.963	4.972	4.981	4.990	5.000	5.009	5.018
1020	5.018	5.027	5.037	5.046	5.056	5.065	5.074	5.083	5.092	5.102	5.111
1030	5.111	5.120	5.130	5.139	5.148	5.158	5.167	5.176	5.185	5.195	5.205
1040	5.205	5.214	5.223	5.233	5.242	5.252	5.261	5.270	5.280	5.289	5.299
1050	5.299	5.308	5.318	5.327	5.337	5.346	5.356	5.365	5.375	5.384	5.394
1060	5.394	5.403	5.413	5.422	5.432	5.441	5.451	5.460	5.470	5.480	5.489
1070	5.489	5.499	5.508	5.518	5.528	5.537	5.547	5.556	5.566	5.576	5.585
1080	5.595	5.595	5.605	5.614	5.624	5.634	5.643	5.653	5.663	5.672	5.682
1090	5.682	5.692	5.702	5.711	5.721	5.731	5.740	5.750	5.760	5.770	5.780
1100	5.780	5.789	5.799	5.809	5.819	5.828	5.838	5.848	5.858	5.868	5.878
1110	5.878	5.887	5.897	5.907	5.917	5.927	5.937	5.947	5.956	5.966	5.976
1120	5.976	5.986	5.996	6.006	6.016	6.026	6.036	6.046	6.055	6.065	6.075
1130	6.075	6.085	6.095	6.105	6.115	6.125	6.135	6.145	6.155	6.165	6.175
1140	6.175	6.185	6.195	6.205	6.215	6.225	6.235	6.245	6.256	6.266	6.276
1150	6.276	6.286	6.296	6.306	6.316	6.326	6.336	6.346	6.356	6.367	6.377
1160	6.377	6.387	6.397	6.407	6.417	6.427	6.433	6.443	6.453	6.463	6.473
1170	6.473	6.483	6.493	6.503	6.513	6.523	6.533	6.543	6.553	6.563	6.573
1180	6.580	6.591	6.601	6.611	6.621	6.632	6.642	6.652	6.663	6.673	6.683
1190	6.683	6.693	6.704	6.714	6.724	6.735	6.745	6.755	6.766	6.776	6.786
1200	6.786	6.797	6.807	6.818	6.828	6.838	6.849	6.859	6.869	6.880	6.890
1210	6.890	6.901	6.911	6.922	6.932	6.942	6.953	6.963	6.974	6.984	6.995
1220	6.995	7.005	7.016	7.026	7.037	7.047	7.058	7.068	7.079	7.089	7.100
1230	7.100	7.110	7.121	7.131	7.142	7.152	7.163	7.173	7.184	7.194	7.205
1240	7.205	7.216	7.226	7.237	7.247	7.258	7.269	7.279	7.290	7.300	7.311
1250	7.311	7.322	7.332	7.343	7.353	7.364	7.375	7.385	7.396	7.407	7.417
1260	7.417	7.428	7.439	7.449	7.460	7.471	7.482	7.492	7.503	7.514	7.524
1270	7.524	7.535	7.546	7.557	7.567	7.578	7.589	7.600	7.610	7.621	7.632
1280	7.632	7.643	7.653	7.664	7.675	7.686	7.697	7.707	7.718	7.729	7.740
1290	7.740	7.751	7.761	7.772	7.783	7.794	7.805	7.816	7.827	7.837	7.848
1300	7.848	7.859	7.870	7.881	7.892	7.903	7.914	7.924	7.935	7.946	7.957
1310	7.957	7.968	7.979	7.990	8.001	8.012	8.023	8.034	8.045	8.056	8.066
1320	8.066	8.077	8.088	8.099	8.110	8.121	8.132	8.143	8.154	8.165	8.176
1330	8.176	8.187	8.198	8.209	8.220	8.231	8.242	8.253	8.264	8.275	8.286
1340	8.286	8.298	8.309	8.320	8.331	8.342	8.353	8.364	8.375	8.386	8.397
1350	8.397	8.408	8.419	8.430	8.441	8.453	8.464	8.475	8.486	8.497	8.508
1360	8.508	8.519	8.530	8.542	8.553	8.564	8.575	8.586	8.597	8.608	8.620
1370	8.620	8.631	8.642	8.653	8.664	8.675	8.687	8.698	8.709	8.720	8.731
1380	8.731	8.743	8.754	8.765	8.776	8.787	8.799	8.810	8.821	8.832	8.844
1390	8.844	8.855	8.866	8.877	8.889	8.900	8.911	8.922	8.934	8.945	8.956
1400	8.956	8.967	8.979	8.990	9.001	9.013	9.024	9.035	9.047	9.058	9.069
1410	9.069	9.080	9.092	9.103	9.114	9.126	9.137	9.148	9.160	9.171	9.182
1420	9.182	9.194	9.205	9.216	9.228	9.239	9.251	9.262	9.273	9.285	9.296
1430	9.296	9.307	9.319	9.330	9.341	9.353	9.364	9.375	9.387	9.397	9.410
1440	9.410	9.421	9.433	9.444	9.456	9.467	9.478	9.490	9.501	9.513	9.524
1450	9.524	9.536	9.547	9.558	9.570	9.581	9.593	9.604	9.616	9.627	9.639
1460	9.639	9.650	9.662	9.673	9.684	9.696	9.707	9.719	9.730	9.742	9.753
1470	9.753	9.765	9.776	9.788	9.799	9.811	9.822	9.834	9.845	9.857	9.868
1480	9.868	9.880	9.891	9.903	9.914	9.926	9.937	9.949	9.961	9.972	9.984
1490	9.984	9.995	10.007	10.018	10.030	10.041	10.053	10.064	10.076	10.088	10.099
1500	10.099	10.111	10.122	10.134	10.145	10.157	10.168	10.180	10.192	10.203	10.215
1510	10.215	10.226	10.238	10.249	10.261	10.273	10.284	10.296	10.307	10.319	10.331
1520	10.331	10.342	10.354	10.365	10.377	10.389	10.400	10.412	10.423	10.435	10.447
1530	10.447	10.458	10.470	10.482	10.493	10.505	10.516	10.528	10.540	10.551	10.563
1540	10.563	10.575	10.586	10.598	10.609	10.621	10.633	10.644	10.656	10.668	10.679
1550	10.679	10.691	10.703	10.714	10.726	10.738	10.749	10.761	10.773	10.784	10.796
1560	10.796	10.808	10.819	10.831	10.843	10.854	10.866	10.877	10.889	10.901	10.913
1570	10.913	10.924	10.936	10.948	10.959	10.971	10.983	10.994	11.006	11.018	11.029
1580	11.029	11.041	11.053	11.064	11.076	11.088	11.099	11.111	11.123	11.134	11.146
1590	11.146	11.158	11.169	11.181	11.193	11.205	11.216	11.228	11.240	11.251	11.263
1600	11.263	11.275	11.286	11.298	11.310	11.321	11.333	11.345	11.357	11.368	11.380
1610	11.380	11.392	11.403	11.415	11.427	11.438	11.450	11.462	11.474	11.485	11.497
1620	11.497	11.509	11.520	11.532	11.544	11.555	11.567	11.579	11.591	11.602	11.614
1630	11.614	11.626	11.637	11.649	11.661	11.673	11.684	11.696	11.708	11.719	11.731
1640	11.731	11.743	11.754	11.766	11.778	11.790	11.801	11.813	11.825	11.836	11.848
1650	11.848	11.860	11.871	11.883	11.895	11.907	11.918	11.930	11.942	11.953	11.965
1660	11.965	11.977	11.988	12.000	12.012	12.024	12.035	12.047	12.059	12.070	12.082
1670	12.082	12.094	12.105	12.117	12.129	12.141	12.152	12.164	12.176	12.187	12.199
1680	12.199	12.211	12.222	12.234	12.246	12.257	12.269	12.281	12.292	12.304	12.316
1690	12.316	12.327	12.339	12.351	12.363	12.374	12.386	12.398	12.410	12.421	12.433
1700	12.433	12.444	12.456	12.468	12.479	12.491	12.503	12.514	12.526	12.538	12.549
1710	12.549	12.561	12.572	12.584	12.596	12.607	12.619	12.631	12.642	12.654	12.666
1720	12.666	12.677	12.689	12.701	12.712	12.724	12.736	12.747	12.759	12.770	12.782
1730	12.782	12.794	12.805	12.817	12.829	12.840	12.852	12.863	12.875	12.887	12.898
1740	12.898	12.910	12.921	12.933	12.945	12.956	12.968	12.980	12.991	13.003	13.014
1750	13.014	13.026	13.037	13.049	13.061	13.072	13.084	13.095	13.107	13.119	13.130
1760	13.130	13.142	13.153	13.165	13.176	13.188	13.200	13.211	13.223	13.234	13.246
1770	13.246	13.257	13.269	13.280	13.292	13.304	13.315	13.327	13.338	13.350	13.361
1780	13.361	13.373	13.384	13.396	13.407	13.419	13.430	13.442	13.453	13.465	13.476
1790	13.476	13.488	13.499	13.511	13.522	13.534	13.545	13.557	13.568	13.580	13.591
1800	13.591	13.603	13.614	13.626	13.637	13.649	13.660	13.672	13.683	13.694	13.706
1810	13.706	13.717	13.729	13.740	13.752	13.763	13.775	13.786	13.797	13.809	13.820
1820	13.820										

**More  
Books!**



yes  
**I want morebooks!**

Buy your books fast and straightforward online - at one of world's fastest growing online book stores! Environmentally sound due to Print-on-Demand technologies.

Buy your books online at  
**[www.morebooks.shop](http://www.morebooks.shop)**

Kaufen Sie Ihre Bücher schnell und unkompliziert online – auf einer der am schnellsten wachsenden Buchhandelsplattformen weltweit! Dank Print-On-Demand umwelt- und ressourcenschonend produziert.

Bücher schneller online kaufen  
**[www.morebooks.shop](http://www.morebooks.shop)**



[info@omniscryptum.com](mailto:info@omniscryptum.com)  
[www.omniscryptum.com](http://www.omniscryptum.com)

OMNIScriptum

